Behavioral Responses to Frequency-specific Head-related Transfer Functions as Filtered by the Facial Ruff in the Barn Owl (*Tyto alba*)

Von der Fakultät für Mathematik, Informatik und Naturwissenschaften
der RWTH Aachen University zur Erlangung des akademischen Grades
einer Doktorin der Naturwissenschaften genehmigte Dissertation

vorgelegt von

Diplom-Biologin/MBA

Elena Laura Hausmann

aus Aachen

Berichter: Universitätsprofessor Dr. Hermann Wagner

Universitätsprofessor Dr. Harald Luksch

Tag der mündlichen Prüfung: 23. September 2010

Diese Dissertation ist auf den Internetseiten der Hochschulbibliothek online verfügbar.

Contents

List of Figures

List of Tables

Nomenclature

AAr auditory arcopallium

FFT Fast Fourier Transform

HRIR Head-related impulse responses

ICx external nucleus of the inferior colliculus

IID interaural intensity difference

LSO lateral superior olive

HRTF head-related transfer function

ILD interaural level difference

ITD interaural time difference

SD standard deviation

1 Summary

The barn owl is, due to its numerous morphological and neuronal adaptations to sound localization, a long-established model animal for the auditory system. Besides extensive research on the topic within the last decades, it is still unclear how direction- and frequency-dependent physical cues (interaural time differences (ITDs), level differences (ILDs) and monaural spectra) contribute to sound localization especially in the elevational plane. A further open question is to what extent frequency integration is needed for accurate localization, and how the owl can resolve spatial coding ambiguities.

Although the dichotic stimulation via headphones allows to introduce and manipulate ITDs and ILDs independently, it does not reflect the monaural frequency characteristics that are usually present in free-field stimuli. This problem can be overcome when sound stimuli are filtered by the animal's characteristic head-related transfer functions (HRTFs), creating a Virtual Auditory Space.

In the present thesis, I investigated the properties of HRTFs in the American Barn owl (*Tyto alba pratincola*, L.). The shape of the owls' HRTFs is crucially influenced by the filtering properties of the facial ruff. Therefore, I analyzed the physical cues used for sound localization which are contained in the HRTFs after filtering by the outer ear and ruff. Furthermore, I tested the impact of HRTFs measured under different conditions and in various frequency bands on the owls' sound localization ability in a behavioral task.

During the experiments, two methodological approaches were used. First, HRTFs were measured and analyzed under various conditions. The binaural and monaural cues to sound location were assessed in a large set of barn owl HRTFs, including existing HRTFs measured in earlier experiments. Either anesthetized or dead animals were used for a detailed analysis of whether the physiological condition or the body temperature have any influence on the sound localization cues. The analysis focused especially on the low-frequency range ($<2\,\mathrm{kHz}$), the role of which is still obscure in the owl. At low frequencies, the owl's ears might act as pressure difference receivers, with both ear cavities being coupled through the interaural canal. In that case, the low-frequency ITD range would be predicted to increase compared to the high-frequency range. However, I did not find such an effect, which argues against the hypothesis of a pressure difference receiver characteristic of the owl's ears.

Second, HRTF-filtered stimuli were calculated for stimulation of barn owls in a Virtual Acoustic Space. The sound localization ability of three owls was tested in a behavioral paradigm utilizing saccadic head-turn responses as a measure for the perceived sound source location. In a first approach, the influence of the facial ruff was investigated by virtual removal of the ruff. This was done by comparing azimuthal and elevational head-turn reactions to normal, individualized HRTFs with reactions to normal, non-individualized respectively to "ruffcut" HRTFs. The HRTFs used for that part of the thesis had been recorded near the eardrum of the respective owl during stimulation with tonal sweeps. Measurements had

been repeated after successively removing the ruff feathers of a reference owl (owl 39), which resulted in a set of HRTFs for representative spatial sound source locations and with different ruff conditions, depending on which part of the ruff feathers were removed.

As expected from the directionality of the ruff, I found that the owls were impaired in their localization ability when the ruff feathers were virtually removed. This impairment included an inability to distinguish stimuli containing the same ITD, but coming from either the front or the rear hemisphere, respectively. The owls distinguished such stimuli only when the HRTFs had been measured with intact ruff, but not after virtual ruff removal. Furthermore, elevational sound localization was severely reduced in the latter stimulus condition.

In a second experimental series, the influence of 1/3 octaveband-filtered HRTFs with center frequencies ranging from 1 to 9 kHz was tested in the same behavioral paradigm. The owls localized the stimuli with good azimuthal accuracy, but located stimulus elevation accurately only for frequencies above 3 kHz. Localization errors depended on center frequency. When the ILD of 1/3 octaveband-filtered stimuli with 5 kHz center frequency was fixed to 0 dB, the owls seemed to experience phantom sound sources and were unable to discriminate stimulus elevation, as they did with unmanipulated stimuli.

The results presented in the thesis demonstrate that the facial ruff of barn owls alters incoming sound in a frequency-specific way that is not only crucial for accurate sound localization in both azimuthal and elevational planes, but can also be predicted from the filtering properties of the ruff.

2 Zusammenfassung

Die Schleiereule ist dank ihrer Vielzahl morphologischer und neuronaler Anpassungen an die Schalllokalisation ein etabliertes Modelltier für das auditorische System. Trotz ausgedehnter Forschung in den letzten Jahrzehnten ist jedoch noch unklar, wie genau richtungs- und frequenzabhängige physikalische Parameter (interaurale Zeitdifferenzen (ITDs), interaurale Pegeldifferenzen (ILDs) und monaurale Spektra) zur Schalllokalisation insbesondere in der vertikalen Ebene beitragen. Eine weitere offene Frage ist, in welchem Ausmaß Frequenzintegration für eine exakte Lokalisation notwendig ist, und wie die Eule räumliche Mehrdeutigkeiten auflösen kann.

Obwohl dichotische Stimulation über Kopfhörer es ermöglicht, ITDs oder ILDs unabhängig voneinander gezielt zu manipulieren, reflektieren solche Stimuli nicht die natürlicherweise vorkommenden monauralen Frequenzcharakteristika. Dieses Problem kann umgangen werden, wenn Schallreize mit den charakteristischen Kopfübertragungsfunktionen (HRTFs) des Tieres gefiltert werden und so eine Virtuelle Akustische Umgebung erzeugt wird.

In der vorliegenden Doktorarbeit wurden die Eigenschaften von Kopfübertragungsfunktionen (HRTFs) der Amerikanischen Schleiereule (*Tyto alba pratincola*, L.) untersucht. Die Höhe der nach Filterung durch Kopf und Außenohr in den HRTFs enthaltenen monauralen und binauralen Schalllokalisationsparameter wird von den Filtereigenschaften des Gesichtsschleiers beeinflusst. Der Schwerpunkt dieser Dissertation lag daher sowohl auf der Analyse der Lokalisationsparameter in HRTFs, die unter verschiedenen Bedingungen gemessen wurden, als auch auf der Vorhersage des Lokalisationsverhaltens, das aus der Stimulation mit HRTF-gefilterten Stimuli in verschiedenen Frequenzbändern resultiert.

Es wurden zwei methodische Ansätze verfolgt. Zum einen wurden HRTFs unter verschiedenen Bedingungen gemessen und die binauralen und monauralen Lokalisationsparameter in den HRTFs zahlreicher Schleiereulen analysiert, einschließlich einiger aus früheren Messungen stammender HRTF-Sätze. Der Einfluss von physiologischem Zustand und Körpertemperatur auf die Lokalisationsparameter wurde durch einen Vergleich entweder anästhesierter oder toter Tiere untersucht. Der Fokus der Analyse lag dabei auf dem tieffrequenten Bereich ($<$2 kHz), dessen Bedeutung in der Schleiereule noch weitgehend ungeklärt ist. In diesem Frequenzbereich könnte Schall die Trommelfelle der Eule von beiden Seiten erreichen und diese dadurch als Druckdifferenz-Rezipient fungieren, sofern sie über den interauralen Kanal miteinander gekoppelt wären. Für diesen Fall wäre die Vorhersage, dass die ITD-Spanne im niederfrequenten Bereich stark ansteigt. Dies habe ich jedoch in meinen Experimenten nicht beobachtet, was gegen eine mögliche Funktionsweise als Druckdifferenz-Rezipient der Eulen-Ohren spricht.

Im zweiten methodischen Ansatz wurden HRTF-gefilterte Stimuli für die Verwendung in einem komplexen Verhaltensparadigma berechnet, in dem der Kopfdrehwinkel als Indikator für die empfundene räumliche Position der Schallquelle diente. Die Lokalisationsfähigkeit

der Eulen für solche Stimuli wurde getestet, indem den Tieren verschiedene virtuelle Stimuli per Kopfhörer vorgespielt wurden.

In einer ersten Versuchsreihe wurde der Gesichtsschleier der Eulen virtuell entfernt, um dessen Einfluss auf das Lokalisationsverhalten zu testen. Für diesen Zweck wurden Kopfdrehsakkaden in der Azimut- und Elevationsebene als Reaktion auf normale, individualisierte HRTFs mit solchen auf "Schleier entfernt"-HRTFs verglichen. Die HRTFs für diese Versuchsreihe wurden kurz vor dem Trommelfell der jeweiligen Eule bei zeitgleicher Stimulation mit logarithmisch ansteigenden Tonreizen aufgenommen. Für ein Referenztier wurde die Messung nach sukzessiver Entfernung des Gesichtsschleiers wiederholt, was in HRTFs für repräsentative räumliche Positionen resultierte, sowohl mit intaktem als auch ohne Schleier.

Wie auf Grund der Richtungssensitivität des Gesichtsschleiers erwartet, war die Fähigkeit der Eulen, virtuelle Schallquellen zu lokalisieren, nach virtueller Entfernung des Schleiers eingeschränkt. Die Einschränkung umfasste sowohl die Fähigkeit, die Stimuluselevation zu bestimmen, als auch die, Stimuli mit zwar gleicher ITD, aber mit Ursprung in der vorderen bzw. hinteren Hemisphäre, voneinander zu unterscheiden. Solche Reize konnten die Tiere nur mit intaktem Schleier unterscheiden, nicht jedoch nach dessen virtueller Entfernung.

In einer zweiten Versuchsreihe wurde im selben Verhaltensparadigma der Einfluss von 1/3-Oktavband-gefilterten HRTFs mit Zentrumsfrequenzen von 1 bis 9 kHz getestet. Die Eulen lokalisierten diese Stimuli mit hoher azimutaler Genauigkeit, konnten aber die Stimuluselevation nur für Frequenzen über 3 kHz bestimmen. Das Ausmaß der Lokalisationsfehler hing dabei von der Stimulusfrequenz ab. Wenn die ILD von oktavbandgefilterten Reizen mit 5 kHz Zentrumsfrequenz künstlich auf Null gesetzt wurde, schienen die Eulen nicht nur Phantomquellen zu lokalisieren, sondern konnten auch, anders als bei den unmanipulierten Oktavbandreizen derselben Zentrumsfrequenz, die Stimuluselevation nicht mehr bestimmen.

Die Ergebnisse der vorliegenden Arbeit zeigen, dass der Gesichtsschleier der Eule Schall frequenzspezifisch in einer Weise verändert, die nicht nur notwendig für präzise Lokalisation von virtuellen Schallquellen in der Azimut- und Elevationsebene ist, sondern auch aus den Filtereigenschaften des Schleiers vorhergesagt werden kann.

3 General Introduction

Humans mainly rely on visual information to orient in their environment. However, it is often a sound stimulus that tells somebody where to look, and oral communication would be severely hampered without the ability to detect and localize sounds and to provide auditory information with meaning. Thanks to a vast range of research studies including both humans and model animals, many of the basic principles of auditory processing made substantial progress and are nowadays applied in computational sciences or medicine, for example for cochlear implants and other hearing aids.

While deaf people in the modern world do not suffer from life threatening restrictions, the aforementioned features are crucial for animals that hunt prey using mainly auditory information. Such animals, like the barn owl (*Tyto alba*), are due to their behavioral and neuronal specializations to sound localization a well established model organism for auditory perception and processing.

In this thesis, I investigated the contribution of direction-dependent physical cues, as introduced by the facial ruff of the barn owl, to azimuthal and elevational sound localization. Specifically, I simulated virtual ruff removal and frequency-specific filtering using the Virtual Auditory Space (VAS) method. This method involves stimuli filtered with the owls' head-related transfer functions that are delivered independently to each ear. The VAS has been shown to be appropriate for the investigation of sound localization tasks, since it reflects all relevant factors that are also present in free-field sounds. The fundamentals of the technique are explained in section 3.2, followed by a brief overview of how this thesis was designed.

3.1 Barn owls as a model for sound localization

Sound localization can be performed by exploiting the fact that certain characteristics of a sound wave are modified in a specified way while it travels, as well as when it encounters an object. In animals that possess two ears, there are two major binaural cues to sound localization, first, interaural time differences (ITDs), and second, interaural level differences (ILDs). The latter occur because the frequency components of a sound are attenuated in a frequency-dependent manner at both ears, even more strongly at the ear that is opposed to the direction of the sound source. The head of a subject attenuates frequencies with a wavelength in the range of or smaller than the head diameter, while frequencies with a larger wavelength travel around it without being strongly affected. Hence, the smaller the wavelength with respect to the head diameter is, the stronger is the corresponding frequency component attenuated. In other words, high frequencies are stronger attenuated than low frequencies. The resulting ILD helps mammals to localize sound sources in the high-frequency range (Middlebrooks and Green, 1991). Barn owls use them to localize sounds

in the vertical plane (Knudsen and Konishi, 1979; Moiseff, 1989a,b; Takahashi et al., 1984), because their asymmetric ear positioning results in ILDs that change along the vertical axis.

For sound sources outside the midsagittal plane, the sound arrives first at one ear, the side of which is called ipsilateral, and with a certain time delay at the other ear, which is the contralateral ear. This interaural time difference (ITD) – or external delay – increases with increasing head diameter. ITD also depends on the angle of the sound source location relative to the midline between both ears. That is, if the midline is set to 0°, then a sound coming from 90° (or perpendicular to the right ear) respectively -90° (perpendicular to the left ear) results in the largest ITDs in a classical spherical head model.

Mammals use ITDs only in the low frequency range where accurate encoding of the phase of the signal's carrier frequency is still possible (<1500 Hz in humans; Blauert, 1997) to localize sound sources in the horizontal plane. Barn owls, in contrast, with their ability to encode a signal's phase up to a frequency of 9 kHz (Köppl, 1997) can determine azimuth using ITDs over their whole hearing spectrum (Coles and Guppy, 1988; Knudsen and Konishi, 1979; Konishi, 2003; McAlpine et al., 2001; Middlebrooks and Green, 1991; Wagner et al., 2007).

Thus, mammals and barn owls use the identical physical cues in different ways, which is due to several morphological and neurological specializations of the owl.

Barn owls have a characteristic, parabolically shaped facial ruff that is directionally sensitive for frequencies ≥ 4 kHz and enhances incoming sound up to 20 dB (Brainard et al., 1992; von Campenhausen and Wagner, 2006; Coles and Guppy, 1988; Keller et al., 1998; Olsen et al., 1989). In contrast to other birds and to mammals, the ears of barn owls are asymmetrically arranged. The left ear opening lies higher at the head, and is, therefore, more sensitive to sounds coming from the lower hemisphere, whereas the right ear opening is upwards directed and sensitive to sounds coming from the upper hemisphere (Brainard et al., 1992; von Campenhausen and Wagner, 2006; Keller et al., 1998; Knudsen et al., 1984). The cochlear basilar papilla is with 11 mm not only longer than in most other birds, but half of its length is devoted to frequencies above 5 kHz resulting in an 'auditory fovea' in this frequency range (Köppl et al., 1993). The lowest hearing threshold of owls is as low as -18.5 dB SPL between 3 and 9 kHz, with an upper frequency limit of 12 kHz (Dyson et al., 1998; Konishi, 1973a; Wagner, 1993).

These adaptations of the owl result in an extremely effective auditory system that allows sound source localization with an accuracy of 3° for both azimuthal and elevational components (Bala et al., 2003; Knudsen et al., 1979; Konishi, 1973a). However, this high spatial resolution only holds in the frontal field. The more lateral or elevated the sound source is, the larger become localization errors (Bala et al., 2003, 2007; Knudsen et al., 1979; Poganiatz et al., 2001). This is mainly due to underestimation of the sound source angle.

While localization performance in the frontal field does not differ significantly for azimuthal and elevational components even in free-flight experiments (Bala et al., 2007; Knudsen et al., 1979; Konishi, 1973b), it strongly decreases for eccentric sound sources especially for the

vertical plane. Here, the localization error for the elevational component increased up to 27.9° at +70° elevation and 0° azimuth (Knudsen et al., 1979). The localization of elevational sound source components at eccentric locations was half as accurate, thus significantly lower, as for azimuthal components in several studies (Bala et al., 2007; Knudsen et al., 1979; Konishi, 1973b; Poganiatz and Wagner, 2001; Poganiatz et al., 2001).

It is required that ITD and ILD have neuronal correlates in order to preserve and exploit their information and use it for sound localization. ITD and ILD are processed in two separate pathways up to the level of the inferior colliculus in the auditory brainstem nuclei of the barn owl (Moiseff and Konishi, 1981a; Takahashi et al., 1984). ITD and ILD pathways converge again at the level of the lateral shell of the IC (ICls) (Takahashi and Konishi, 1988; Takahashi et al., 1988).

Integration of ITD and ILD allows the formation of an auditory space map in the external nucleus of the inferior colliculus (ICx, Knudsen and Konishi, 1978), where the receptive fields of each space-specific neuron corresponds to a spatial position either in the contralateral hemifield or ipsilateral near the midline (Euston and Takahashi, 2002; Knudsen and Konishi, 1978; Konishi, 2003; Takahashi et al., 2003). When two concurrent sound sources emit amplitude-modulated uncorrelated noise bursts, space-specific neurons are able to resolve the two sources lying within their spatial receptive fields by encoding the phase of the amplitude modulations (Keller and Takahashi, 2005). That ability and the restricted receptive fields of space-specific neurons is crucial to separate adjacent sound sources from each other (Keller and Takahashi, 2005).

Since the external time delay of a sound signal arriving at both ears varies systematically with the position of the sound source relative to the listener's head, the source location can be calculated on a neuronal basis by internally compensating the external delay. This requires an array of coincidence detectors tuned to different ITDs, with maximum responses to coinciding signals from both sides, a model which has first been proposed by Jeffress (1948). In the barn owl's nucleus laminaris (NL), a brainstem nucleus of the auditory pathway, neuronal delay lines fulfill this function within each frequency channel (Carr and Konishi, 1988; Wagner, 2002). A spike train which is generated in response to incoming sound travels along these delay lines. Due to the external ITD, the sound signal reaches the eardrum on the contralateral side later than on the ipsilateral side. Accordingly, transmission of the signal by the basilar membrane of the cochlea and generation of neuronal spikes starts with a time delay that reflects the external ITD. Eventually, the two spike trains coincide at the neuron that represents the external delay, that is, the more contralaterally the sound source is positioned, the longer it travels along the contralateral delay line and the shorter it travels along the ipsilateral delay line. Coincidence detector neurons arranged in a tonotopic array fire maximally when both spike trains arrive isochronously, i.e. the leading signal matches the lagging one.

However, neurons on the level of the NL cannot code for a specific ITD yet, since they are

narrowly frequency-tuned and do not discriminate the stimulus ITD from multiples of its period (Konishi, 2003). Consequently, their ITD tuning curves are cyclic with several equal peaks (Konishi, 2003; Wagner, 2002). This ambiguity leads to the localization of so-called phantom sources until the stimulus exceeds a certain bandwidth (Knudsen, 1981; Saberi et al., 1998, 1999). Thus, with tonal or very narrowband stimulation, the owl experiences the sound source as being located either at the real source location (as predicted by the ITD) or at a position indicated by the real source's ITD ± n times the period duration of the stimulus frequency, with n as an integer (Saberi et al., 1998).

Auditory space can either be represented by the slope of the ITD tuning curves (slope-code) as suggested for mammals (Harper and McAlpine, 2004), or by the peak (maximum firing rate) of the ITD tuning curves, each representing a specific spatial location (place-code) by means of axonal delay lines as implemented in the owl (Carr and Konishi, 1988). The mammalian slope-code model predicts that neurons represent only phases up to one-half of the period duration, but not outside this range because the maximum slope would suffice to encode all spatial positions within the physiologically relevant range. This limited ITD representation has been named "π limit" because the distribution of neurons responding to specific ITDs when plotted against frequency resembles the shape of the greek letter pi.

In the barn owl's inferior colliculus, however, neurons in the low-frequency range represent not only ITDs outside the physiologically relevant range of approximately ±250 µs, but also outside the π limit (Wagner et al., 2007). This finding further supports that in the owl, auditory space is represented by a place-code. It has been proposed that the curvature of ITD-cross-correlation patterns after integration across frequencies may explain why owls can detect ITDs five times larger than the naturally occurring ITDs (Saberi et al., 2002). The least curved trajectory of this cross-correlation pattern would represent the real ITD at which neuronal response peaks coincide across all frequencies, while responses to the phase multiples (real ITD ± n times period duration, see above) would result in stronger curvature (Wagner et al., 1987). In narrowband stimuli or tones, across-frequency integration is restricted.

At low frequencies (<2 kHz), the period duration is too long for phantom sources to appear within the physiological relevant range. However, at low frequencies, it may be possible that sound waves reach the owls' eardrums from both sides, directly and indirectly through the interaural canal as is the case in small birds (Larsen et al., 1997, 2006). In small birds, the interaurally coupled ear cavities increase the available ITD range. For higher frequencies, sound attenuation in the owl's interaural canal is too strong to allow a similar functional role of the interaural canal (Moiseff and Konishi, 1981b), but measurements in the low-frequency range are missing so far.

The wavelength of the stimulation tone determines the maximum phase difference, from which the ITD that can occur for this tone at a given head diameter is calculated. If the owl is stimulated with e.g. a 5 kHz tone – with a period of 200 µs – the maximum ITD

calculated from 180° phase difference is 100 µs. Larger phase differences cannot occur with this tone because the signals arriving at both ears then start to get back in phase. Due to the limited maximum phase difference that can occur for a tone of a given frequency, the azimuthal position of experienced phantom sources in the owl is limited. Apart from the owl's head diameter, it depends on the sound's ITD as well as on its frequency (cf. Table 7). A signal arriving at one ear can either be matched with the leading or with the lagging phase to calculate the ITD, both coding for ambiguous sound source azimuths in the opposite hemispheres. If the maximally occurring ITD of tonal or narrowband stimuli lie within the physiologically relevant range, the owl can experience phantom sound source locations whose positions can be derived from the stimulus ITD and period duration (Saberi et al., 1998).

When owls were stimulated with a 5 kHz tone with an ITD of either +50 µs (right side leading) or -150 µs (left side leading), one of two owls always turned its head to -50°, while the second owl turned its head to +20° (Saberi et al., 1998). The owls reacted to two concurring sound images by choosing either the more centrally or the more peripherally located source. With reversed algebraic signs, the signs of the head turn responses were likewise reversed. The first owl responded with a head saccade to +50° when the stimulus ITD was either -50 µs or +150 µs. With this stimulation, the second owl experienced the sound source at -20°.

All of these sound source positions were predicted by either adding or subtracting the stimulus ITD from the stimulus period (for example, 200 − 50 = 150 µs (corresponding to 50° azimuth, based on the change of 2.5 µs ITD per degree as measured by von Campenhausen and Wagner, 2006) and -200 + 150 = -50 µs (corresponding to -20°), indicating that owls experience the sound source at different locations depending on whether the signal is interpreted as left or right ear leading (Saberi et al., 1998). With higher frequencies, the period of a tone decreases and correspondingly the owl's head turning angle decreased.

For broadband stimulation, the ambiguity can be resolved in a higher processing station, the external nucleus of the inferior colliculus (ICx). Here, the tuning curves from the varying frequency components of the stimulus are integrated and yield one main peak and several smaller side peaks (Takahashi and Konishi, 1986). Hence, ICx neurons are broadly frequency tuned, a crucial prerequisite for the integration across frequencies.

3.2 Head-related transfer functions

Processing of ITD and ILD allows for a high auditory resolution in the horizontal and, in the owl in contrast to mammals and most other birds, even in the vertical plane. In a classic spherical head model that holds for humans and most animals with symmetrically arranged ears at opposite ends of the sphere, sound sources lying along the surface of a head-centered 'cone of confusion' (Blauert, 1997) result in constant – thus indistinguishable – ITDs. Each

ITD corresponds to two spatial positions: first, in the frontal hemisphere, and second, in the rear hemisphere.

The barn owl might resolve this ambiguity due to the unique, unambiguous combination of a specific ITD with a specific ILD in the frontal hemisphere (Moiseff, 1989b) in order to create an auditory space map in the external nucleus of the inferior colliculus (ICx), which is then combined with visual information in the optic tectum in the midbrain (Knudsen, 1981; Wagner, 1993). If the combination of ITD and ILD is indeed the crucial factor for the owl to distinguish ambiguous positions, then this discrimination ability should disappear when the facial ruff is removed, because it is only the ruff that creates the characteristic distribution of binaural cues (von Campenhausen and Wagner, 2006). The investigation of this question was one of the goals of the present thesis (see section 5).

Ambiguity is reduced furthermore because the outer ear of most animals is formed asymmetrically with respect to the frontal plane (Searle et al., 1975), and because ear, head and body have different diffraction and reflection properties. These differences may introduce disparities to the monaural frequency spectra that help to distinguish spatial positions along the cone of confusion (Blauert, 1997). In contrast to many other species, for example cats, the pinna in barn owls cannot be moved. The same holds for humans. Pinna movements serve to bring auditory targets into visual focus, similar to head movements in humans or owls. Sound localization can also be performed monaurally by moving the pinna or head and evaluate the resulting changes in the monaural spectra (Searle et al., 1975; Slattery and Middlebrooks, 1994; Wanrooij and Opstal, 2004).

However, animals with moveable pinnae face the problem that eye and ears can be moved independently, but both cues need to be integrated in order allow adequate orienting responses (Drager and Hubel, 1975; Harris et al., 1980; Hartline et al., 1995; King and Calvert, 2001; Meredith and Stein, 1986). In the cat, auditory and visual cues are integrated into auditory and visual space maps in the superior colliculus (Gordon, 1973; Hartline et al., 1995; Middlebrooks and Knudsen, 1984). This is possible because the divergence between sound source and gaze direction is compensated by shifts of the spatial receptive fields of auditory neurons. Pinna movements of the contralateral ear cause auditory spatial receptive fields in neurons of the superior colliculus of anesthetized cats to systematically shift peripherally and upward (Middlebrooks and Knudsen, 1987), similar to what is also observed in primates (Jay and Sparks, 1984). When cats turned their ipsilateral pinna sidewards, the areas where the neurons responded best moved frontally (Middlebrooks and Knudsen, 1987).

Besides these differences in the neural representation, the working principle of the pinna itself is always the same: its structure filters incoming sound linearly and in a direction dependent fashion (Blauert, 1997) by attenuating certain frequencies while other components are enhanced. The result is a direction-specific and individually different monaural frequency spectrum. The difference between the monaural spectra of both ears additionally introduces ITDs and ILDs. Thus, free-field stimuli are characteristically filtered during transmission

to the eardrum. The filter function is called a head-related transfer function (HRTF) and depends on individual differences in the exact shape of the outer ear, head and shoulder. The importance of these characteristic properties is even more emphasized by studies that show that, if only ITD and ILD cues are varied in a stimulus, the sound source position is perceived as lying inside the head (Plenge, 1974).

Stimuli that are filtered with the individual HRTF, in contrast, are externalized, thus perceived as coming from outside the head (Fujiki et al., 2002; Hartmann and Wittenberg, 1996; Wightman and Kistler, 1989a,b). Any free-field stimulus that is filtered with the individual HRTF and presented via in-ear phones (at a location similar to the recording site) will appear like a real free-field stimulus, as Keller et al. (1998) or Poganiatz et al. (2001)demonstrated for barn owls showing head turn responses that corresponded to free-field stimulation. In the barn owl, the facial ruff filters incoming sound and results in characteristic distributions of physical cues (von Campenhausen and Wagner, 2006; Coles and Guppy, 1988).

The HRTF can be determined by stimulating the subject with, for example, broadband noise or other signals containing the relevant frequency spectrum, and measuring the output signal that reaches the eardrum with in-ear microphones (for details see section 4.2.2). It was previously shown that ITD and interaural phase differences (IPD) change systematically with azimuth, while ILD changes with azimuth for frequencies below 5 kHz respectively with elevation for higher frequencies (Brainard et al., 1992; von Campenhausen and Wagner, 2006; Keller et al., 1998; Moiseff, 1989b; Poganiatz and Wagner, 2001; Poganiatz et al., 2001; Wagner, 1993). Thus, the measured HRTFs indeed contain all relevant information to enable sound localization. The complexity of the HRTFs increases with more lateral and rear spatial positions of the sound source, where the auditory sensitivity of barn owls decreases compared to the midline of their line of sight (Knudsen and Konishi, 1979).

When the HRTFs of barn owls were virtually manipulated, so that all spectral parameters of the filtered noise stimulus were maintained except the ITD, Poganiatz et al. (2001) found that ITD was the only relevant parameter for the owl to determine sound azimuth. Correspondingly, if only ILD was varied, the owl responded with head turning behavior into the direction that was predicted by the extent of ILD variation that the manipulated HRTF provided. However, the elevational head movement contained an azimuthal component that could only be explained by assuming an indirect influence of ITD on the perception of elevation mediated by frequency-specific cues (Egnor, 2001; Poganiatz and Wagner, 2001).

Since the owl can barely move its eyes (DuLac and Knudsen, 1990; Steinbach, 1972), the amplitude of head turning saccades can be used as a direct measure for the perceived sound source location (Knudsen et al., 1979, 1984; Moiseff and Konishi, 1981a). The possibility to measure HRTFs and manipulate certain of its characteristics in association with the behavioral head turn response provides an elegant and powerful way to investigate the importance of single HRTF characteristics on sound localization.

3.3 Aim and design of the thesis

Since the main goal of fundamental research on auditory processing is to apply the gained knowledge in humans, for example to improve hearing implants or localization robots, it is of specific interest to find out which physical cues are really needed to localize sound sources. As a consequence, the relevant cues can be preserved or simulated while discarding nonessential information, so as to reduce computational efforts in numerous auditory applications, including the creation of Virtual Auditory worlds also for humans.

In the last decade, HRTFs were measured and presented to barn owls via headphones in order to create virtual environments (Keller et al., 1998; Saberi et al., 1998, 1999) or to manipulate ITD and ILD systematically (Egnor, 2001; Keller et al., 1998; Poganiatz and Wagner, 2001; Poganiatz et al., 2001). However, these HRTFs reflected the filter properties of the owl's head and facial ruff 'as a whole'. In the present thesis, I therefore attempted to resolve the major contribution of the facial ruff and its filtering properties to sound localization in the barn owl. The ruff contains two types of feathers. Its outer border consists of several rows of reflector feathers which are stiff and whose main duty is to collect and amplify sound (von Campenhausen and Wagner, 2006; Coles and Guppy, 1988). The center of the facial disk is filled with fluffy auricle feathers, which are 'acoustically transparent' and protective (von Campenhausen and Wagner, 2006; Payne, 1971; Wagner, 2002).

Coles and Guppy (1988) investigated how the types of ruff feathers contribute to sound perception by measuring sound pressure levels in the outer ear cavity and at the round window of the cochlea. They used tones for stimulation of anesthetized owls and stated that the facial ruff alone amplified tones up to maximally 12 dB between 5 and 8 kHz, with a sharp decrease above 9 kHz. The external ear, including the ear cavity, enhances frequencies between 3 and 9 kHz up to 20 dB, with directional sensitivity (Coles and Guppy, 1988). The cited study focused on physical properties of the ruff for sound analysis without quantifying results in a behavioral context, which was one of the goals of the present thesis.

Previous studies opened a good insight into which information contained in sound stimuli is used for auditory localization, and how the owl implements them (Coles and Guppy, 1988; Knudsen et al., 1979, 1984; Knudsen and Knudsen, 1986; Konishi, 2003; Payne, 1962; Poganiatz and Wagner, 2001; Poganiatz et al., 2001; Takahashi et al., 1984; Wagner, 2002). However, it is still unclear to what extent the owl's localization performance depends on the facial ruff as a unique morphological adaptation. Is the ruff or the ear asymmetry the crucial factor, or only the combination of both features? Are the cues that result from filtering of sound by the ruff relevant for behavioral tasks? And if so, for what tasks are the cues needed? Last but not least, the question of how information within specific frequency channels can be extracted and used for localization tasks is of major relevance. The results gained from systematic manipulation of frequency-specific cues can further promote the discussion of whether across-frequency integration is a prerequisite for successful localization or not. The

present thesis therefore attempts to answer the above raised questions by investigating the impact that the filtering of incoming sound by the facial ruff has on sound localization. Three major aspects are tackled:

- First, what physical parameters (ITD, ILD and monaural cues) are present in barn owl HRTFs in individual frequency bands in both low- and high-frequency ranges, and are they influenced by body temperature or physiological state of the owl? What relevance may physical cues in the low-frequency range have for the functional role of the owl's ears? The presented results have previously been published in Hausmann et al. (2010).

- Second, to what extent does virtual removal of the facial ruff influence sound localization precision with broadband stimuli, and does the use of individualized versus non-individualized HRTFs play a role?

- And third, does the owl use the broadband-ILD for sound localization, or can it make use of the narrowband-ILD of individual frequency bands? If so, does the narrowband-ILD help to resolve spatial ambiguities?

Each of the main aspects will be outlined in a separate chapter (chapters 4 to 6) which also include the methods I used, followed by a general discussion (chapter 7).

4 Properties of barn owl HRTFs in the low-frequency range

*The most conspicuous features of the barn owl (*Tyto alba*) are the directionally-sensitive facial ruff and the asymmetrically arranged ears. The frequency-specific influence of these features on sound has consequences for sound localization that might differ between low and high frequencies. Whereas the high-frequency range (>3 kHz) is well investigated, less is known about the characteristics of head-related transfer functions for frequencies below 3 kHz. In the present study, I compared 1/3 octaveband-filtered transfer functions of barn owls with center frequencies ranging from 0.5 to 9 kHz. The range of interaural time differences was 600 µs at frequencies above 4 kHz, decreased to 505 µs at 3 kHz and increased again to about 615 µs at lower frequencies. The ranges for very low (0.5-1 kHz) and high frequencies (5-9 kHz) were not statistically different. Interaural level differences and monaural gains increased monotonically with increasing frequency. No systematic influence of the body temperature on the measured localization cues was observed. These data have implications for the mechanism underlying sound localization and I suggest that the barn owl's ears work as pressure receivers both in the high- and low-frequency ranges.*

4.1 Introduction

Barn owls are an exception to most birds in concerns of sensory processing. The American subspecies *pratincola* is middle-sized with a weight between 420 and 550 g. The head has a skull diameter of about 4 cm (Knudsen, 1981), much larger than in similar-sized birds such as the pigeon (Columbia livia) with a skull width of about 19 mm (Johnston, 1990). Moreover, the barn owls' ruff increases the effective head size to a diameter of 8 to 10 cm. The ruff serves as an acoustic amplifier and is the basis for the low hearing threshold in this bird (Coles and Guppy, 1988; Dyson et al., 1998).

The hearing range of barn owls lies between frequencies between about 200 Hz and 10 kHz (Dyson et al., 1998). This is much broader than the typical hearing range of other birds (Okanoya and Dooling, 1987). Konishi (1973b) demonstrated the importance of frequencies above 3 kHz for sound localization, as was recently confirmed by Singheiser et al. (2010) and what I also measured (section 6). So far, not much is known about the behavioral role of the low frequencies. In the following, the range from 3-10 kHz will be called the high-frequency range. By contrast, the range below 3 kHz will be referred to as low-frequency range. The frequency-specific influences of the head and body on sound signals may be determined as so-called head-related transfer functions (HRTFs) (for a review see Blauert, 1997). Keller

et al. (1998) were the first to provide a complete set of HRTFs for the barn owl. The main focus of their study was on the high-frequency range. These authors derived the monaural gains and the main sound-localization cues, the interaural time difference (ITD) and the interaural level difference (ILD) from the HRTFs.

The barn owl uses the ITD of a sound to compute the amplitude of azimuthal head turns (Moiseff and Konishi, 1981a; Poganiatz et al., 2001), while the ILD is an important cue for vertical sound localization (Egnor, 2001; Keller et al., 1998; Moiseff, 1989b,a; Poganiatz and Wagner, 2001). Campenhausen and Wagner(2006) demonstrated that an intact ruff increases ILDs and enlarges the maximum range of the ITD at high frequencies. However, the authors did not study the low-frequency range (<3 kHz) in enough detail. If the distributions of ITDs and ILDs in the low-frequency range were known, this would allow for a better understanding of their role in behavior.

Knowledge about the range of ITDs at the low frequencies could help to answer another question that has long been debated: do the ears of the barn owl function as pressure or as pressure-difference receivers? In a pressure receiver, the left and right ears work independently, because sound that enters, for example, the right ear is strongly attenuated within the skull so that its amplitude when reaching the left eardrum indirectly is insufficient to affect eardrum motion. Consequently, the motion of the left eardrum is only influenced by sounds entering the left ear directly and vice versa. In other words, the sound cannot travel between the two sides within the skull. Mammalian ears work as pressure receivers (for a review see Blauert, 1997).

By contrast, in pressure-difference receivers, motion of the eardrum on each side is influenced by sounds entering either ear, which may lead to directionally-sensitive interactions of the direct and indirect sounds at each tympanum. Crickets (Michelsen and Larsen, 2008; Weber et al., 1981), reptiles (Christensen-Daalsgard and Manley, 2005; Fay and Feng, 1987), and some birds (Calford, 1988; Larsen et al., 2006; Lewald, 1990) possess pressure-difference receivers. Although is has been claimed that barn owl ears may work as pressure-difference receives (Coles and Guppy, 1988), the available evidence clearly speaks against this principle because in the high-frequency range, the attenuation between the ears is too strong (Moiseff and Konishi, 1981b). The situation in the low-frequency range remained unclear so far.

Measuring HRTFs is not trivial, specifically in the low-frequency range, where the receiver characteristics of the ears may change. Larsen and coworkers (1997) showed that the directionality of the ears of small birds may be impaired during anesthesia, because the animals then stop venting the Eustachian tube. Consequently, outer and inner ear pressures are not equalized. The overpressure from the outer ear thus leads to a decreased motility respectively to an inwards-movement of the eardrum.

A similar effect could occur due to a decrease in temperature caused by anesthesia (Larsen et al., 1997), causing changes in atmospheric pressure which exceed the pressure variations that sound waves induce. In both cases, the hampered motility of the tympanum acts as a

high-pass filter, which should influence both the ITD and ILD ranges in the low-frequency range.

In this chapter of the thesis, I explored the question of whether the sound localization cues (ITD, ILD, monaural gain) in barn owls change in the low-frequency range compared to high frequencies, and whether body temperature has an effect on localization cues. For this purpose, I calculated the maximum ITD and ILD ranges as well as monaural gains from 1/3 octaveband-filtered head-related transfer functions (HRTFs) with center frequencies from 500 Hz to 9 kHz. Possible implications of the results are discussed in the context of research.

4.2 Methods

4.2.1 Animals and Handling for HRTF measurements

For this part of the thesis, HRTFs of 17 barn owls were analyzed. HRTFs from eleven out of these had been measured earlier (owls H, P, S, J, G, Isi, X, 19, M, U and V). Among these previously measured HRTFs were also those of owls H, S and P which were used for the later behavioral experiments. Anesthesia was done using Valium (1 mg/kg/h) and Ketamin (20 mg/kg/h). Salivation was prevented by administering Atropine sulfate (0.05 mg i.p.) at the beginning of the measurements. Details on the anesthesia and handling of the owls during HRTF recording were as described in Campenhausen and Wagner (2006). Care and treatment of the owls were in accordance with the guidelines for animal experiments as approved by the Landespräsidium für Natur, Umwelt und Verbraucherschutz Nordrhein-Westfalen, Recklinghausen, Germany, and complied with the NIH Guide for the use and care of laboratory animals. From eleven living owls, five were female (owls H, P, Z, Ind, J) and six were male (owls 14, G, Isi, Q, S, X). Data from four dead owls (owls 19, M, U, V) were already included in Campenhausen and Wagner (2006). Owls O and XM, used for the comparison of HRTFs under various conditions, were both male. The latter two owls were first anesthetized and then sacrificed in the course of the measurements.

4.2.2 HRTF measurements

The linear convolution of free-field sound input $x(t)$, filtering by the external ear, and output $y(t)$ at the eardrum is described in the time domain by the convolution integral

$$y(t) = \int_{-\infty}^{\infty} h_{\text{sys}}(\tau) \cdot x(t-\tau) d\tau \tag{1}$$

where $h_{sys}(t)$ is the impulse response of the system for a given time point t. The impulse responses (head-related impulse response, HRIR) can be transformed into the frequency domain via Fast Fourier transformation (FFT), which yields the head-related transfer function

$Y_0(f)$ of the system. If the Fourier transforms of two functions - in this case, $X(f)$ as the FFT of the sound input $x(f)$, and the HRTF $H(f)$ - are multiplied, then their product is equivalent to their convolution in the time domain:

$$Y(f) = H(f) \cdot X(f) \tag{2}$$

Analogously, convolution of two FFTs in the frequency domain corresponds to their multiplication in the time domain.

Hence, the HRTFs describe the filtering properties of the owl's ruff in the frequency domain, whereas HRIRs refer to the time domain. HRTF and HRIR can be easily transformed from one domain into the other. The signals were always recorded as HRIRs, transformed into the frequency domain for easier calculation and manipulation of stimulus parameters, and then transformed back into the time domain for their use in the behavioral experiments. For simplicity, I will use the term HRTF to refer to the transfer functions in both domains.

All experiments were performed in a sound-attenuating chamber (IAC 403A, Industrial Acoustics, Niederkrüchten, Germany). For measurement of the transfer function $Y_{\mathrm{owl+sys}}(f)$, the owls – either anesthetized or dead – were wrapped into a cloth jacket to prevent motion and support the animal's body. The head was attached to a thin metal rod with the help of a metal headholder that had been implanted into the owl's skull prior to the experiments. The metal rod was installed on the ground as a part of the setup framework and fixated the owl in a natural posture in the center of a moveable circular metal hoop with 90 cm radius.

A loudspeaker (MacAudio ML-103E) was mounted on the hoop (Fig. 1). The distance between the speaker and the owl's head was 90 cm. By rotating the hoop along its vertical axis, the loudspeaker could be moved to azimuthal values of -160° azimuth (left hemifield) to +160° azimuth (right hemifield) with 0° azimuth and 0° elevation directly in front of the owl. The loudspeaker could also be moved along the hoop from -70° elevation (lower hemisphere) to +60° elevation (upper hemisphere) with 0° elevation in front of the owl as demonstrated in Fig. 1B+C. Throughout this thesis, azimuthal and elevational stimulus angles and the corresponding localization cues were plotted into a two-dimensional Cartesian coordinate system.

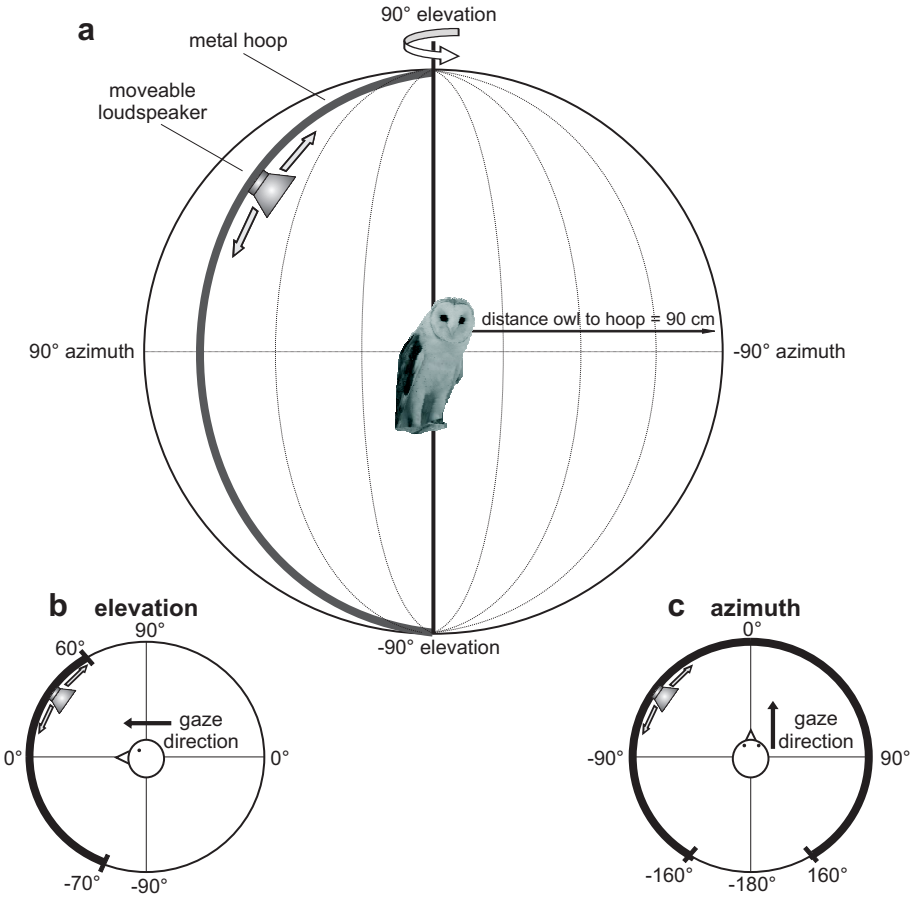

Figure 1: Schematic of the setup for HRTF measurements

A) During HRTF measurements, the anesthetized owl was fixated with the help of a jacket in the center of a metal hoop. A loudspeaker could be moved upwards or downwards along the hoop, allowing variation of the vertical stimulus angle from -70° (lower hemisphere) to 60° (upper hemisphere) as shown in panel B). The hoop could be rotated along its vertical axis, which allowed positioning of the hoop at azimuthal values from -160° (left to the owl in the rear hemisphere) to 160° (right to the owl in the rear hemisphere), with 0° being directly in front of the owl as shown in panel C).

During the measurements, probe tubes (Sennheiser KE4 211-2 microphones) were inserted 15 mm inside the right and left ear canals, respectively, i.e. about 2 mm in front of the eardrum. This is adequate to measure the sound pressure at the eardrum (Keller et al., 1998). HRIRs were recorded by playing a sweep signal (logarithmically rising from 20 Hz to 16 kHz within 500 ms, see Fig. 3) five times from the loudspeaker, recording the resulting signals close to the eardrum and averaging the five repetitions. The recorded signals were amplified, filtered (20 kHz cutoff frequency, 60 dB roll-off within 3 kHz) and recorded for 510 ms after stimulus onset. The spatial resolution was at least 20°. A finer spatial resolution was achieved by interpolation.

The utilized hardware components influenced the recorded HRTFs because they have specific transfer functions themselves, which are confounded with the measured impulse responses. In other words, the transfer function $Y_{\text{owl+sys}}(f)$ can in the first place only be measured for the system as a whole, containing all hardware components used for stimulus presentation (such as the amplifier, loudspeaker etc with their transfer function $X_{\text{sys}}(f)$ and the microphones with the transfer function $T_{\text{sys}}(f)$) as well as the owl's external ear with its directionally specific transfer function $H_{\alpha\varepsilon}(f)$, depending on stimulus azimuth α and stimulus elevation ε.

Contortion of the HRTF recordings can be excluded by measuring the transfer function $Y_{\text{sys}}(f)$ of the hardware components as a reference and divide the recorded transfer functions $Y_{\text{owl+sys}}(f)$ by this reference measurement (eq. 3).

The reference measurement $Y_{\text{sys}}(f)$ measured with the microphones only contain all the hardware components of the sound delivery system as well, but are conducted without the owl. Only the microphones were placed in the center of the hoop at a position corresponding to the position of the owl's ears, the sweep signal was played five times and the resulting signals were recorded. Since the transfer properties of the owl's external ear lack in this measurement, the direction-dependent HRTF of the owl, $H_{\alpha\varepsilon}(f)$, can be gained by dividing both transfer functions:

$$H_{\alpha\varepsilon}(f) = \frac{Y_{\text{owl+sys}}(f)}{Y_{\text{sys}}(f)} = \frac{H_{\alpha\varepsilon}(f) \cdot X(f) \cdot T_{\text{sys}}(f)}{X(f) \cdot T_{\text{sys}}(f)} \tag{3}$$

Thereby, the HRIRs recorded at the owl's eardrum were corrected for the influence of the microphone and hardware components by transforming the HRIRs into the frequency domain, and dividing the FFT for each spatial position by that of the reference measurement. When the signal was transformed back into the time domain, it was bandpass filtered from 300 Hz to 12 kHz to reduce noise.

4.2.3 Calculation of 1/3 octaveband-filtered HRTFs

For the analysis in narrow frequency bands, the owls' HRTFs were passband-filtered with 1/3 octaveband filters (Fig. 2). Such octaveband filters correspond to the filter properties of the cochlea, where the "critical filter width", below which adjacent frequencies cannot be resolved, approximates 1/3 octaveband (Quine and Konishi, 1974). The same holds for humans(Fletcher, 1940). On a linear scale, the bandwidth of the octaveband filters increases with increasing frequency (see Fig. 3A), whereas on a logarithmic scale, the width remains constant (see Figs. 2 and 3B). This is due to the overrepresentation of high frequencies on the cochlea. The use of linear filters with constant bandwidth across frequencies instead of octaveband filters would either allow for an integration across several frequency channels at higher frequencies, because each passband filter would then exceed the critical bandwidth for cochlear frequency resolution, or the energy contained at low frequencies would be too low.

For the analysis of HRTF properties as well as for the later calculation of stimuli for behavioral experiments, a series of 1/3 octaveband filters was calculated using the MatLab (MathWorks) function oct3dsgn. Filter calculation was based on a 3rd order butterworth filter according to the Order-N specification of the AISI S.1.-1986 standard[1]. Each octaveband filter was centered at a specific center frequency, from 1 kHz to 9 kHz in steps of 1 kHz. Above and below the respective center frequency, the amplitude of the filtered signal decreased as defined by the width of the octaveband filter (Fig. 2). With each doubling of the frequency (= one octave), the amplitude of the input signal was decreased by 50 dB. Exemplary, the upper and lower cutoff frequencies at which the signal's amplitude reached a certain attenuation in dB are provided for each 1/3 octaveband filter in Table 11 in the appendix.

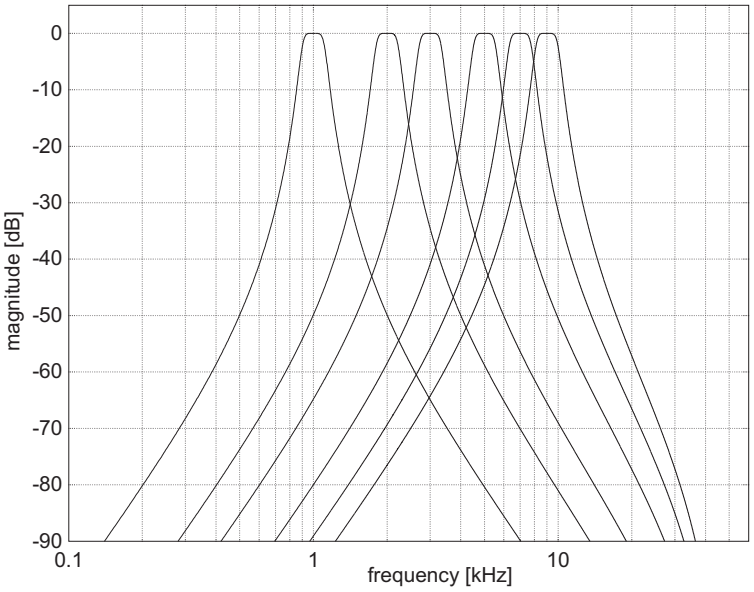

Figure 2: 1/3 octaveband filters
For center frequencies from 1 kHz to 9 kHz, a series of 3rd order butterworth 1/3 octaveband filters were calculated, with which the signal for each spatial direction was filtered. The filters attenuated signals by 50 dB per octave. The x-axis shows the center frequency in kHz, the y-axis denotes the relative amplitude in dB.

After 1/3 octaveband filtering, only the localization cues in that frequency band remained, whereas the energy in other frequency bands was strongly attenuated (Fig. 2). Octaveband-

[1] ASA 65-1986: Specifications for Octave-Band and Fractional-Octave-Band Analog and Digital Filters, 1993

filtered HRTFs still contain all naturally occurring localization cues, but the narrow bandwidth prevents integration across large frequency bands. Thus, the bandwidth of such HRTFs exceeds that of pure tones, but falls below that of broadband HRTFs.

4.2.4 Calculation of ITD and ILD ranges and monaural gains

The distributions of physical parameters like ITDs, ILDs and monaural gains were analyzed. The minimum (i.e., the sound is maximally leading at the left ear) and maximum (i.e., the sound is maximally leading at the right ear) ITDs were calculated by cross-correlating the impulse responses in 1/3-octaveband-filtered HRTFs after these were corrected for the influence of the microphones and hardware components by division of the corresponding Fast Fourier Transforms (for details see von Campenhausen and Wagner, 2006). The range of ITDs as the difference between minimum and maximum ITDs (in µs) will be called ITD span in the following.

ILDs were calculated as the average binaural level difference in dB for each 1/3-octaveband relative to the reference measurement. The ILD span was being defined as the difference between the most negative (left ear louder) to the most positive (right ear louder) ILD within each 1/3-octaveband.

Monaural gains were the relative enhancement or damping, respectively, of incoming sound. The area of 3 dB gain (cf. Figs. 4+7, gray shaded) includes spatial positions at which the gain was within 3 dB of the maximum gain, providing a measure of directionality as defined in Campenhausen and Wagner (2006). The range, or span, of monaural gains was the difference between the maximum gain, i.e. maximum enhancement, and the minimum gain, i.e. maximum damping.

Unless noted otherwise, a two-tailed t-test was used for statistical comparison of two samples. We tested if data samples came from a Gaussian distribution using a Kolmogorov-Smirnov test with Dallal-Wilkinson-Lillie for P value. A Pearson correlation test was used for correlation analysis if the data were normally distributed, and a Spearman correlation test if not.

4.3 Results

For this part of the thesis, I analyzed head-related transfer functions of 17 American barn owls (*Tyto alba pratincola*). Out of these, eleven animals were alive and anesthetized (see Methods) during HRTF recordings, four were dead, while two owls (O and XM) were first anesthetized and then dead. The four dead animals had been deep-frozen and were unfrozen for the measurements. Owls O and XM were tested either with temperature controlling or without. Data from these two owls are presented in a separate section.

4.3.1 Qualitative description of low-frequency HRTFs

I calculated 1/3 octaveband-filtered HRTFs in the low-frequency range with center frequencies of 500, 600, 750, 900, 1000, 1250, 1500 and 1750 Hz, as well as from 2 kHz to 9 kHz in steps of 1 kHz. Frequencies below 500 Hz were not considered because the quality of the signal used for HRTF recordings was poor for lower frequencies (Fig. 3). Figure 3 also shows that the width of the octaveband filters is constant across frequencies on a logarithmic scale (Fig. 3A), corresponding to the logarithmic representation of frequencies on the cochlea, but that on a linear scale, the filter width increases with increasing frequency (Fig. 3B). The change in the sweep's frequency content over time is also shown in Fig. 3C in a color-code, with red indicating high energy and blue indicating low energy.

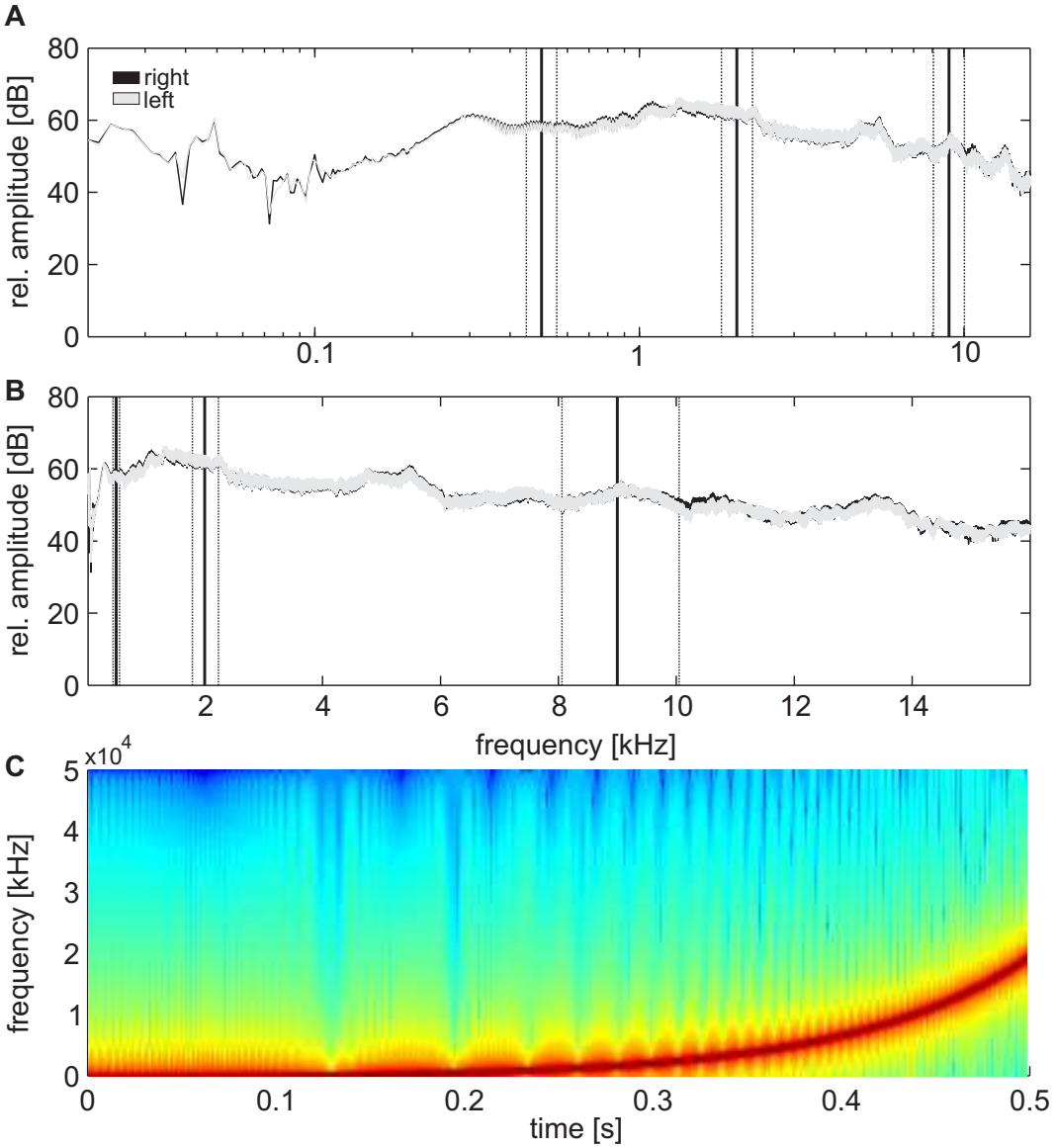

Figure 3: Signal quality for HRTF recording

Stimulation for HRTF recordings was with a logarithmically rising sound sweep running from 200 Hz to 16 kHz within 500 ms. The signal was recorded approximately 2 mm in front of the owl's eardrums via microphone tubes and is shown for the left (gray) and right (black) ear, respectively. Y-axis is in dB, x-axis depicts the frequency in Hz. The signal below about 500 Hz was less regular than at higher frequencies and, therefore, this range was not considered for calculation of 1/3 octaveband filters. Vertical black lines show the position of a 1/3 octaveband filter at 500, 2000 and 9000 Hz centre frequency with minimum and maximum borders (dotted lines) on a **A**) logarithmic scale and **B**) a linear scale. **C**) shows the color-coded frequency spectrum of the signal with high energy in red and low energy in blue.

The distributions of physical cues (ITDs, ILDs and monaural gains) exhibited frequency-specific characteristics as described in the following. For all frequencies, ITDs increased monotonically with increasing azimuthal angle in the frontal hemisphere (Fig. 4, left column) up to a maximum at about 90° to 110°, depending on the frequency. The spatial positions at which ITDs were maximal (i.e., the sound is leading maximally at the right ear) and minimal (i.e., the sound is lagging maximally at the right ear) shifted respectively towards the periphery with increasing frequencies (Fig. 4, left column).

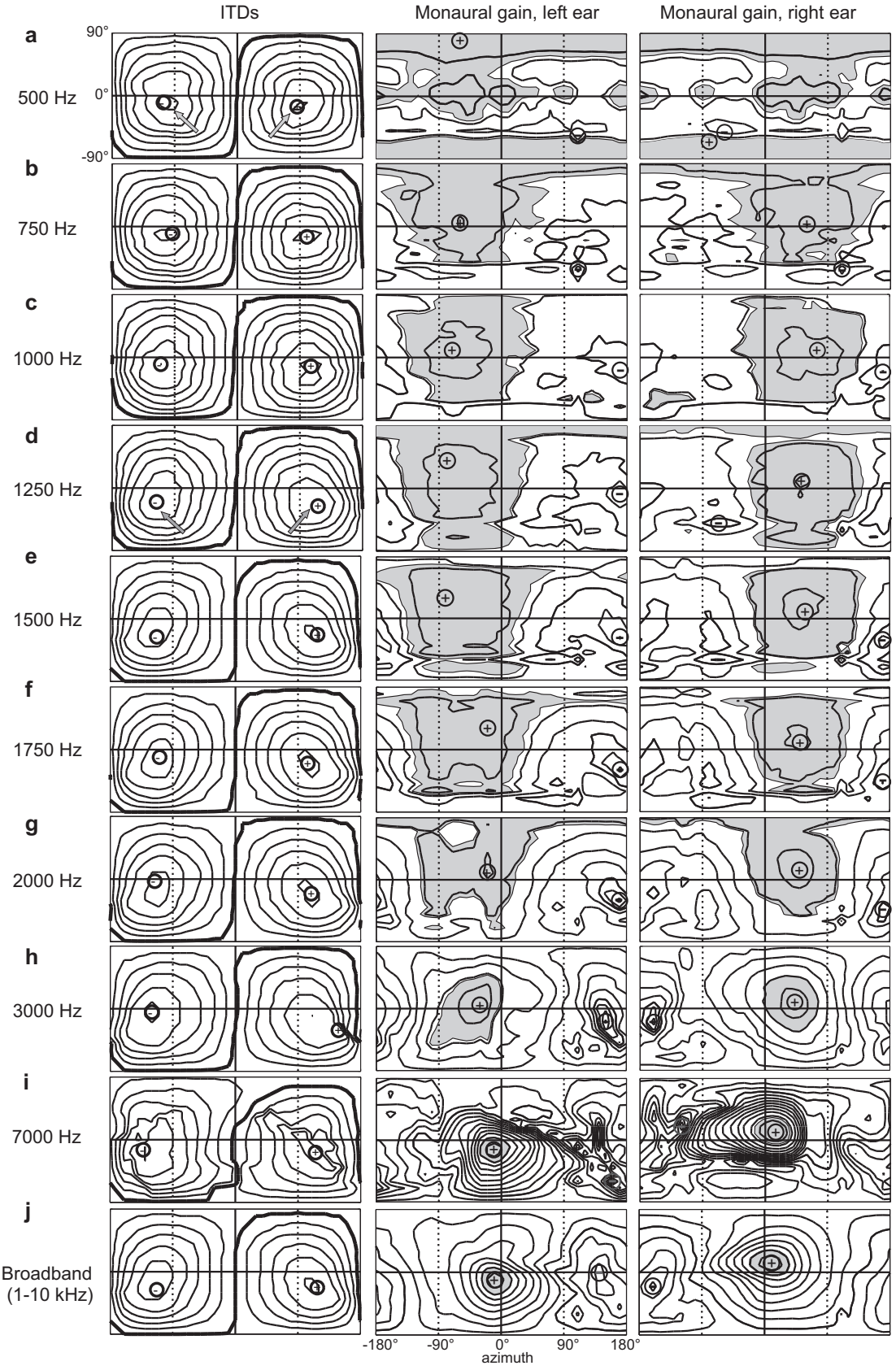

Figure 4: Frequency-dependent changes of ITDs, ILDs and monaural gains

One-third octaveband-filtered HRTFs are shown for owl H for increasing center frequencies (top to bottom) as denoted on the left side of each row. Left column: Black lines show positions along which the ITD is constant (iso-ITD lines). Stepsize is 50 µs. Bold black lines represent 0 µs ITD. The horizontal and vertical axes denote the azimuthal and elevational stimulation angles, respectively. Spatial positions at which minimum and maximum ITDs occur shift from about ±95° azimuth at low frequencies towards the periphery (±110° azimuth) at higher frequencies (see gray arrows, left column; cf. Fig. 9). Middle and right columns: As for the ITDs, the directionality of the monaural gains is shown for the left and right ears, respectively. Iso-gain lines (analogous to the iso-ITD lines) are drawn with a spacing of 2 dB. In the gray shaded areas, the monaural gain is within 3 dB of the ear's maximal gain as defined in von Campenhausen and Wagner (2006). The size of this 3 dB-area decreases with increasing frequency for both ears, hence the directionality increases.

At center frequencies of 500 Hz (Fig. 4A, gray arrows) and of 750 Hz (Fig. 4B) the extrema were close to the 90° of azimuth, corresponding to the situation in humans. At higher frequencies, however, the extrema started to shift towards about ±110° (Fig. 4D, gray arrows) as in the broadband ITD distribution (Fig. 4I). The extrema were located near 90° at 500 Hz center frequency and started to shift towards 110° of azimuth for frequencies between 600 Hz to 1 kHz (Fig. 5). Between 1 and 2 kHz, extrema remained at about 110° azimuth, whereas extrema lay at about 130° between 3 and 4 kHz. At higher frequencies, between 5 and 9 kHz, the extrema no longer shifted towards the periphery, but their azimuthal position decreased again towards a relatively stable location at approximately 110° (Fig. 5).

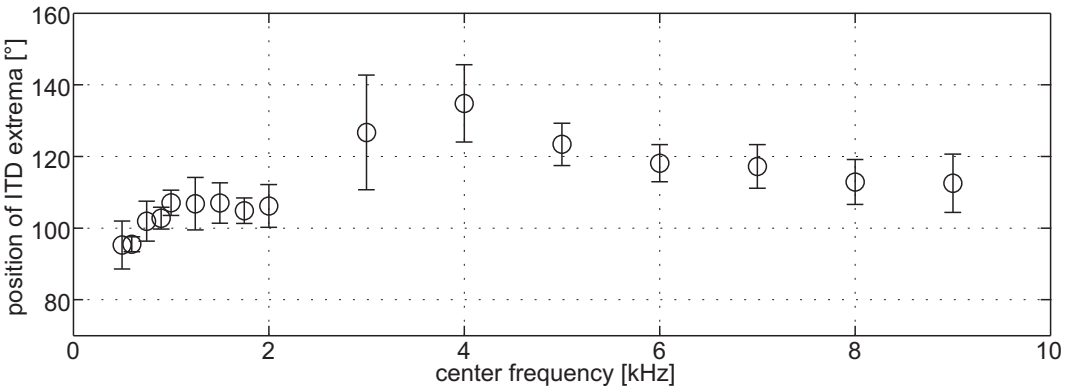

Figure 5: Shift of ITD maxima with frequency
With increasing frequency, the ITD maximum and minimum, respectively, shifted from about ±95° at 500 Hz center frequency towards about ±110° azimuth for 1 kHz, then were located at about ±130° azimuth between 3 and 4 kHz and finally ended in a plateau at about ±110° at frequencies >4 kHz.

The distribution of ILDs was as shown and described in detail in Campenhausen and Wagner (2006) or Keller et al. (1998), with an almost exclusive increase of ILDs with azimuth, but not with elevation at low frequencies, and strong elevational changes of the ILD at high frequencies (cf. Fig. 9, middle left column).

Examples of ILD distributions are shown in Fig. 9 (middle left column) for owl XM, and also in Fig. 27 for owls H, S and P. The respective monaural gains for the left and right ears increased slowly with frequencies below 3 kHz (Fig. 4, middle and right columns). For frequencies >2 kHz, the directivity gradually approximated the spatial pattern also present at broadband sounds (Fig. 4J), meaning that the position of minimum and maximum monaural gains shifted towards the central auditory space and their spatial distribution changed from a more diffuse pattern at low frequencies (Fig. 4A) towards a sharply circumscribed maximum at higher frequencies (Fig. 4I).

4.3.2 Quantitative analysis of sound localization cues

This analysis was based on HRTFs of 15 owls, excluding owls O and XM, whose data are presented in a separate section for a detailed analysis of the influence of body temperature on HRTF characteristics.

ITD span

The change of the ITD span with frequency was similar in all owls, whether dead or alive during HRTF recording. In the 11 anesthetized owls, the mean ITD span was 586 ± 24 µs (mean ± SD) or 14 µs larger than in the four dead owls with 572 ± 24 µs. Since the difference was not significant (Mann-Whitney test, $p = 0.2828$), data from all owls were pooled for further analysis. The ITD range at higher center frequencies (5-9 kHz) was 600 ± 7 µs (mean ± SD) and dispersions were not significantly different between frequencies (one-way ANOVA, $p > 0.05$, Fig. 6A).

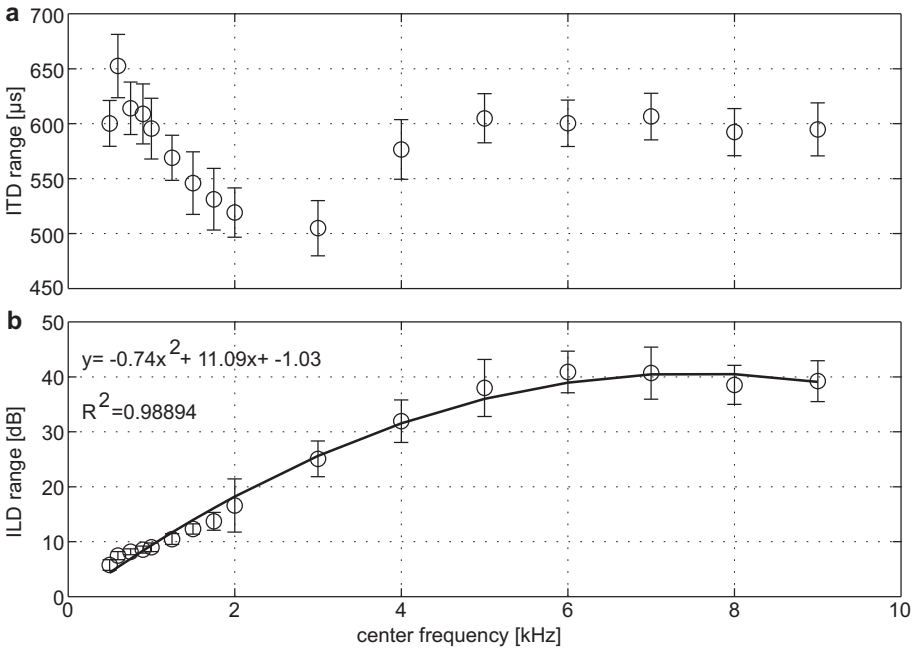

Figure 6: Frequency-specific ITD and ILD ranges in barn owl HRTFs

A) The mean ITD span was about 600 µs for frequencies ≤1 kHz as well as for centre frequencies ≥5 kHz. Between 2 and 4 kHz, the ITD span decreased to a minimum of 505 µs at 3 kHz. **B**) The mean ILD span (in dB) increased with increasing center frequency from about 6 dB at 500 Hz to about 40 dB at frequencies ≥7 kHz. This increase was well described by a polynomial fit ($y = -0.74x^2 + 11.09x - 1.03$, goodness of fit: $R^2 = 0.9889$).

Below a center frequency of 5 kHz, the ITD span started to decrease. It reached a value of 576 ± 27 µs at a center frequency of 4 kHz. The minimum ITD span occurred at a center frequency of 3 kHz, where it was 505 ± 25 µs (mean ± SD). For frequencies below 3 kHz, the ITD span increased again, and reached a maximum of 652 ± 28 µs (mean ± SD) at a center frequency of 600 Hz. The mean value of the 5 data points taken at frequencies below 1 kHz was 614 ± 26 µs (mean ± SD). When the ITD ranges of 500 Hz to 1 kHz centre frequency were compared to those at 5-9 kHz, no significant difference was revealed with a Wilcoxon

matched pairs test ($p = 0.1875$). Thus, no increase in the ITD span in the low-frequency range was observed.

ILD span

The ILD span increased monotonically from about 6 dB at 500 Hz center frequency to a saturation value of about 40 dB at 6 kHz (Fig. 6B). The contribution of left and right ears, respectively, to the ILD span (i.e. the absolute values of negative and positive ILDs) was not significantly different (Wilcoxon matched pairs test, $p = 0.8092$). Differences between living and dead owls were not significant ($p = 0.3589$), hence the data from all owls were pooled.

The relationship between ILD range and frequency was well approximated by a polynomial fit ($y = -0.74x^2 + 11.09x - 1.03$, goodness of fit: $R^2 = 0.9889$, Fig. 6B), meaning that, relatively, the ILD span increased more strongly in the low-frequency range than at higher center frequencies. At frequencies $\geq$5 kHz, ILDs reached a plateau where they did no longer rose, thus the increase of ILDs with growing center frequency would probably be more accurately described by a saturation fit. However, since the barn owl's hearing range is limited to 10 kHz (Dyson et al., 1998) and since I only analyzed HRTFs up to 9 kHz center frequency, a proper evaluation of how ILDs change with even higher frequencies was impossible. Therefore, I chose a polynomial approximation.

Monaural gains

With increasing frequency, the monaural directionality in terms of maximum positive gain (i.e., enhancement of incoming sound in dB) increased. The maximum monaural gains for left and right ears started at 2.12 $\pm$ 1.07 dB (mean $\pm$ SD) at 0.5 kHz and increased to 19.04 $\pm$ 2.84 dB at 9 kHz (Fig. 7A). The dependence of monaural gains on center frequency was well fitted by polynomial functions for both ears (left: $y = -0.27x^2 + 4.45x + 0.75$, goodness of fit: $R^2 = 0.94088$; right: $y = -0.29x^2 + 4.69x + 0.6$, $R^2 = 0.96949$). As for the ILDs, maximum monaural gains seemed to reach saturation at a value of about 20 dB for each ear.

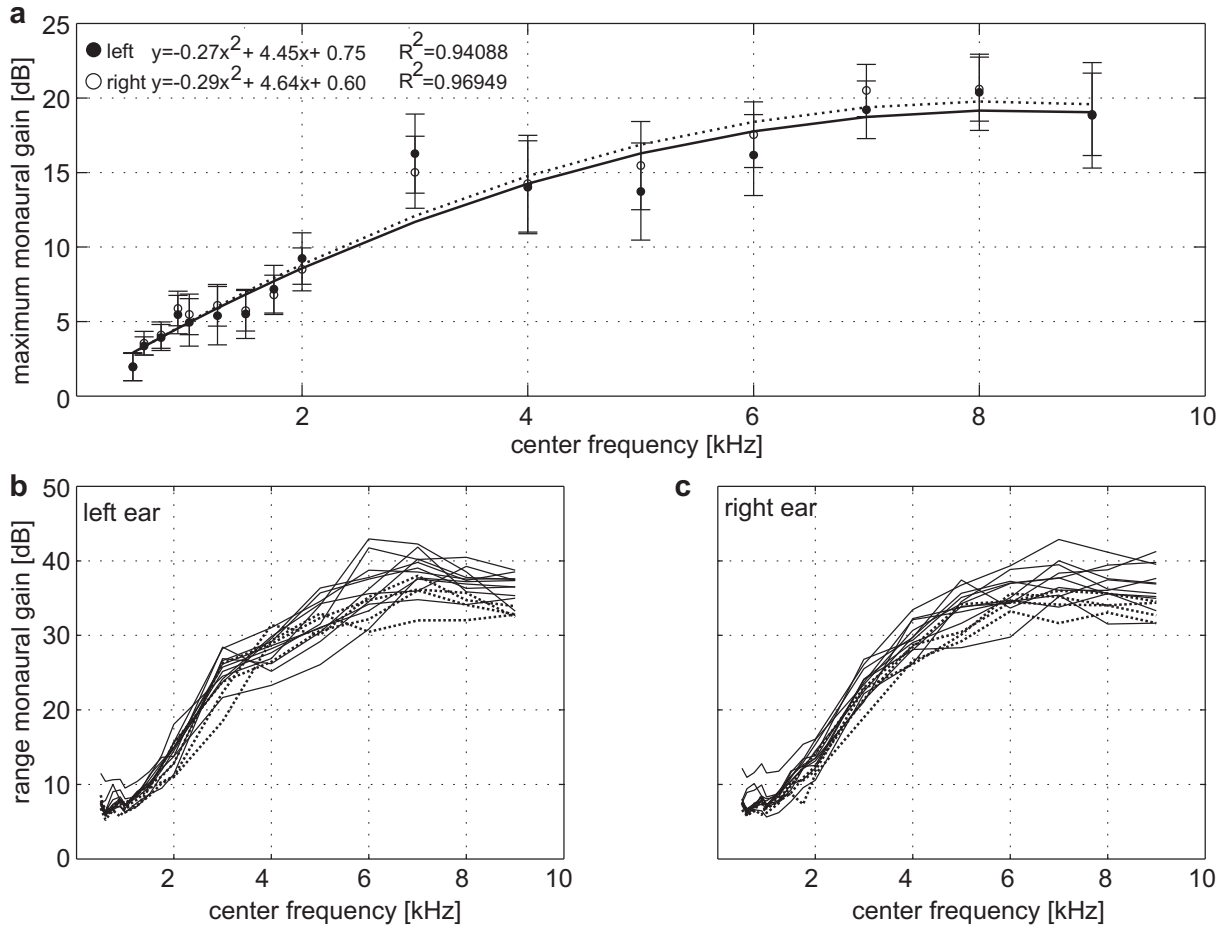

Figure 7: Frequency-specific monaural gains

A) The range of monaural gain for left and right ears, respectively (in dB, mean ± SD of pooled data from all owls) increased from about 7 dB at 0.5 kHz up to about 36 dB at 7 kHz where it ended in a plateau. There were no significant differences between the monaural gain of left and right ears, respectively. **B**+**C**) Monaural gains as in A) are plotted for both ears against center frequency in kHz for living owls (continuous lines) and dead owls (dotted lines) individually. Gains increased from 7 dB at 500 Hz to about 36 dB at 9 kHz.

The maximum gains for left and right ears, respectively, were not significantly different from each other (Wilcoxon matched pairs test, $p = 0.2009$, Fig. 7A). The same held for the range of monaural gains (Wilcoxon matched pairs test, $p = 0.8463$, Fig. 7B+C). Similarly, the size of the area of 3 dB gain (gray shaded in Fig. 4, center and right columns for the left and right ear, respectively) decreased gradually with increasing frequency and approximated the broadband situation for a frequency of 7 kHz (Fig. 4J, middle and right columns).

Furthermore, the spatial position at which monaural gains were maximal shifted towards the frontal auditory space, with the maximum for the left ear being located slightly below and the maximum for the right ear being located slightly above the horizontal midline. Thus, not only are the monaural gains and therefore the directionality of the ear enhanced at higher frequencies, but also the position of maximum gain shifts more and more towards the central auditory space close to the midline (Figs. 4 and 9, right columns).

4.3.3 Effect of body temperature on HRTFs

The body temperature has been implicated in having an effect on physical cues to sound location (Larsen et al., 1997). To test the influence of body temperature on ITD, ILD and monaural gains in barn owls, I measured HRTFs at 20° resolution of two anesthetized owls under various conditions while recording the body temperature. Room temperature in the experimental chamber was constant within 0.7°C over a course of 10 hours. The owl was wrapped into a heater blanket. A rectal sensor measured body temperature and kept it constant. In owl O, body temperature increased from initially 38.1°C directly after the initiation of anesthesia to 38.6 °C after 90 minutes (Fig. 8A).

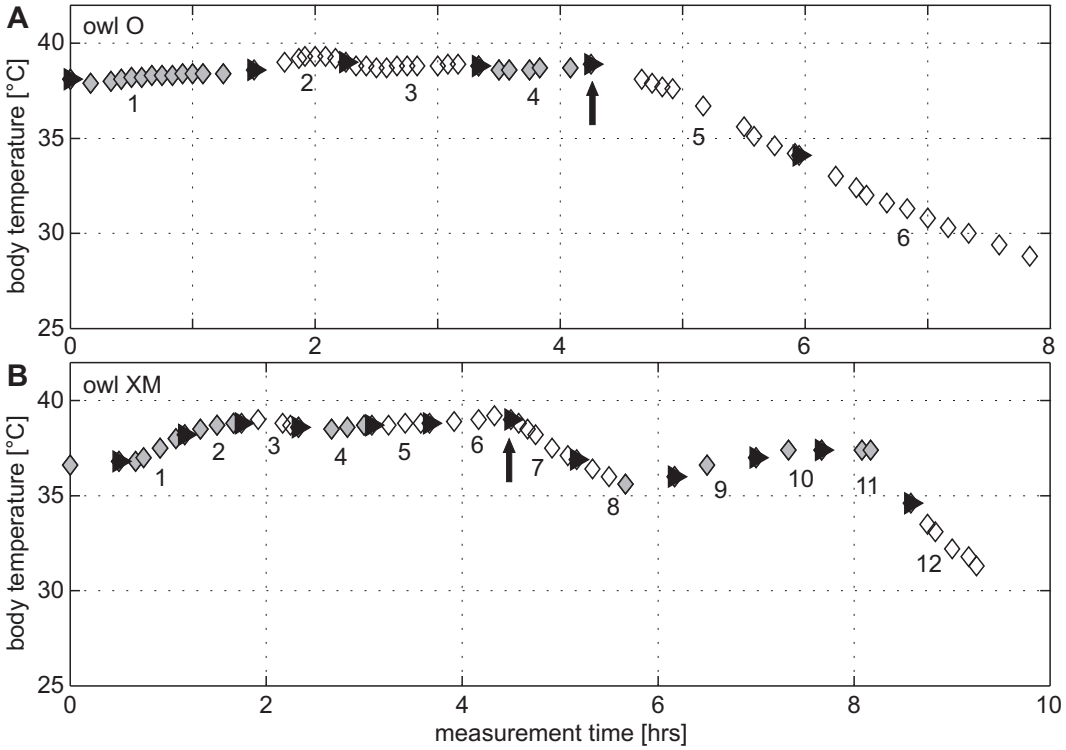

Figure 8: Body temperature in owls O and XM during HRTF measurements

Temperature in °C is plotted as a function of recording time for owl O (**A**) and owl XM (**B**). Posture and anesthesia were identical to other HRTF measurement experiments. Black triangles mark the onset of a new HRTF measurement (gray diamonds: heater on, white diamonds: heater off). The body temperature did not decrease when the owl was not heated compared to the situation with heater as long as the animal was alive. The black arrow in each panel marks the time point at which the owl was killed. Numbers below each measurement denote the number of measurement for better identification.

A similar effect was seen in owl XM. In this bird, body temperature increased from 36.6 °C to 38.8 °C 105 minutes after the initiation of the anesthesia (Fig. 8B). The heater was then switched off. Owl O immediately regulated its body temperature up to about 39.2 °C, where it remained stable over the next two hours. In owl XM, the temperature varied between 38.6 and 38.9 °C. When the heater blanket was switched on again, using the last measured temperature as the new regulation temperature, body temperature settled down between 38.5 to 38.9 °C in both owls.

After several further measurements of body temperature (see Fig. 8), the owl was killed, and HRTFs were measured again while the body cooled down. The heater was turned off in

owl O right away, and body temperature decreased to 28.8 °C within 3 hours. By contrast, in owl XM the heater was off for the first two HRTF measurements after the owl was killed. The body temperature dropped from 39.0 °C to 35.6 °C during this period. Then the heater was turned on for the next two measurements. During this time, body temperature increased from 35.6 to 37.4°C. After switching off the heater again, body temperature decreased to 31.3 °C within one hour.

The ITD patterns in owl XM (Fig. 9, left column) were similar when the owl was living and when it was dead. This held true for both low frequencies (compare Fig. 9A to B, left column) and high frequencies (compare Fig. 9C to D, left column). Equivalent observations were made for the ILD patterns (second column from the left).

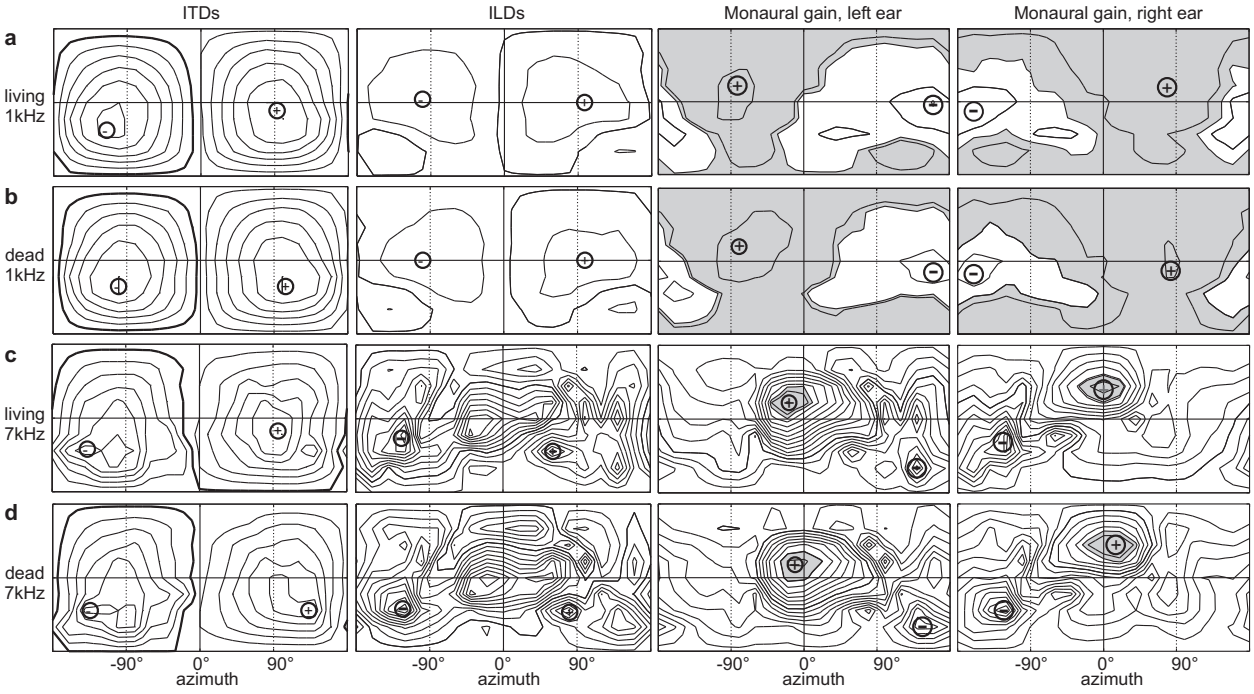

Figure 9: Frequency-specific HRTFs of owl XM

HRTFs of owl XM are shown for a low frequency (1 kHz, **A**+**B**) and a high frequency (7 kHz, **C**+**D**) analogous to Fig. 4. The owl was alive during the measurements shown in A and C, whereas it was dead during the measurements shown in B and D. Mean body temperature, based on all temperature samples taken during the corresponding HRTF measurement (cf. Fig. 8), for the living owl was 38.55 ± 0.26 °C (measurement 2 in Fig. 8B), and 32.75 ± 1.22 °C for the dead owl (measurement 12 in Fig. 8B). The left column shows the ITDs, each line representing 50 µs (bold line represents 0 µs ITD). The distributional patterns of ILDs (second column from the left, each line represents 2 dB) and monaural gains (third column from the left: left ear, right most column: right ear) did not differ between dead and living owl.

The amplitude of ITDs and ILDs of owls O and XM fell within the range of the other owls whose HRTFs we analyzed (one-way ANOVA, ITDs: $p = 0.3520$, 17 cases, ILDs: $p = 0.9118$, 17 cases). ITDs for individual center frequencies did not differ between the two owls O and XM (owl O: 567.95 ± 36.19 µs (mean ± SD), owl XM: 565 ± 17 µs, Mann-Whitney test, $p = 0.6923$), so data from both owls were pooled. None of the treatments (alive or dead, with heater or without heater) had a significant influence on the ITD ranges (Fig. 10A, one-way ANOVA, $p \geq 0.0955$).

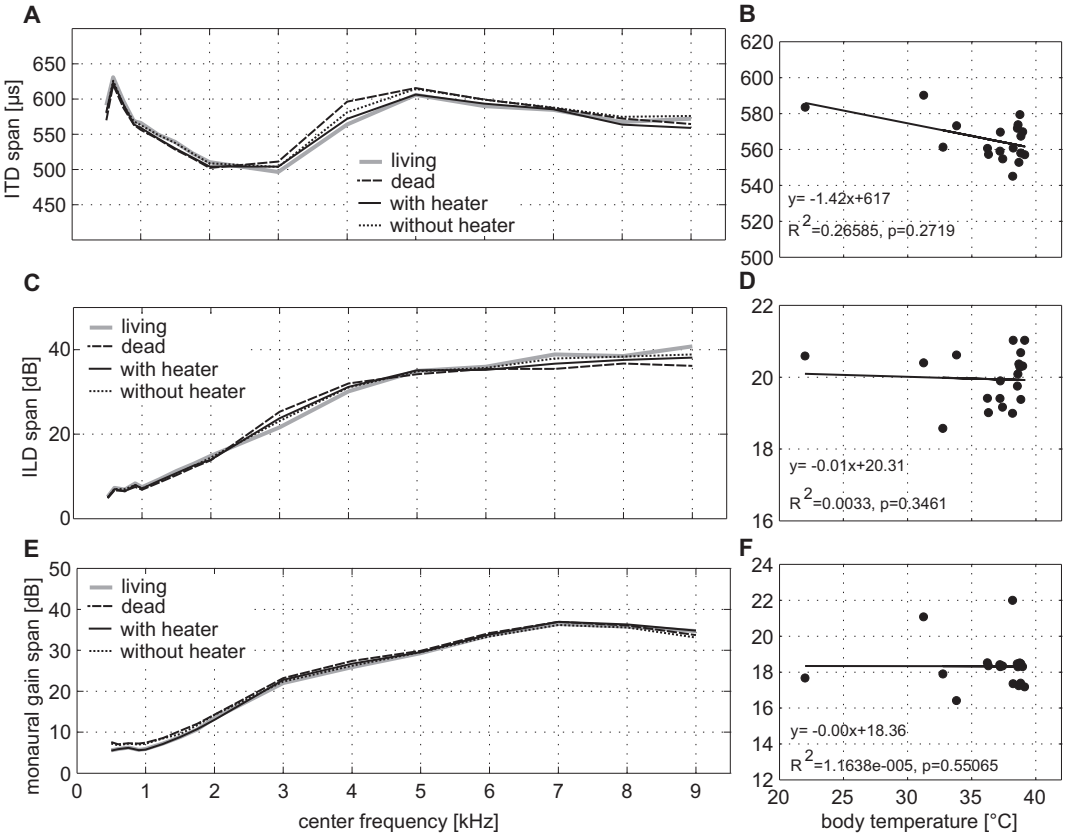

Figure 10: Influence of body temperature on ITDs, ILDs and monaural gains

A) The ranges of ITD, **B**) ILD or **C**) monaural gain (mean for left and right ears) did not significantly change for measurements with the living or dead owls O and XM, or whether the heater was on or off, respectively (one-way ANOVA, p>0.05). The lines show the mean ranges (black: living owls, gray: dead owls, dotted: with heater, dashed: without heater). **D**) ITD spans, **E**) ILD spans and **F**) monaural gains were tested for correlation with the mean body temperature in °C, but no significant correlation was observed for any of the parameters (Spearman correlation test, p = 0.2719). Slopes of a linear regression and goodness of fit (R^2) were low.

Furthermore, ITD spans were not correlated with the mean body temperature determined in the respective measurement, even though a trend towards a decrease in ITDs with increasing temperature was visible (y = -1.42x + 617, goodness of fit: R^2= 0.26585, Spearman correlation test: p = 0.2719, Fig. 10B).

ILDs spans were also alike between the two owls (owl O: 20.67 ± 14.50 dB, owl XM: 19.52 ± 13.03 dB, paired t-test, p = 0.07, Fig. 10C). When ILD ranges were compared for each individual center frequency, no significant differences were found for either condition (Fig. 10C). A linear regression (y = -0.0101x + 20.314, R^2= 0.0033, p = 0.3461) showed no correlation with the body temperature during the respective measurement (Fig. 10D).

Monaural gains were not different between measurements with the living and dead owl for both animals, neither concerning the distribution of monaural gains (see Fig. 7, third (left ear) and fourth (right ear) columns from the left) nor the range (one-way ANOVA, p = 0.05, Fig. 10F). As for ITDs and ILDs, monaural gains of owls O and XM were not different from the other owls (one-way ANOVA, p = 0.9078). To test whether the body temperature correlated with changes in the monaural gains, these were plotted against the mean temperature during the corresponding measurement. Again, the correlation was not significant (y = -0.0011x + 18.36, p = 0.55065).

4.4 Discussion

I analyzed HRTFs in 17 owls under varying conditions for the distribution and ranges of ITDs, ILDs and monaural gains. I did not observe a marked change in ITD span when low and high frequencies were compared. The different conditions of the owls did not have an influence on the localization cues. I will first set our findings into the context of earlier studies, then discuss their relevance for the question of whether the barn owl's ear functions as a pressure or a pressure-difference receiver, before we speculate about the functional role of the low frequencies.

4.4.1 Distribution of localization cues

Wit a barn owl's skull size of 4 cm, it is surprising to measure an ITD span as large as 600 µs. Several studies with barn owls have reported similar values, if the relationship between ITD and azimuth is used for comparison (Brainard et al., 1992; Keller et al., 1998; Moiseff and Konishi, 1981a). The ITD span reduced to about 440 µs after all head feathers were removed (von Campenhausen and Wagner, 2006).

The simple calculation with a head width of 4 cm and a sound velocity of 340 m/s results in an ITD span of only ±120 µs. This shows that sound propagation around the barn owl's head is complex, and that the ITD span is larger than predicted by the physical separation of the ears. A similar observation has been made in chickens (Hyson et al., 1994) and in the budgerigar (Larsen et al., 2006). The data from the chicken (Hyson et al., 1994) would suggest that the ITD span should increase by a factor of 2 for low frequencies, as is the case in many bird species such as kestrel, zebra finch, quail or grass owl (Calford and Piddington, 1988). This was not observed in the barn owl. Instead, the ITD range was just 2.5 % larger in the barn owl for frequencies below 1 kHz than it was for high frequencies (5-9 kHz).

The increase of the ILD span and of the monaural gains with increasing frequencies were as expected from other animals (birds: Calford, 1988; Larsen et al., 2006; Lewald, 1990, cat: Tollin and Koka, 2009, guinea pig: Sterbing et al., 2003, rhesus monkey: Spezio et al., 2000) and as has been observed by others in the barn owl (Brainard et al., 1992; Coles and Guppy, 1988; Keller et al., 1998). Both the ILD span and the span of monaural gains were small for low frequencies, and their spatial changes were sparse. This means that neither monaural spectral cues nor ILDs are useful for sound localization in the low-frequency range.

4.4.2 Properties of pressure difference receivers

The morphology of the avian skull and Eustachian tube suggested that internal transmission of sound form the left to the right ear was possible (Wada, 1924). This was later confirmed physiologically in several avian species (Hill et al., 1980; Rosowski and Saunders, 1980; Lewald, 1990; Schwartzkopff, 1952, for a review see Klump, 2000).

On the other hand, Moiseff and Konishi (1981b) showed that the interaural pathway of the barn owl is not involved in sound localization, since it attenuated high-frequency sound too strongly. Calford and Piddington (1988) demonstrated that the interaural canal enhances the interaural delay. Delays measured at high frequencies were close to those expected from the path length around the head, but delays measured at low frequencies could be up to three times this expectation. The predictions were based on a model of the function of the interaural canal (Calford, 1988).

Since, in the barn owl's inferior colliculus, neurons were found having maxima in the response-vs-ITD function far outside of the physiological ITD range as determined with broadband stimuli (Vonderschen and Wagner, 2009; Wagner et al., 2007), it was interesting to test whether in the barn owl, the ITD span for frequencies below 1 kHz would increase well beyond the ITD span measured for high frequencies. This was not the case, which provides indirect evidence that the barn owls' ears do not function as pressure-difference receivers even at low frequencies.

However, this conclusion has to be considered with reservation, because the ITD was not derived from measurements of the eardrum motion directly or via cochlear microphonics, but just from the pressure in the external ear close to the tympanum. Keller et al. (1998) found that this measurement location faithfully reflects the pressure at the eardrum. Nevertheless, direct measurements of eardrum motion would be useful.

The threshold to evoke cochlear microphonics (CM) in the barn owl has shown to be insensitive to frequency changes up to 10 kHz (Köppl and Gleich, 1997). Even though CMs might more accurately reflect what the owl actually perceives, Köppl and Gleich (1997) also showed that audiograms derived from CM thresholds were upwards shifted in their sensitivity compared to behavioral and neuronal thresholds. Secondly, measurements of the CM are not useful for comparison of dead and alive owls, because CM amplitude decreases when the owl is dead (Köppl and Gleich, 1997). Furthermore, Coles and Guppy (1988) showed that the directionality of CM between 3 and 9 kHz were different from those of the external ear.

Another caveat may be that anesthesia influences directionality and timing through the interaural canal (Larsen et al., 1997, 2006). This may be due to a closure of the Eustachian tubes, especially if body temperature drops. For this reason, we controlled the body temperature in two owls and tested both dead and living owls. We did not find an influence of body temperature on ITD span, nor did the killing of the bird influence the ITD span. In addition, no change in the spectral gradient of monaural gains as expected from Larsen et al.(1997, their Fig. 1) was observed in any of the conditions tested. Furthermore, Calford and Piddington (1988) reported an increase in the low-frequency ITDs under ketamine hydrochloride anesthesia. Hence, if relevant for the barn owls' hearing, we would expect to observe an increased ITD range despite the ketamine anesthesia.

Thus, all the data suggest that the interaural canal plays, if at all, a marginal role in barn owl hearing even in the low-frequency range. However, my data do not provide the basis

for a definite answer on the functional role of the owls' ears in the low-frequency range. For that reason, it would be interesting to obtain data with a laser vibrometer to find out to what extent the pressures we measured here represent the motion of the eardrum.

4.4.3 Possible functional role of the low frequencies

The low frequencies are represented in the ascending auditory pathway of the barn owl (Koeppl 1997, Wagner et al. 2002, Vonderschen and Wagner 2009). However, a representation of low frequencies is missing in the external nucleus of the inferior colliculus, a nucleus which has been shown to be important for sound localization (Wagner, 1993).

The low-frequency information available in forebrain neurons has been implied to be relevant for hemispheric shifts of attention rather than precise sound localization (Vonderschen and Wagner 2009). Indeed, the localization precision for low frequencies as tested in the laboratory is much lower than the one for high frequencies (Singheiser et al., 2010).

The fact that the owl does not use low-frequency information for precise sound localization (Konishi, 1973a,b) might be the reason why the ITDs at low frequencies are not optimally represented in this animal (Harper and McAlpine, 2004; Wagner et al., 2007). While the range of ITDs would be suitable, but is not used, for sound localization, the ILD range and the monaural gains in the low-frequency range are too small to serve as valid sound-localization cues.

What then may be the role of the low frequencies in the barn owl? It is less well known that barn owls produce communication sounds in the low-frequency range (Bühler and Epple, 1980). They communicate with their babies in the typically dark nest with low-frequency sounds (Bühler and Epple, 1980). If an owlet stops to produce begging sounds, it will be overtaken by the siblings (Roulin et al., 2000; Roulin, 2001).

Male barn owls display courtship "songs" at the prospective nesting site. These courtship songs also contain mainly low-frequency information (Bühler and Epple, 1980). Thus, it seems that in the barn owl, the communication system and sound-localization system are spectrally separated, with communication using the low-frequency range and the sound-localization using the high-frequency range. It has only been speculated on how the information in the different frequency bands was combined in the forebrain (Vonderschen and Wagner, 2009), or what kind of tasks it is specifically used for.

4.5 Conclusions

It is clear that barn owls' HRTFs contain a broad range of physical parameters that the owl can use for sound localization. Among these, the two binaural cues ITDs and ILDs have been shown in previous studies to suffice for localization of sound sources in both horizontal and vertical planes. Monaural spectral cues may play an additional role, but do not seem to be needed for accurate localization (Poganiatz and Wagner, 2001). The distributions and ranges of physical parameters are not influenced by the owl's body temperature or physiological state, which suggests that it is mainly the head size and the shape of the outer ear which influence incoming sound.

Based on the spatial distributions of ITDs and ILDs, one can make certain predictions on the sound localization ability of owls in behavioral experiments. For example, ITD distributions are largely frequency-independent. That makes them a reliable cue for azimuthal sound localization over all frequencies, disregarding phase ambiguities that can occur at high-frequency narrowband sounds (Saberi et al., 1998).

On the other hand, ILDs at low frequencies are small and do not vary much with elevation. Thus, ILDs should only be of use for sound localization at higher frequencies, mainly in the vertical plane. If ILDs are present, they could also help the owl to resolve spatial ambiguities and thereby distinguishing real sound sources from phantom sources as described by Saberi et al. (1998), a question that will be investigated in chapter 6.

The fact that the ITD and ILD distributions are characteristically shaped by the owl's facial ruff (von Campenhausen and Wagner, 2006) raises the question of how the owl's localization performance is altered if the influence of the ruff is removed. This issue will be tackled in the following section.

5 Virtual Removal of the Facial Ruff

When sound arrives at the eardrum it has already been filtered by the body, head and outer ear. This process is mathematically described by the head related transfer functions (HRTFs), which are characteristic for the spatial position of a sound source and for the individual ear. HRTFs in the barn owl are shaped by the facial ruff, which alters interaural time differences (ITD), interaural intensity differences (ILD) and the frequency spectrum of the incoming sound. Here I created novel stimuli to simulate the removal of the barn owl's ruff in a virtual acoustic environment, thus creating a situation similar to passive listening in other animals, and used these stimuli in behavioral tests.

HRTFs were recorded from an owl before and after removal of the ruff feathers. Normal and ruff-removed conditions were created by filtering broadband noise with the HRTFs. Under normal virtual conditions, no differences in azimuthal head-turning behavior between individualized and non-individualized HRTFs were observed. The owls were able to respond differently to stimuli from the back than to stimuli from the front having the same ITD. By contrast, such a discrimination was not possible after the virtual removal of the ruff. Elevational head-turn angles were smaller with non-individualized than with individualized HRTFs. The removal of the ruff resulted in a further decrease in elevational head-turning amplitudes.

The findings show that the facial ruff a) prevents front-back confusions by increasing the ITD range and b) enables elevational sound localization in the frontal field by introducing a shift of iso-ILD lines out of the midsagittal plane, which causes ILDs to increase with increasing stimulus elevation. The changes at the behavioral level were related to the changes in the binaural physical parameters (ITD and ILD) that occurred after the virtual removal of the ruff. These data provide new insights in the design of external hearing structures and open the possibility to apply the results on autonomous agents, creation of virtual auditory environments for humans or in hearing aids.

5.1 Introduction

The barn owl (*Tyto alba*) as an effective nocturnal hunter has developed a unique morphological specialization, the directionally sensitive facial ruff (Coles and Guppy, 1988). While it seems clear that the ruff plays a role in prey capture and sound localization (Knudsen, 1981), its behavioral relevance is poorly understood at a quantitative level.

Barn owls localize sound by making saccadic head-turns towards the sound emitting source (Knudsen and Konishi, 1979). The contribution of auditory cues to azimuthal and elevational sound localization was investigated by stimulating both ears with earphones (Moiseff and Konishi, 1981a) or, more advanced, in a virtual acoustic space (Egnor, 2001; Keller et al.,

1998; Poganiatz and Wagner, 2001; Poganiatz et al., 2001). These experiments identified the interaural time difference (ITD) as the only cue that determines the amplitude of the azimuthal head-turn (Moiseff, 1989b,a; Poganiatz et al., 2001; Saberi et al., 1998, 1999). Interaural level differences (ILDs) were found to be an important cue for elevational sound localization (Egnor, 2001; Keller et al., 1998; Moiseff, 1989b,a; Poganiatz and Wagner, 2001). ITD and ILD are processed independently in separate neural pathways (Takahashi et al., 1984). Further cues, like the monaural spectra, may help to resolve ambiguities, for example if ITD and ILD have identical values at several positions in space (Brainard et al., 1992; von Campenhausen and Wagner, 2006; Saberi et al., 2002).

Since the body, head and outer ear (facial ruff of the owl) influence ITDs, ILDs and the monaural characteristics of sounds arriving at the eardrum in a direction-dependent and frequency-specific manner, recording of the so-called head-related transfer functions (HRTFs) and convolution of any free-field sound with the appropriate HRTF for a given spatial position creates virtual acoustic stimuli (VAS). Presentation of VAS via earphones allows for externalization of sounds in humans (for a review see Blauert, 1997). Likewise for the barn owl, HRTFs contain all relevant information for sound localization (Poganiatz and Wagner, 2001; Poganiatz et al., 2001). Poganiatz et al. (2001) showed that barn owls responded to VAS in the same way as they responded to free-field sounds.

Since the barn owl can barely move its ear flaps or eyes (Steinbach, 1972), the amplitudes of the head saccades can be used as a direct measure for the perceived sound-source position. A full set of HRTFs in the barn owl was first measured by Keller et al. (1998). Recently, von Campenhausen and Wagner (2006) quantified the physical changes of sound-localization cues based on HRTFs recorded before and after removing the ruff feathers. After removal of the ruff, the ITD range was decreased and ILDs did no longer change with elevational stimulus position in the frontal hemisphere. The VAS derived from the HRTFs may be manipulated for example by shifting ITDs (Poganiatz et al., 2001) or by altering the correlation of binaurally presented noise (Egnor, 2001). These manipulations allow current studies to go beyond earlier studies (Knudsen, 1981).

I made use of these possibilities to virtually remove the ruff. This has the advantage that the ruff of the respective owl does not need to be cut off, which might influence the birds' behavior and would create an instable situation due to regrowth of feathers. Another advantage of VAS is that HRTFs from one individual may be used in the same (individualized HRTF), but also in other individuals (non-individualized HRTFs). This allows for a better generalization of the effects of stimulus parameters.

I here address the question to what extent the ruff influences azimuthal and elevational sound localization, and whether its function is accurately reflected by the changes that it introduces to the ITD and ILD distributions.

5.2 Methods

5.2.1 Animals and Training

Three American barn owls (*Tyto alba pratincola*, L.) participated in the behavioral experiments, two of which were female and one was male. Care and treatment of the owls was in accordance with the guidelines for animal experiments as approved by the Landespräsidium für Natur, Umwelt und Verbraucherschutz Nordrhein Westfalen, Recklinghausen, Germany, and complied with the NIH Guide for the use and care of laboratory animals. For the behaving owls (owl H, owl P and owl S), a virtual-space environment was created. The ruff of these owls was not removed. In this way, they were not impaired in their orienting and social behavior outside experimental sessions, and fixed reference HRTFs could be used for every owl that participated in the behavioral experiment. The owls experienced the changed HRTFs only during the daily experimental session. Thus, they did not get used to the slightly different spatial sensations of non-individualized HRTFs.

As a reference animal, HRTFs of an anesthetized barn owl (owl 39) were recorded in earlier experiments von Campenhausen and Wagner (2006) before and after removal of the ruff feathers. Details of the anesthesia may be found in Wagner et al. (2007).

5.2.2 Creating a virtual acoustic environment using HRTFs

For the behavioral experiments described in this section, I used HRTFs that had been measured earlier as described in 4.2.2. After recording a set of HRTFs with the intact ruff, the reflector feathers and the auricular feathers in the center of the facial disk were completely removed, leaving only the body feathers on the rear of the head intact. For details on the feather removal see von Campenhausen and Wagner (2006). HRTFs from the owls which participated in the later behavioral experiments (owl H, owl S, owl P) had been recorded with normal ruff under anesthesia.

The HRTF measurements were carried out in the same sound attenuating chamber (IAC 403A, Industrial Acoustics, Niederkrüchten, Germany) that was used for the behavioral experiments. A loudspeaker (MacAudio ML-103E) could be moved along a semicircular track (hoop) as shown in Fig. 1 and described in section 4.2.2. The hoop could be rotated on a vertical axis. In effect the loudspeaker could be placed at virtually every spatial position on a sphere of 90 cm diameter from the centre of the owl's head. A microphone (Sennheiser KE4 211-2) with an attached silicone tube was placed 2 mm in front of the eardrum, close enough for precise measurement, but without running the risk of damaging the eardrum (Keller et al., 1998). HRTFs for owls H, S and P were measured at positions from -170° to +160° azimuth and from -70 to +80° elevation with 10° resolution. Negative positions refer to left or downward, respectively.

Calculation of the virtual acoustic stimuli was done as described in section 4.2.2 and 4.2.3, with the exception that the HRTFs were broadband-filtered from 1 to 12 kHz with an 8th

order butterworth filter.

The virtual stimuli were presented at the entrance of the ear canal via earphones (Sony MDR-E831LP), which in turn have a characteristic transfer function. To prevent that this influence of the earphones compromised the virtual stimuli when these were replayed to the owl, the influence of the earphones had to be removed from the VAS before using them for stimulation in order to accurately simulate any stimulus coming from the azimuth α and the elevation ε. For this purpose, another reference measurement, $Y_{\text{earphone}}(f)$, for the earphones was required. This reference measurement reflected the influence of the earphones, ear canal as well as of the recording microphones with their transfer function $T_{\text{sys}}(f)$ and hardware components with their transfer function $X_{\text{sys}}(f)$. For the virtual stimuli used for behavioral experiments, all owl-specific transfer functions ($Y_{\text{owl+sys}}(f)$) had to be divided by the reference measurement $Y_{\text{earphone}}(f)$ rather than by the microphone-reference alone ($Y_{\text{sys}}(f)$). The resulting stimuli were identical to the HRTFs after correction of the microphone alone (see section 4.2.2), but the influence of the earphones was additionally removed. The latter was re-introduced during behavioral tests because the stimuli were replayed by the corresponding earphones. Hence, $C_{\alpha\varepsilon}(f)$ is the HRTF after correction for the influence of the ear canal and earphones:

$$C_{\alpha\varepsilon}(f) = \frac{Y_{\text{owl+sys}}(f)}{Y_{\text{earphone}}(f)} = \frac{H_{\alpha\varepsilon}(f) \cdot X(f) \cdot T_{\text{sys}}(f)}{X(f) \cdot T_{\text{sys+earphone}}(f)} \tag{4}$$

For the purpose of measuring $Y_{\text{earphone}}(f)$, the owl was provided during HRTF recording with the headphones that were also used in the following experiments. The tonal sweep stimuli were then played via the earphones and the resulting impulse response was recorded in the same manner described above (section 4.2.2), 2 mm in front of the eardrum. Each owl-specific HRTF was then divided by the earphone reference measurement $Y_{\text{earphone}}(f)$ following eq. 4. A separate impulse response exists for each spatial position. The impulse response was cut to a length of 128 sample points and multiplied with a Tukey filter window of the same length that set the first and the last measurement value to zero. The described calculations led to a set of HRTFs for each owl and ruff status (normal versus removed ruff feathers) that could be presented to owls in behavioral experiments to investigate the contribution of single ruff features for sound localization behavior.

In sum, if an analysis of the distribution of localization cues was performed, the recorded transfer functions were corrected for the influence of the hardware components including the microphones and attached tubes by dividing its FFT through the FFT of a reference measurement of the microphones alone (without the owl) as described in section 4.2.2. For virtual stimulation, in contrast, the reference measurement included the influence of the earphones used in the behavioral experiments (eq. 4).

In the latter case, all HRTFs were corrected for the influence of the ear canal of the corresponding owl, which differed between the behavioral owls and owl 39. This introduced a systematic error when comparing localization of non-individualized HRTFs, due to the

slightly different ear canal. Since HRTFs contain all relevant information for sound localization (Poganiatz and Wagner, 2001; Poganiatz et al., 2001), the owl can derive any spatial sound source position indirectly from the characteristics that the impulse response recorded at a given spatial position provides. Hence, if impulse responses corresponding to a certain spatial position are presented via earphones, the owl should respond with a head turn movement into that direction. If non-individualized HRTFs are used for the calculation of stimuli, the head turn responses may vary systematically – given that HRTFs describe a linear system – depending on the owl from which the impulse responses were recorded. However, comparison of non-individualized HRTFs with and without facial ruff, respectively, considers the influence of the ruff only.

For a given HRTF, a cross-correlation of the left and right ear's impulse response was performed in order to derive the ITD. Broadband ILDs were calculated by subtracting the average level (within the range of 1-12 kHz) of the left ear's from the right ear's impulse response. Throughout this thesis, the resulting ITD and ILD distributions were plotted in a Cartesian coordinate system as shown in Fig. 14 or Figs. 4 and 9.

The calculations led to sets of HRTFs for each owl and stimulus condition (normal or removed ruff feathers, respectively) that were stored as finite impulse response filters (FIR) for the right and left ear on a digital controller, HUGO (Institute for Technical Acoustic, Aachen, Germany). Thereby, any incoming signal could be filtered with the HRTFs of a defined spatial position to simulate a free-field sound coming from the corresponding direction (virtual loudspeaker). For stimulation, broadband noise (300 Hz to 15 kHz) was computer generated and converted it to an analogous signal by a TDT DA3-4 digital/analog converter (Tucker-Davis Technologies, Alachua, Florida, USA). A TDT F6 device was included to prevent aliasing.

5.2.3 Procedure for Behavioral Experiments

All behavioral experiments were conducted in the same sound-attenuating chamber that was used for HRTF recording. The owl was placed on a perch in the center of the chamber in front of a feeder table. The virtual stimuli were presented at the entrance of the ear canal via earphones (Sony MDR-E831LP) after correction for the frequency response of the earphones and the ear canal. The headphone device included the receiver of a real-time tracking system (MiniBird, Ascension Technology Corporation, Burlington, Vermont, USA). Since the earphone device was attached to a metal plate implanted in the owl's skull, it was in a reproducible, fixed position over all experimental sessions. The transmitter detected changes of current flow in a magnetic field induced when the receiver moved within the magnetic field. The corresponding azimuthal and elevational head coordinates reflected the owl's head movements along these axes and were transmitted with 80 Hz sampling rate to the personal computer during the whole experimental session.

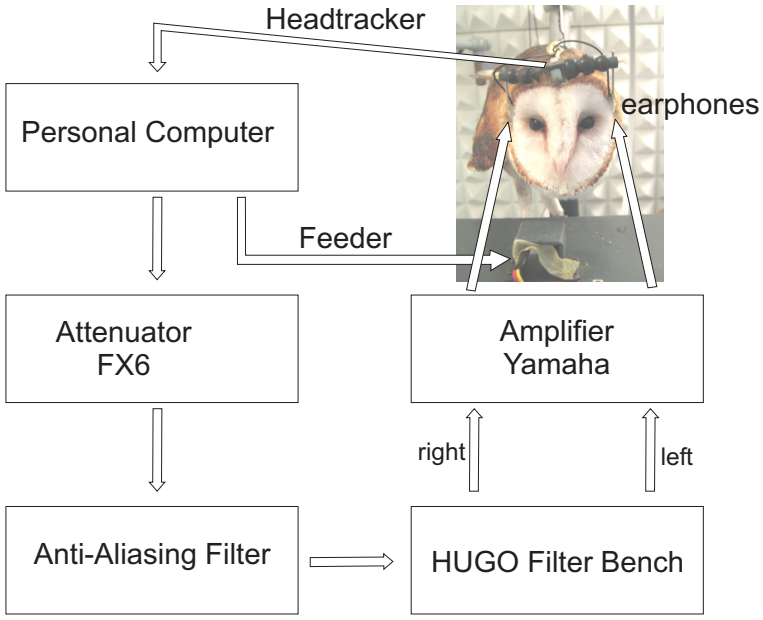

Figure 11: Setup for the behavioral experiments
During behavioral experiments, the owl was sitting in the sound-attenuating chamber with a headtracker device on the skull. The stimulus is computer-generated, attenuated to about 25 dB above hearing threshold (cf. section 5.2.4) and splitted into two identical signals, each of which is filtered with the according HRTF for each ear (left and right) of the selected spatial position before they are presented to the owl via headphones.

During an initial training phase of several months, the owl triggered the next stimulus by fixating a frontal (relative to the owl's natural line of sight) "zeroing window" for some 100 ms. Stimuli consisted of HRTF filtered, static broadband noise with varying length (100-1000 ms). Stimulus positions were selected pseudo-randomly in a range of -140° to +140° in azimuth and -40 to 40° in elevation in steps of 10°. The owl had to turn its head into the correct direction, defined by the azimuthal and elevational components that the stimulus provided, within a target window of ±10° azimuthal and elevational deviation from the target position. If the target window was fixated for at least 150 ms, the owl was automatically rewarded with several hundred milligrams of meat (one day old chicken) from the feeder apparatus. Otherwise, no reward was provided. The training phase continued until the owl showed high performance (>50% of the trials were within the target window).

The actual experimental sessions corresponded to the training procedure, but stimuli had duration of 100 ms and responses were randomly rewarded in 60% of trials. This percentage sufficed to keep the owl motivated for 30 to 100 trials per day. Individualized HRTFs were presented in 60 % of trials, non-individualized HRTFs with intact (20 %) and removed ruff (20 %) were interspersed in the remaining trials in pseudo-randomized order. The number of trials, n, depended on the stimulus position. We tested each position in steps of 20° azimuth (from -140° to 140°) at least 18 times. Since the stimulus software determined the HRTF to be used for stimulation depending on the owl's initial head position by rounding to integer steps of 10°, the owl was stimulated in few trials at stimulus positions other than steps of 20° azimuth. Positions with trial numbers smaller than $n = 6$ were not included into statistical analyses.

5.2.4 Hearing thresholds

Since it was important that the stimuli were well audible for the owls during behavioral experiments, hearing thresholds were determined for each of the three animals (owls H, S and P) using a Go-NoGo-Paradigm. That means, HRTF-filtered broadband noise identical to that used in later experiments was replayed via headphones. If the owl heard the stimulus, it turned its head towards the virtual sound source, at either -40° or +40° azimuth, and 0° elevation, and was rewarded with a small amount of meat. If the owl showed no head turn (as defined by the criteria in section 5.2.5), the trial was counted as a no-reaction trial. Threshold measurement served to set the stimulus amplitude in the later experiments to about 25 dB above threshold. This was the case for 33 dB attenuation in the hardware system used, corresponding to 36 dB SPL. Background noise in the room was at 23 to 26 dB SPL at the position of the owl's head.

During threshold measurements, the attenuation (in dB) of the stimuli, relative to the maximum amplitude the sound system could generate, covered the range from 38 dB (the loudest stimulus) to 74 dB in steps of 4 dB. Additionally, 60 dB attenuation were tested. Stimuli were presented in pseudo-randomized order at least 10 times (maximally 20 times) per azimuth and attenuation. If the owl reacted with a head turn, the trial was counted as "correct response". The percentage of correct responses was plotted against the attenuation in dB, separately for -40° and 40° azimuth (Fig. 12A-C = logistic fit, D-F = Boltzman) fit.

All measured thresholds were then converted to dB SPL by measuring the sound amplitude with a sound level meter (Brüel & Kjaer). A logistic psychometric function was fitted to the data points based on a Monte Carlo simulation with 2000 runs for estimation of the variability of the fitted parameters. The threshold was defined as the attenuation at halfwidth of the logistic fit, i.e. at 50 % of the maximum percentage of correct responses. Thresholds were at 59.1 dB relative attenuation, corresponding to -0.4 dB SPL for owl H, respectively at 60.8 dB, corresponding to -1.8 dB SPL, for owls S and P without significant differences between the owls (Wilcoxon signed rank test, 95 % confidence interval, $p \geq 0.1934$).

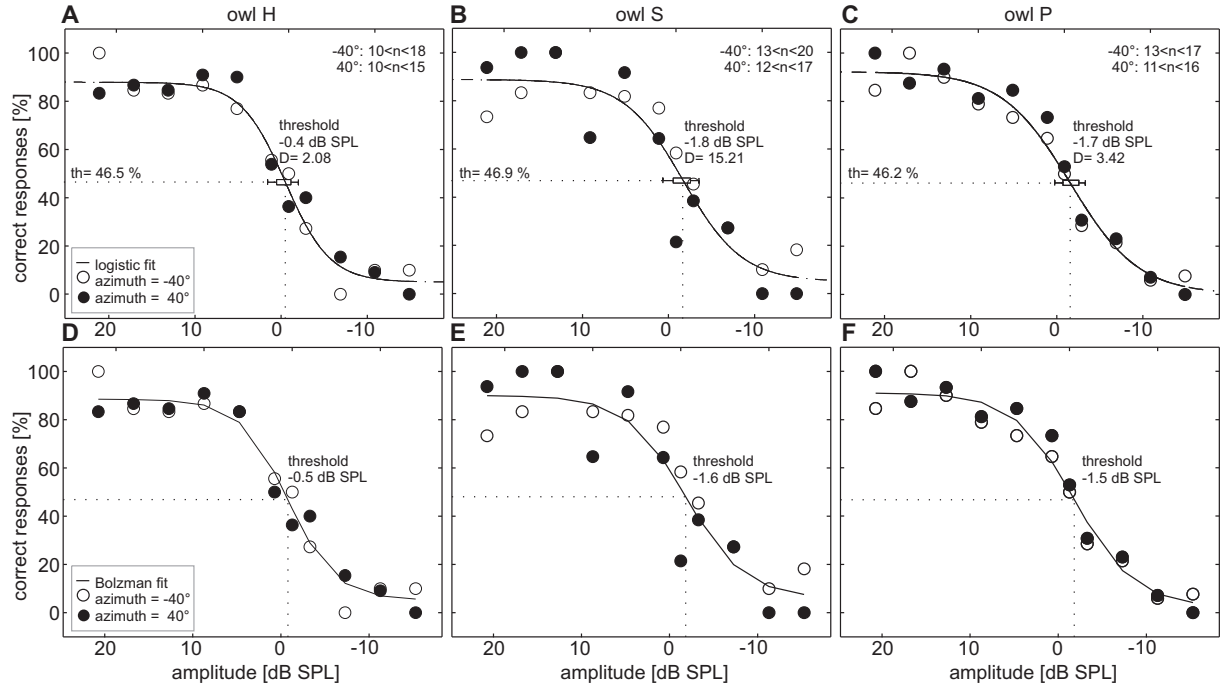

Figure 12: Hearing thresholds of the behaving owls

For each of the three owls (H, S and P), hearing thresholds were measured at ±40° azimuth. A correct response was a head turn as defined by the error criteria. A-C) The percentage of correct responses (head turns) is plotted for -40° (white circles) and 40° (black circles) stimulus azimuth (at 0° elevation) for each of the three owls. Hearing thresholds were determined at 50 % of the maximum percentage correct of a logistic fit through the data points. Thresholds for all owls were at about 60 dB attenuation in the sound system used, corresponding to about -1 dB SPL. Each data point includes at least 10 trials (n). The whisker error bars signify ±1 standard deviation (box) and ±2 standard deviations (whiskers) from the mean. D is the deviance statistic, with cpe as the cumulative probability estimate. D-F) As in A-C, but a Boltzman fit was plotted to the data points. Hearing thresholds did not differ from those calculated with the logistic fit.

Determination of the threshold had only the purpose to provide a rough estimate of when the stimulus was well detectable for the behaving owl. For this reason, false-alarm trials (i.e. head-turns without preceding stimulus or head-turns into the wrong direction) were not taken into account for simplicity, the more as they occurred in less than 1% of trials (owl H: 2 out of 264 trials = 0.76%, owl S: 0 of 277 trials = 0%, owl P: 4 of 369 trials = 1.08%). Thresholds estimated using a Go-NoGo-Paradigm can be distorted because one cannot tell whether a no-reaction trial was due to inaudibility (i.e., a miss) or because the animal didn't make the effort of reacting. Therefore, thresholds usually have to be corrected for the proportion of false alarms for an accurate estimation (cf. Dyson et al., 1998).

However, stimulus conditions here were similar to those in the later experiments, so the proportion of stimulus-independent false alarm were assumed to be constant during threshold estimation trials as well as in later experimental trials. Furthermore, the owls were trained to fixate a frontally mounted light diode until a stimulus appeared which usually prevented head saccades without preceding stimulus. For these reasons, the estimated thresholds were considered sufficient for their purpose, even though they were calculated without considering the false-alarm rates.

The estimated thresholds in my experiments lay about 20 dB below the level of the background noise, which corresponds closely to what Konishi (1973a) and Dyson et al. (1998) measured.

5.2.5 Data Analysis

The head movements of the owls were tracked by the MiniBird tracking device (Ascension Technology Corporation, Burlington, Vermont, USA). Head movements with velocities exceeding 20°/s were defined as head-turns. For each trial, the head-turn track was corrected for the owl's initial head-turn position by subtracting the azimuthal head position from the azimuthal component of the track, and the initial elevational head-turn position from the elevational component of the track. This correction allowed to define the initial head-turn position as 0° azimuth and 0° elevation and enabled comparison of head-turn angles between individual trials. Figure 13A shows a typical head-turn, segregated into the azimuthal (Fig. 13B) and elevational head-turn component (Fig. 13C).

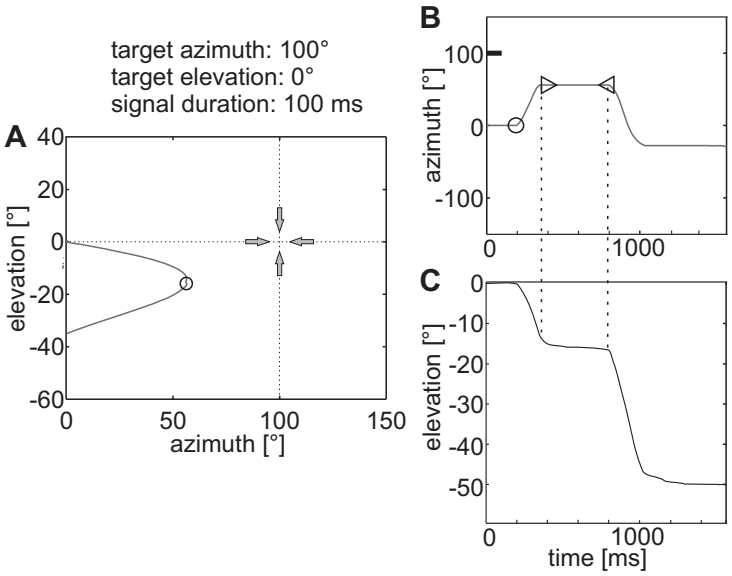

Figure 13: Head-turn movements with azimuthal and elevational components

A) A typical head turn movement tracked with the MiniBird device is shown for a trial with owl H. The stimulus position was 100° azimuth and 0° elevation (arrows). The owl's initial head position was defined at 0° azimuth and 0° elevation on a head-centered coordinate system. The owl's final fixation position (head turn velocity <20°/s) is marked by the circle. The owl then turned its head back to the feeder device (close to 0° azimuth and -50° elevation). **B**) The azimuthal head-turn component of the trial shown in A) is plotted on a linear time scale. Stimulus duration (100 ms) is indicated by the bold black line. The head turn started at the position marked by the circle. The owl fixated the azimuthal position marked by the triangles (defined as the head turn angle) before turning back to the position of the feeder. **C**) As in B), the elevational head-turn component is plotted against time (in ms). The dotted lines delineate the time points between about 380 and 800 ms and mark the elevational gaze direction during target fixation.

Azimuthal and elevational components were analyzed separately. The fixation point was defined as that point at which head-turn velocity fell below 20°/s for at least 150 ms. If the owl fixated the target position shorter, or if it had response latencies (the time between trial initiation and onset of the head-turn) of less than 50 ms or more than 500 ms, the trial was counted as an error. Only trials that met the criteria (non-errors) were included in the analysis. For comparison of two data-sample groups (e.g., the fixation points of two different owls at the same stimulus position), a two-way ANOVA with Scheffé post-hoc test was used to reveal dependences of head-turn angles on stimulus parameters and, for further evaluation, a Mann-Whitney test (two-tailed, 95% confidence interval). For the Boltzman

fit to the azimuthal head-turn angles (dependent variable) as shown in Fig. 18, the lower asymptote, A1, and the upper asymptote, A2, were estimated from the azimuthal head-turn angles using a nonlinear least squares regression. The Boltzman fit was calculated following the equation

$$f(x) = \frac{A1+A2}{1+e^{\frac{x-x0}{dx}}} \qquad \text{(eq. 1)}$$

with x0 as x at $\frac{y}{2}$ or $\frac{A1+A2}{2}$ and dx as a time constant.

5.3 Results

Experiments were carried out with three tame barn owls from the institute's breeding stock, owls H, S and P. My hypothesis was that ruff removal influences sound localization and that the effect of ruff removal can be related to changes in the distributions of ITDs and ILDs. To test this hypothesis, it was first important to determine the distributions of ITDs and ILDs on an individualized ("normal, individualized condition" or stimulus condition 1) and non-individualized basis ("normal, non-individualized condition" or stimulus condition 2), then to show that non-individualized HRTFs are adequate for stimulation by comparing the behavioral responses to stimulus condition 2 with those to stimulus condition 1.

Finally, I quantified how non-individualized HRTFs with removed ruff ("ruffcut condition" or stimulus condition 3) influence sound localization and relate the changes in sound localization induced by ruff removal to the accompanying changes in sound-localization parameters.

5.3.1 Patterns of ITDs and ILDs in the HRTFs

In HRTFs recorded with intact facial ruff, ITDs changed continuously with azimuth up to about 110° and were largely independent of stimulus elevation. The most prominent feature of the ITD distribution was a shift of the extrema of the ITD to the rear hemisphere (minimum ITD at about -110° azimuth/ -20° elevation, maximum ITD at about +110° azimuth/ +20° elevation; Fig. 35A-D in the appendix). The most eye-catching feature of the ILD distribution in the barn owl with its asymmetrical ears was a rotation of the axis with the largest ILD gradient from the azimuthal axis, resulting in a minimum of the ILD at about -20° azimuth/-20° elevation and a maximum of the ILD at about +20° azimuth/ +20° elevation (Fig. 35F-I).

ILD is unambiguously related to varying elevational sound positions in an area spanning about ±40° in elevation and about ±60° in azimuth. At more peripheral positions (>±100° azimuth), ILD does not change with stimulus elevation and should, therefore, not be a reliable cue for elevation (see also Fig. 27). Only in the frontal field (within approximately ±60° where auditory resolution is highest, Bala et al., 2007), both sound source azimuth and elevation are unambiguously coded by a specific combination of ITD and ILD under

normal conditions (Euston and Takahashi, 2002; Knudsen and Konishi, 1978; Takahashi et al., 2003).

Qualitatively, the distributions of ITDs and ILDs were similar between owls, but slight differences occurred. For example, in owl S, the main ILD extrema were shifted towards approximately ±135° azimuth and ±10° elevation, but there were local extrema at the positions indicated above (Fig. S1F). I quantified the differences between the varying conditions by subtracting the corresponding ITDs and ILDs, respectively. The data of owl 39 with intact facial ruff served as a reference. The normal individualized ITD and ILD distributions from the experimental owls H, P and S were compared with those of owl 39 (Fig. 14: ILDs, exemplary for owl H). For that purpose, the distributional patterns for ITDs or ILDs, respectively, of owl 39 and the behaving owl were overlaid (Fig. 14C) and subtracted from each other for each spatial position, resulting in a difference map (Fig. 14D). Two-dimensional plotting of these difference distributions yielded difference maps as shown in Fig. 15.

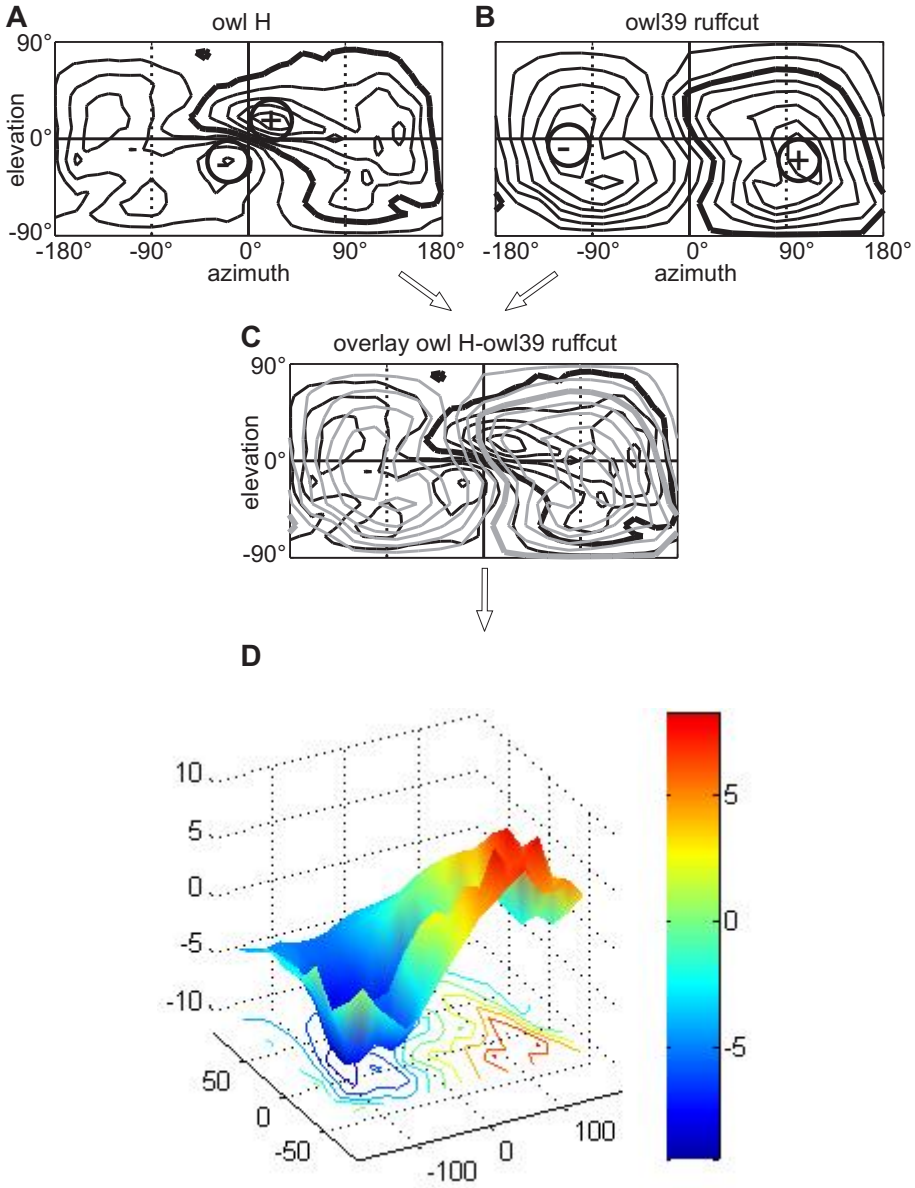

Figure 14: Calculation of difference maps for spatial cues

The calculation of a difference map for ILDs is exemplary shown for **A**) owl H and **B**) owl 39 after feather removal. Both maps were overlaid (**C**, black: owl H, gray: owl 39) and the differences in ILDs were calculated for each spatial position (from -180 to 180° azimuth, -60 to 80° elevation, interpolated) as shown in the surface plot in (**D**).

For example, ITD differences between owl H and owl 39 normal ranged from -10 to +30 µs (Fig. 15A). ILD differences ranged from about -2 to +5 dB (Figs. 14D and 15C). The differences were only slightly higher for owls S (-50 to +30 µs) ITD and -3 to +8 dB ILD, Fig. 36 in the appendix). Owl P's HRTFs differed from those of owl H by up to ±40 µs and -9 to +1 dB, and from those of owl 39 normal by -30 to 50 µs ITD and -2 to -8.5 dB ILD, respectively (Fig. 37 in the appendix). Hence, under normal conditions, the patterns of ITDs and ILDs were similar in all owls.

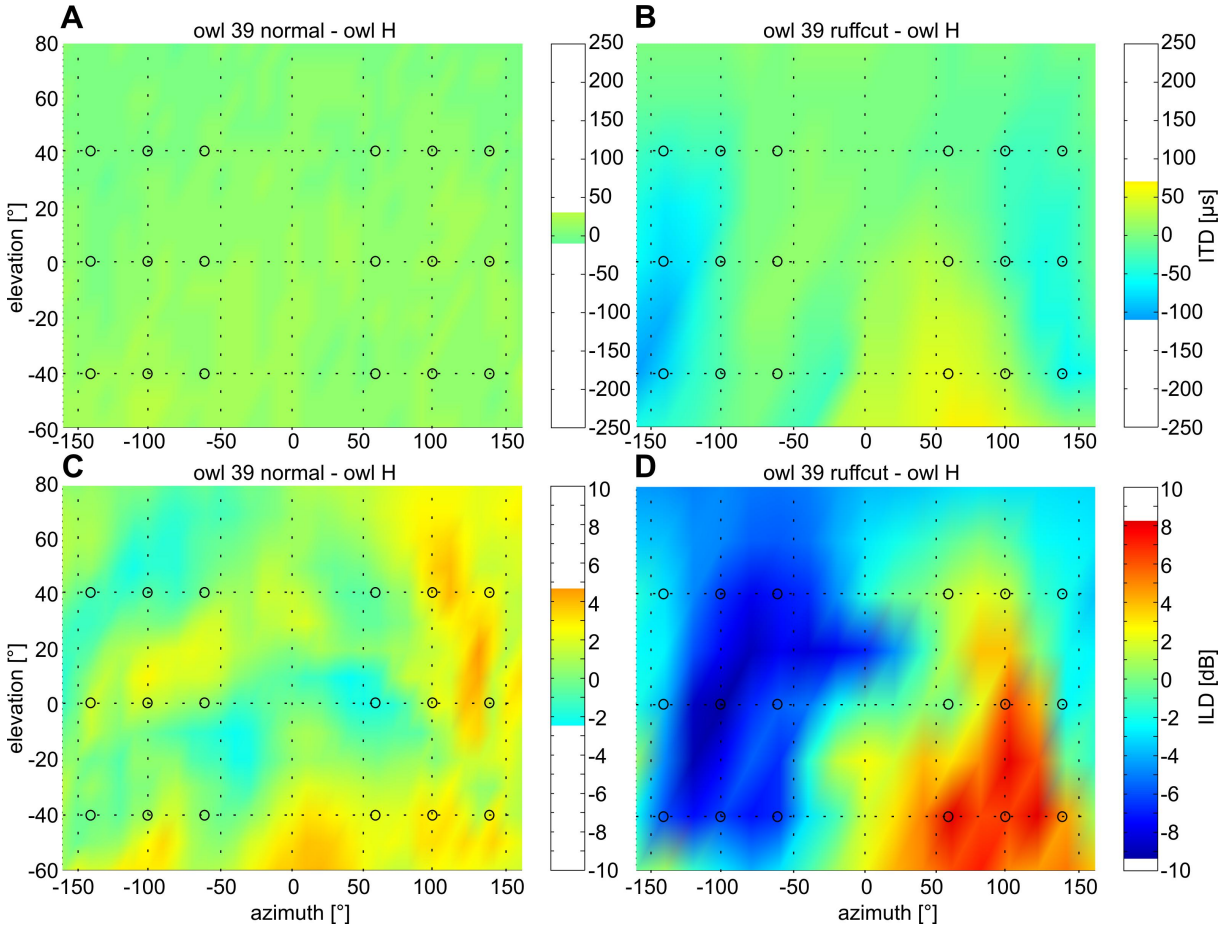

Figure 15: ITD and ILD differences between normal and ruffcut HRTFs

The differences between the ITDs (upper panels) are shown for owl H and owl 39 with **A**) intact and **B**) removed ruff, respectively. Equivalent plots for ILD differences (lower panels) between owl H and owl 39 with **C**) intact and **D**) removed ruff feathers, respectively. Coloration is explained in the bar plots on the side. Blue areas mark positions where the ITDs or ILDs of owl 39 are smaller (nearer to 0 µs or dB) than those of owl H, red areas mean that the ITDs or ILDs of owl 39 are larger (>0 µs or dB). The differences in both, ITDs and ILDs, are larger when the facial ruff was removed than if it was intact (compare A to B and C to D).

The distributions of ITDs and ILDs changed dramatically when the ruff was removed (compare Fig. 14A to B, see also Fig. 35A-D to E for ITDs, and Fig. 35F-I to J for ILDs in the appendix). The most important effect of ruff removal on the distribution of ITDs was a shift of the ITD extrema from the rear hemisphere towards ±90° azimuth and 0° elevation (Fig. 35E), as is the case in species with symmetrical ears (Blauert, 1997). The ITD range decreased from about ±270 µs to about ±240 µs. After the ruff was removed, the characteristic kidney-shaped distribution of the iso-ILD lines (Fig. 35F-I) was lost. ILDs in the ruffcut condition changed with azimuthal sound source position, but did no longer vary with elevation (Fig. 35J). The quantitative analysis demonstrated differences of up to -110 to +70 µs in the ITDs and up to -9 to +8 dB in the ILDs, respectively (15B+D for owl H) between the individualized HRTFs and those of owl 39 after ruff removal. The differences between owl 39 after ruff removal and owls P and S, respectively, were similar (-110 to +60 µs ITD for owl P and -90 to +40 µs ITD for owl S; -14 to 6 dB ILD for owl P and -7 to +8 dB ILD for owl S, Figs. 36 and 37 in the appendix). The largest differences occurred at

the peripheral positions (beyond ±100° azimuth) and in the lower hemisphere. The spatial positions for stimulation of the owls lay within the areas with large differences in ITD and ILD. These were ±60°, ±100° and ±140° azimuth at ±40° and 0° elevation (marked with circles in Figs. 15, 36 and 37).

5.3.2 Head-turns and response latencies

The owls were stimulated with broadband noise in a virtual acoustic space. The noise bursts were filtered with different sets of HRTFs, resulting in the three stimulus conditions. Two owls (owls H and S) were stimulated with their own (individualized) HRTFs or stimulus condition 1. All three owls were tested with stimulus condition 2, with HRTFs recorded from a reference owl with intact ruff (owl 39 normal). The third owl, P, was also stimulated with the HRTFs from owl H.

The use of two sets of normal, non-individualized HRTFs in this owl served as a control condition to reveal possible learning effects, such as habituation to non-individualized stimuli which might influence the owl's performance. All three owls were also tested with stimulus condition 3. Comparison of the latter two stimulus paradigms revealed the contribution of the facial ruff for azimuthal and elevational sound localization.

In all three stimulus conditions, the owls responded to HRTF-filtered stimuli from varying azimuths (-140° to 140°) and elevations (±40° and 0°) with a saccadic head-turn into the stimulus direction (Fig. 13). If the stimulation angle was negative, the owl turned its head to the left side. If the stimulus angle was positive, it turned the head to the right side.

Head-turn latency was defined as the time between stimulus onset and the first time point at which the head-turn velocity exceeded 20°/s (circle, Fig. 13B). Head-turn latencies were concentrated between 80 and 200 ms for all owls with medians ranging from 104 to 160 ms depending on the owl and stimulus position (Figs. 16 and 17).

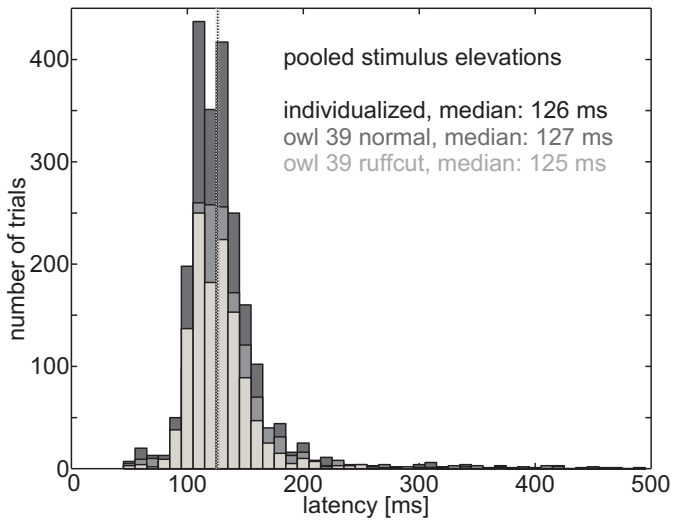

Figure 16: Latencies

Pooled latencies for the owls and stimulus positions are similarly distributed for trials using individualized HRTFs (dark gray, median at 125 ms marked by dark gray line), owl 39 normal (medium gray, median at 125 ms) and owl 39 ruffcut (light gray, median at 127 ms). Trials with latencies larger than 500 ms were excluded from the analysis, because they indicated low motivation or other distracters. No systematic effect of ruff removal on response latency was observed.

These findings accord with previous latency measurements in the barn owl (Knudsen and Konishi, 1979; Poganiatz et al., 2001; Wagner, 1993). In general, latencies did not significantly differ between trials with non-individualized or individualized HRTFs at a particular stimulus position (Wilcoxon signed ranks test, two-tailed, $p>0.05$, Fig. 17). Furthermore, the resemblance of latencies in all stimulus conditions was a first indication that the owls perceived all stimuli similarly.

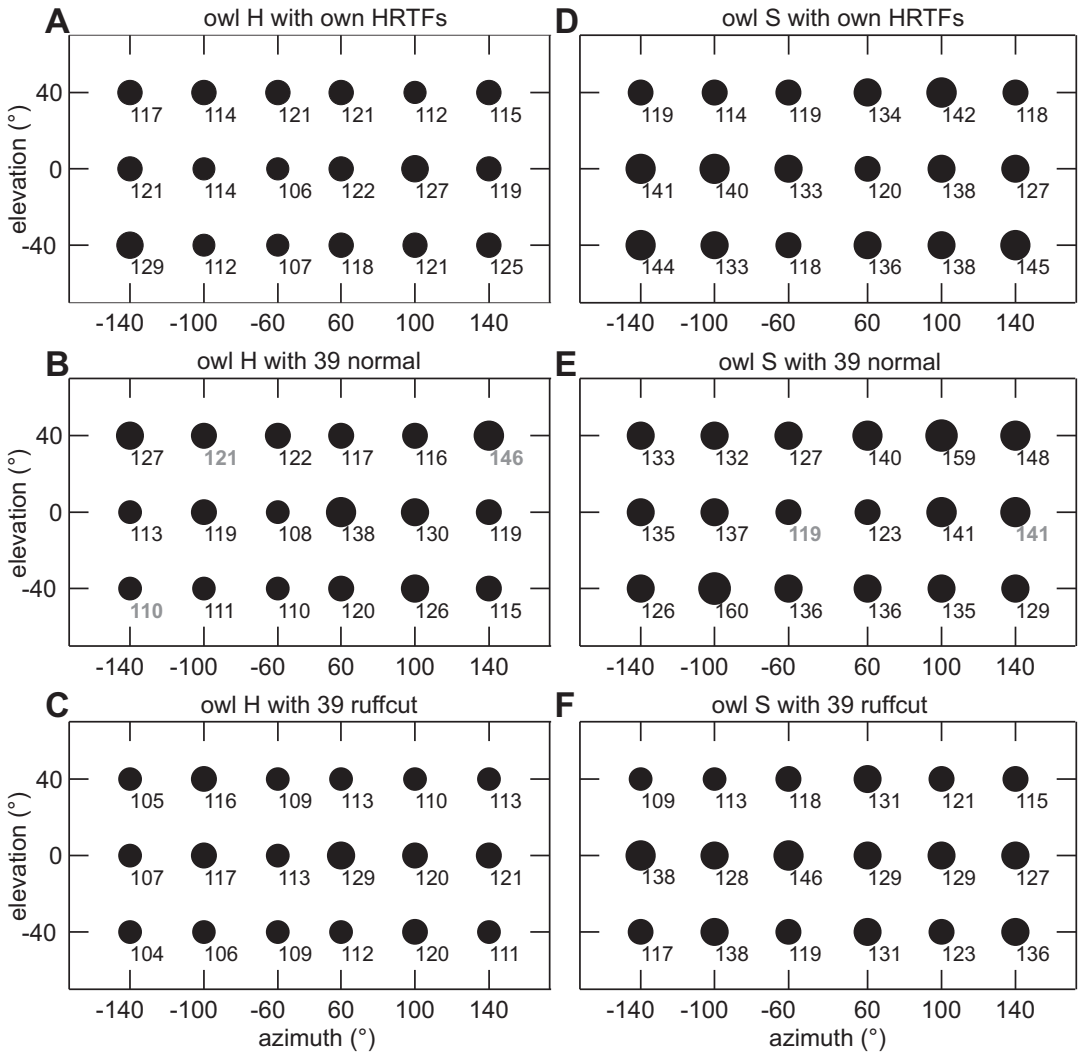

Figure 17: Latencies for responses to different HRTFs at various stimulus positions
A-C) owl H, D-F) owl S. The diameters of the black circles represent median reaction times in response to stimulation with individualized HRTFs (A+D), normal HRTFs of owl 39 (B+E) and HRTFs of owl 39 with removed facial ruff (C+F) at the three stimulus elevations. Gray numbers indicate significant deviation (Mann-Whitney test, $p<0.05$) of the latency from that measured at the corresponding stimulation site with individualized HRTFs. No systematic change of the median reaction times occurred when the owls were stimulated with non-individualized HRTFs.

5.3.3 Azimuthal Sound Localization

The mean amplitude of the azimuthal head-turn saccade depended on the stimulus position in an unambiguous way as shown for owl H in Fig. 18A. For both negative and positive stimulus azimuths, respectively, the absolute value of the amplitude increased in a monotonic way with the absolute value of the stimulus position (Fig. 18A).

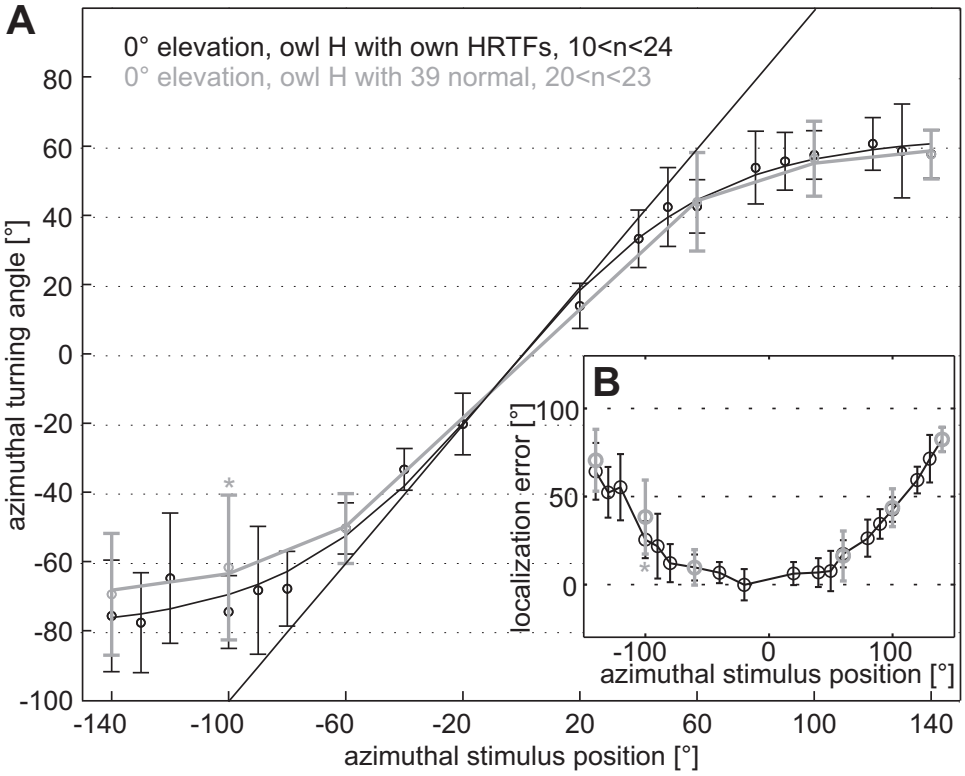

Figure 18: Azimuthal head-turn angles

A) Head-turn angles in degree (mean ± SD) are plotted against the azimuthal-stimulus position in degree, exemplary for owl H with individualized HRTFs at 0° elevation (black) and for stimulation with HRTFs of owl 39 with intact ruff (gray). Localization of the exact stimulus position would result in a line with a slope of 1 (black straight line). The curved black and gray lines are Boltzman fits (see Data analysis) to the azimuthal head-turn angles. Head-turn angles differed only at -100° azimuth (blue asterisk, Mann-Whitney test, $p \leq 0.05$) between the two stimulus conditions (for the other owls, see Fig. 19). The ranges of the number of trials (n) per day point are indicated. **B**) The azimuthal-localization error (difference between stimulus angle and head-turn angle) is plotted as a function of the azimuthal-stimulus angle. Responses to individualized HRTFs are shown in black, those to owl 39 normal in gray. Localization errors were smaller for small stimulus angles than for large stimulus angles, which are reflected by an increasing localization error with increasingly peripheral stimulus angles (see also Fig. 19).

Consequently, a sigmoidal Boltzman function (see Data analysis) fitted the data well for all owls ($R^2 \geq 0.9935$ for individualized and $R^2 \geq 0.9889$ for normal non-individualized HRTFs). This observation meant specifically that the owls were able to respond differently to stimuli coming from the rear hemisphere and to stimuli coming from the frontal hemisphere, even if these stimuli had the same ITD. However, at any azimuthal stimulus position, the amplitude of the head-turn was too small. In other words, the owls undershot the target position. The difference between the owl's head-turn angle and the target angle reflects the azimuthal localization error.

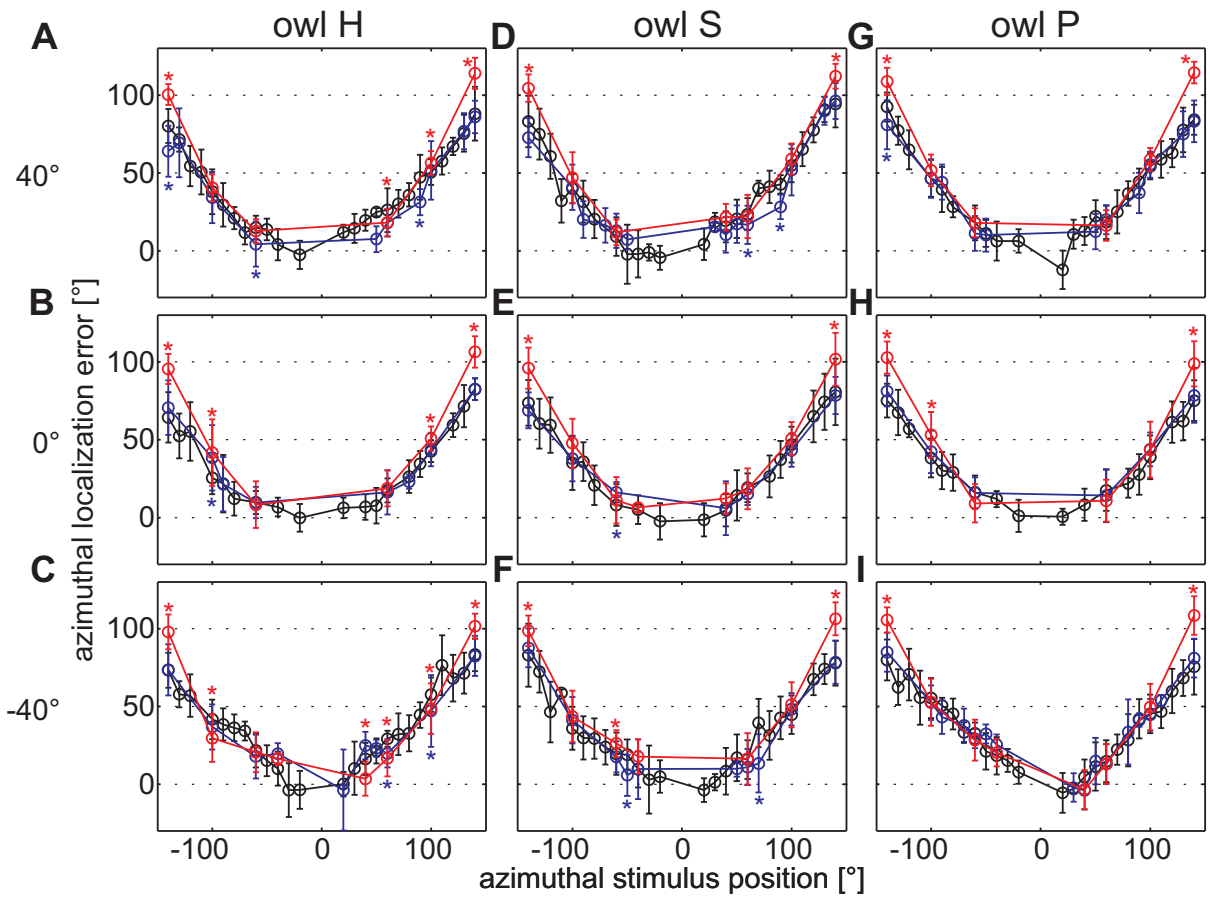

Figure 19: Localization errors for different HRTFs for all owls

The difference between the azimuthal stimulus angle and the corresponding head-turn angle in degree was defined as the localization error. For each stimulus elevation (rows) and owl (columns, A-C: owl H; D-F: owl S; G-I: owl P), localization errors (mean ± SD) are plotted as a function of stimulus azimuth (black lines = individualized HRTFs for owls H and S respectively owl H's HRTFs for owl P, blue = owl 39 normal, red = owl 39 ruffcut). Positive localization errors indicate that the owl fixated a position too close to zero degree ("undershooting"), negative angles indicate overshooting. Positive localization errors gradually increased with increasing stimulus azimuth. Distributions hardly varied between individualized HRTFs and HRTFs of owl 39 normal (significant differences found with a Mann-Whitney test, two-tailed, are marked with blue asterisks), but stimulation with HRTFs of owl 39 with removed ruff resulted in a significantly larger localization error (marked with red asterisks) especially in the peripheral field (±140°, see also Table 2). All data points are shown to give a better picture of the owls' behavior. Statistical comparisons were only performed for data points including at least $n = 3$ trials. Blue asterisks mark positions with significant differences (Mann-Whitney test, $p \leq 0.05$) between individualized HRTFs (owl P: owl H's HRTFs) and owl 39 normal, respectively owl 39 ruffcut (red asterisks).

For stimulus angles beyond ±100°, the amplitude of the azimuthal head-turns approached a plateau of about ±60° (Fig. 18A). The effect of the elevation was significant ($p \leq 0.023$, two-way ANOVA) for each of the three owls, as were the interaction terms of elevation and azimuth ($p \leq 0.001$), respectively elevation and stimulus condition (owl H: $p \geq 0.036$, owl S: $p \geq 0.029$; owl P: $p \geq 0.062$). Due to the increase of the undershooting with stimulus azimuth, the localization error exhibited a U-shaped dependence on azimuth (Fig. 18B for owl H at 0° elevation; for the other owls and stimulus elevations see Fig. 19). The elevation of the stimulus influenced the amplitude of the azimuthal head-turn (Fig. 20). For both elevational

positions of -40° and +40°, the mean azimuthal head-turn amplitude was reduced compared to the situation when stimulus elevation was 0° (Mann-Whitney test, $p \leq 0.05$, Fig. 20).

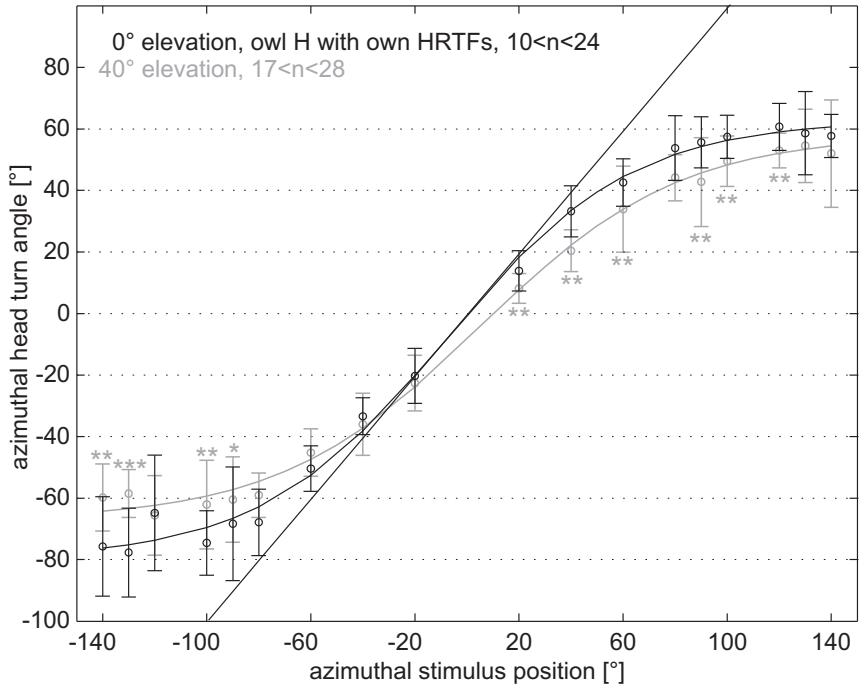

Figure 20: Azimuthal head-turn angle dependent on stimulus elevation
Azimuthal head-turn angles [°] are plotted against azimuthal stimulus angle, exemplary for owl H. A stimulus elevation of 0° (black circles and errorbars, mean ± SD) resulted in larger azimuthal turning angles than stimulus elevations of either 40° (gray circles and error bars) or -40° (not shown). Positions with significant differences between both conditions are marked with asterisks depending on the significance level (*p<0.05, **p<0.01, ***p<0.001) in a Mann-Whitney test.

The azimuthal localization error varied as much between the owls as it did between individualized stimuli (owls H and S) and owl 39 normal (Table 1). I compared responses at 59 positions (see owls H and S in Fig. 19, note that the number of tested positions exceeds the sum of positions given in Table 1 because the table does only consider stimulus azimuths ≤60°, 100° and 140°, but no positions in between) and found differences with a Mann-Whitney test ($p \leq 0.05$) only at 12 positions (20 %, asterisks in Fig. 19). A difference in the azimuthal turning behavior of owl P when stimulated with the two sets of non-individualized HRTFs was only observed in 1 of 31 tests (3.2 %, Fig. 19).

Table 1: Localization differences between individualized and non-individualized HRTFs
For each owl and stimulus azimuth, it was tested if the head-turn angles differed between HRTFs with intact ruff (owls H and S: individualized; owl P: HRTFs of owl H) and HRTFs of owl 39 normal, respectively owl 39 ruffcut (Wilcoxon signed ranks test, $p<0.05$). The frontal field ($<\pm60°$ stimulus azimuth), a position in the middle field ($\pm100°$) and in the periphery ($\pm140°$) were regarded separately. Differing positions are also marked with blue asterisks (owl 39 normal) and red asterisks (owl 39 ruffcut) in Figure S4. The first number in each column gives the number of pairings without singificant differences in the mean turning angles; the second number is the total number of tested pairings. The percentage is given in brackets. There were highly significantly (Fisher test, $p<0.001$) more differences at $\pm140°$ in the owl 39 ruffcut condition than in the owl 39 normal condition, thus in the periphery, but not in the frontal field.

owl 39 normal	**owl H individualized**	**owl S individualized**	**owl P with owl H's HRTFs**	**owls H and S pooled**
$\leq\pm60°$, frontal	9/11 (81.8 %)	11/14 (21.4%)	13/13 (8.3 %)	20/25 (80.0 %)
$\pm100°$, middle	4/6 (66.7 %)	6/6 (0.0 %)	6/6 (0.0 %)	10/12 (83.3 %)
$\pm140°$, peripheral	5/6 (83.3 %)	6/6 (0.0 %)	5/6 (0.0 %)	11/12 (91.6 %)

owl 39 ruffcut	**owl H individualized**	**owl S individualized**	**owl P with owl H's HRTFs**	**pooled**
$\leq\pm60°$, frontal	5/8 (62.5 %)	9/10 (90.0 %)	8/8 (100 %)	14/18 (77.7 %)
$\pm100°$, middle	1/6 (16.7 %)	6/6 (100 %)	5/6 (83.3 %)	7/12 (58.3 %)
$\pm140°$, peripheral	0/6 (0.0 %)	0/6 (0.0 %)	0/6 (0.0 %)	0/12 (0.0 %)

To compare the results obtained with the three stimulus conditions, the azimuthal head-turn angles were pooled for all owls (Fig. 21A, stimulus condition 1: dotted; stimulus condition 2: black; stimulus condition 3: blue). Differences between conditions 1 and 2 occurred only at a few positions as indicated by the black asterisks in Fig. 21A. The general relationship between stimulus angle and mean head-turn angle, as exemplary described above (Fig. 18), was highly similar for all stimulus conditions with intact ruff. Altogether, these results demonstrated no systematic azimuthal head-turn differences between normal non-individualized HRTFs and individualized HRTFs.

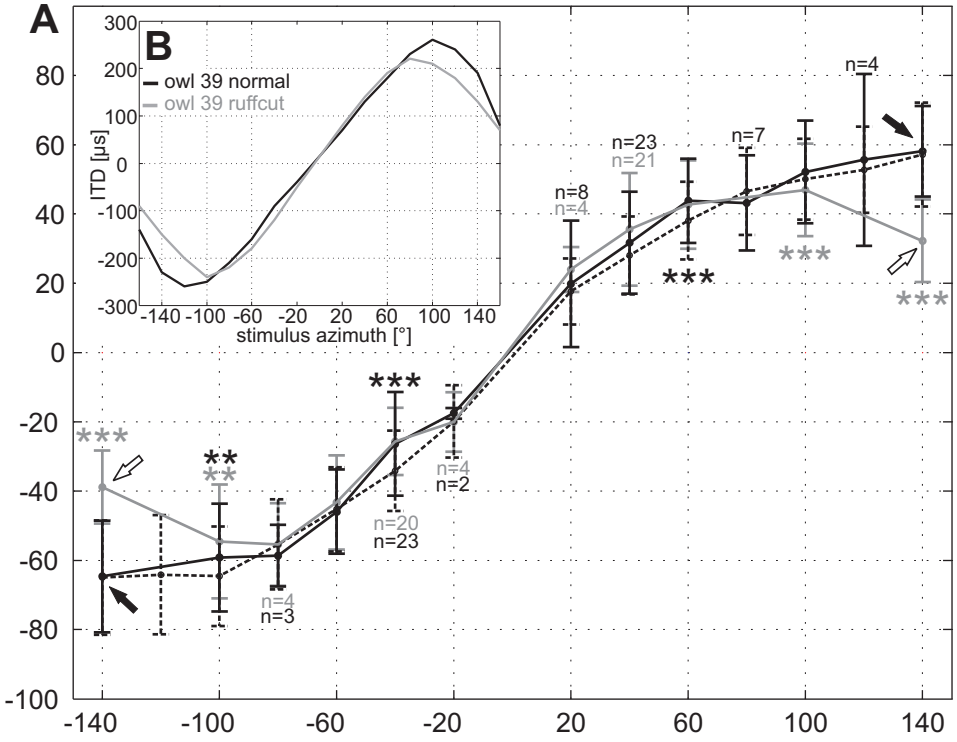

Figure 21: Azimuthal head-turn angles before and after ruff removal

A) Azimuthal head-turn angles were pooled for stimulation with individualized HRTFs (dotted, owls H and S), responses to owl 39 normal (black, all three owls) and to owl 39 ruffcut (gray, all three owls). Stepsize was 20°. Arrows mark ±140° stimulus position, where the azimuthal head-turn angle decreased highly significantly (Mann-Whitney test, $p<0.0001$) in the ruffcut condition. In contrast to the ruffcut condition, the head-turn angles with intact ruff (individualized and owl 39 normal) approach a plateau at about ±60°. Significant differences between stimulus conditions are marked with asterisks depending on the significance level (**$p<0.01$, ***$p<0.001$) in black (individualized versus owl 39 normal) respectively in gray (owl 39 normal versus owl 39 ruffcut). Each data point includes at least 96 trials, unless indicated otherwise by the number of trials (n). **B**) The ITD in µs contained in the HRTFs at 0° elevation is plotted against stimulus azimuth in degree for owl 39 normal (black) and owl 39 ruffcut (blue). Note the sinusoidal course of the ITD. The ITD decreased at peripheral azimuths for both intact and removed ruff, and was smaller in the ruffcut condition.

On the other hand, the removal of the ruff had an influence on peripheral sound localization (stimulus angles outside ±60°). Changes in localization behavior occurred at positions where the differences in ITDs between intact and removed ruff were largest (cf. Fig. 15B). For all owls and stimulus elevations, the angular extent of the azimuthal head-turns decreased highly significantly for stimuli originating at ±100° azimuth (Fig. 21A) and even more strongly for stimuli corresponding to ±140° stimulus azimuth (Fig. 21A, blue, and Fig. 19). For example, when the stimulus was computed from an HRTF corresponding to ±140° in the ruffcut condition, the head-turns had amplitudes that corresponded to those measured for a stimulation from approximately ±40° in the ruff-intact condition (Table 2).

Table 2: Head-turn angles at peripheral stimulus positions

For each owl and stimulus condition (39n = owl 39 normal, 39c = owl 39 ruffcut), the mean azimuthal head-turn angles ± standard deviation (SD) at ±140° stimulus azimuth (azi) is given for the three stimulus elevations (ele). Responses to HRTFs of owl 39 ruffcut were highly significantly (Mann-Whitney test, $p<0.001$) smaller than responses to either individualized (respectively owl H's HRTFs in case of owl P) or owl 39 normal stimuli for any owl and elevation.

		owl H individualized		**owl H with 39n**		**owl H with 39c**	
ele	**azi**	**mean [°]**	**SD**	**mean [°]**	**SD**	**mean [°]**	**SD**
40°	**-140°**	-60.31	10.98	-76.07	16.30	-39.68	6.72
	140°	53.75	10.79	55.79	9.52	25.68	10.07
0°	**-140°**	-75.71	16.15	-69.36	18.00	-44.62	9.66
	140°	57.62	10.95	57.57	7.03	38.50	10.04
-40°	**-140°**	-67.21	11.39	-66.55	16.52	-41.44	11.56
	140°	57.19	10.95	57.57	13.16	38.50	8.27

		owl S individualized		**owl S with 39n**		**owl S with 39c**	
ele	**azi**	**mean [°]**	**SD**	**mean [°]**	**SD**	**mean [°]**	**SD**
40°	**-140°**	-56.92	16.47	-67.35	12.61	-35.51	8.81
	140°	45.86	14.83	43.83	11.53	27.91	7.95
0°	**-140°**	-66.43	14.75	-71.25	11.45	-44.10	13.17
	140°	59.35	21.34	61.65	11.88	38.40	16.94
-40°	**-140°**	-57.21	20.24	-52.39	12.45	-41.55	9.81
	140°	62.35	11.53	61.69	13.97	33.79	10.62

		owl P with owl H		**owl P with 39n**		**owl P with 39c**	
ele	**azi**	**mean [°]**	**SD**	**mean [°]**	**SD**	**mean [°]**	**SD**
40°	**-140°**	-47.63	9.36	-59.06	15.77	-31.23	8.76
	140°	55.87	9.70	56.86	13.36	25.53	7.01
0°	**-140°**	-64.93	10.83	-58.87	9.87	-37.43	10.40
	140°	64.92	13.11	61.59	17.55	41.27	14.48
-40°	**-140°**	-60.28	13.14	-55.19	12.49	-35.54	8.09
	140°	64.57	17.97	59.10	12.37	31.67	12.32

The change in the amplitude of the head-turns was correlated with the decreasing ITDs in the periphery (see also next paragraph). By contrast, localization behavior generally did not differ between the three stimulus conditions within the frontal area of ±60° and only partly at ±100° stimulus angle (Fig. 19A, Table 1). This finding was related to the small differences in ITDs within this area between the three stimulus conditions (cf. Fig. 15B). A two-way ANOVA with a Scheffé post-hoc test showed that the stimulus condition had a highly significant ($p<0.001$) influence on the azimuthal head-turn behavior in dependence of the azimuthal stimulus angle (Table 3). That is, the HRTF alone had no significant influence, whereas stimulus azimuth and elevation as well as combinations of all three factors significantly influenced the owls' head-turn angle (Table 3).

Table 3: ANOVA covariance analysis for azimuthal head-turn angles

For the three owls, a two-way ANOVA revealed how stimulus azimuth (azi), stimulus elevation (ele) and HRTF set (individualized, owl 39 normal or owl 39 ruffcut) influence the azimuthal head-turn angle. Degree of freedom (df), test statistic (F) and significance level (p) as indicated, significant terms ($p<0.001$) are bold printed. $R^2>95\,\%$ for all tests. The interaction terms of stimulus condition (HRTF set) and azimuth respectively elevation were usually significant, whereas the HRTF set alone did not influence the azimuthal head-turn angle.

		owl H		**owl S**		**owl P**	
	df	**F**	**p**	**F**	**p**	**F**	**p**
azimuth	5	3660.795	**0.000**	1980.640	**0.000**	3170.530	**0.000**
elevation	2	3.765	**0.023**	18.812	**0.000**	24.882	**0.000**
HRTF	2	0.983	0.374	0.206	0.814	1.124	0.326
azi*ele	10	5.054	**0.000**	3.885	**0.000**	11.048	**0.000**
azi*HRTF	10	32.413	**0.000**	17.281	**0.000**	34.228	**0.000**
ele*HRTF	4	2.574	**0.036**	2.714	**0.029**	2.251	0.062
azi*ele*HRTF	20	3.140	**0.000**	1.531	0.064	1.748	**0.022**

Since the ANOVA revealed that the azimuthal head-turn angle was not influenced by the stimulus condition (HRTF set) in general, but only by the stimulation with a given HRTF from a specific azimuthal position (Table 3), I analyzed the influence of each stimulus azimuth separately (Table 4 for pooled data from all owls; data for the individual owls can be found in the appendix in Table 10). The stimulus condition mainly influenced peripheral localization, and also interacted with the stimulus elevation (Table 4A). The interaction was mainly based on a difference between the influences of normal versus ruffcut HRTFs at peripheral stimulus positions (Table 4B), which already became apparent from the stronger undershooting at peripheral azimuths (Fig. 20). The Scheffé test revealed furthermore that it was not the use of individualized versus non-individualized HRTFs which influenced the amplitude of azimuthal head-turn angles, but that main differences occurred between individualized HRTFs and 39ruffcut and between stimulus conditions 39normal versus 39ruffcut (Table 4B).

Table 4: Influence of stimulus condition and elevation on azimuthal head-turn angles

A two-way ANOVA with Scheffé post-hoc tests showed the interactions between stimulus elevation (ele) and HRTF set (ind = individualized, 39n = owl 39 normal, 39c = owl 39 ruffcut). Significance level p is given for each factor. Significant terms ($p<0.001$) are bold printed. For simplicity, data from all owls were pooled. A) The HRTF set influenced azimuthal head turn angles only in the periphery, whereas stimulus elevation alone had a stronger influence in the frontal field (60° azimuth). B) A Scheffé post-hoc test revealed that the influence of the HRTF set was due to differences between normal and ruffcut HRTFs rather than between individualized and non-individualized HRTFs. C) The influence of stimulus elevation was mainly explained by the interaction of elevation and a specific HRTF set.

	A) two-way ANOVA			**B) Scheffé test (HRTF set)**			**C) Scheffé test (elevation)**		
azi	**HRTF**	**ele**	**ele*HRTF**	**ind/39n**	**39n/39c**	**ind/39c**	**-40/0°**	**0/40°**	**-40/40°**
-140°	**0.000**	0.459	**0.000**	0.230	**0.000**	**0.000**	**0.000**	**0.000**	0.677
-100°	0.946	0.742	0.559	0.720	**0.024**	**0.003**	0.247	0.289	1.000
-60°	0.283	0.077	0.785	0.055	0.111	0.2963	**0.000**	1.000	**0.000**
60°	0.997	**0.016**	**0.009**	**0.005**	0.692	**0.046**	0.843	**0.009**	0.058
100°	0.173	0.556	0.702	0.843	**0.001**	**0.004**	**0.009**	**0.000**	**0.000**
140°	**0.000**	0.873	**0.000**	0.837	**0.000**	**0.000**	0.988	**0.000**	**0.000**

The impact of stimulus elevation was less clear (Table 4C), since the elevation per se influenced localization in the frontal rather than in the peripheral field (Table 4A), but together with the given stimulus condition, the influence was stronger in the periphery (Table 4A). In other words, the owls exhibited generally smaller head-turn angles at more elevated positions, and this effect was even more prominent in the periphery than in the frontal field (Fig. 20).

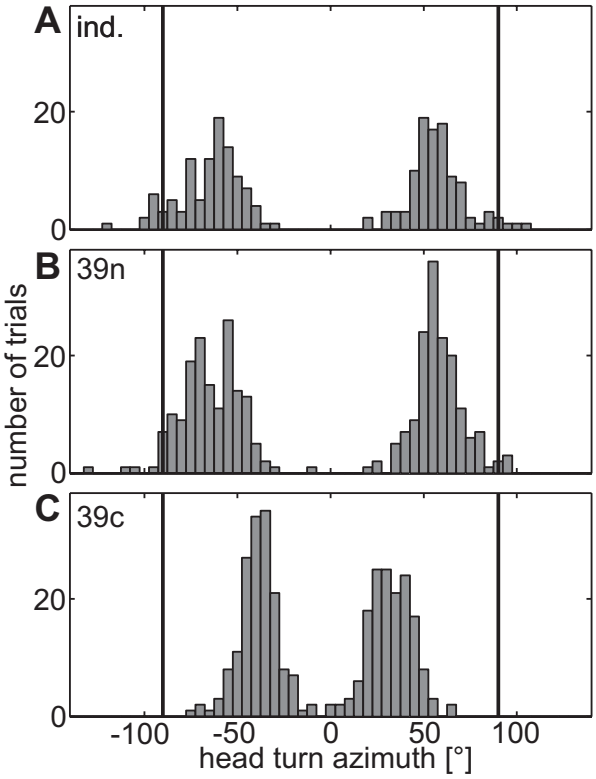

Figure 22: Histogram of azimuthal head-turn angles

The pooled azimuthal head-turn angles of **A**) owls H and S (ind. = individualized), **B**) all owls for HRTFs of owl 39 normal (39n) and **C**) owl 39 ruffcut (39c) are shown in a histogram. The vertical black line indicates 90°. All owls' responses thus lie within the frontal hemisphere. Responses to normal stimuli (A+B) were equally distributed, while those to 39c stimuli were clustered around ±40° azimuth.

Taken together, at ±140° stimulus angle, the head-turn angle was highly significantly smaller in the ruffcut condition than in any stimulus condition with intact ruff for all three owls, irrespective of whether the HRTFs were individualized or non-individualized. In contrast, the differences between conditions with intact ruff was not significant (Fig. 21, Table 4B for pooled data from all three owls and Table 10). This finding also became visible in a histogram of the pooled azimuthal head-turn angles for all owls, allowing comparison of responses to individualized stimuli (owls H and S only) with those to normal and ruffcut stimuli (Fig. 22).

To further analyze the effect of ruff removal, I plotted the azimuthal head-turn angle as a function of ITD (Fig. 23) for the normal condition (intact ruff, black line) and the "ruff removed" condition (blue line).

I reasoned that all head-turn angles should lie on one line, if the owl localized targets in both the frontal and rear hemisphere based on ITD alone. The data points for all stimulus angles up to ±100° fulfilled this expectation. By contrast, a significant deviation from the regression line was observed for stimulus azimuths of ±140° in the normal condition (black arrows and asterisks in Fig. 23, one-sample t-test, $p<0.05$; $p<0.08$ for owl H at -140°). Thus, under normal conditions, the owls associated different positions in space to targets having the same ITD, but originating from different azimuths. This is only possible if the owls used further cues to distinguish between targets with the same ITD. Without the ruff these additional cues apparently cannot be used, since the azimuthal head-turn angle did not deviate from the responses obtained with frontal-hemisphere stimulation in this condition (white arrows in Fig. 23). Thus, in the

ruffcut condition the owls behaved as if they used the ITD as the exclusive cue for stimulus azimuth.

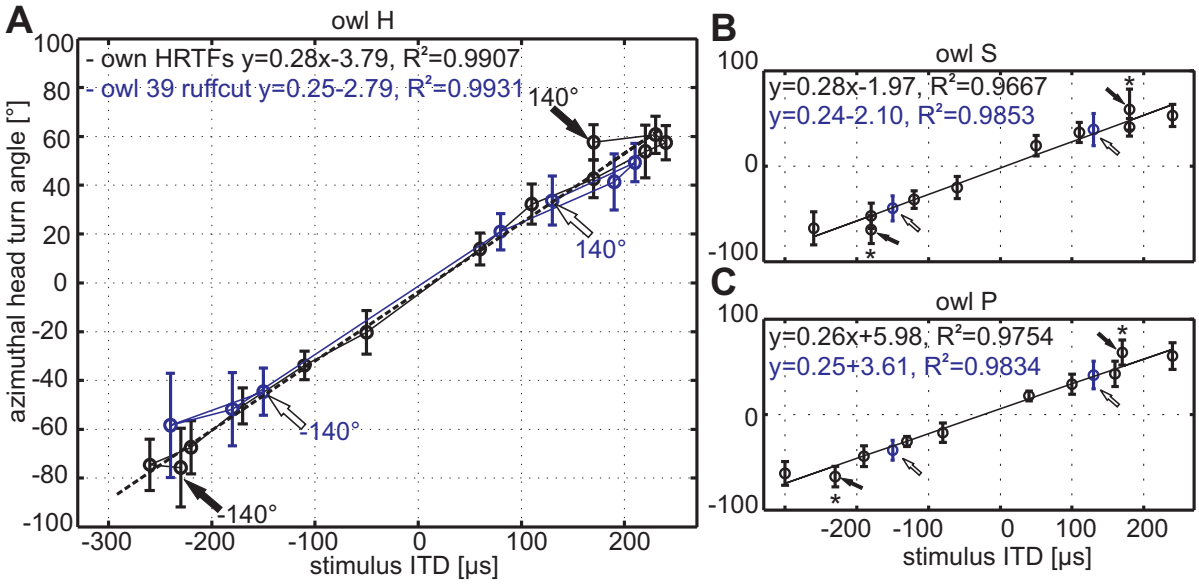

Figure 23: Prediction of azimuthal head-turns from the ITD

The ITD contained at 0° stimulus elevation in the HRTFs of **A**) owl H, **B**) owl S, and **C**) owl P were plotted against the azimuthal head-turn angle in degree. A linear regression (dotted line) through all head-turn angles shows that the owls responded well to the ITD in the HRTFs within the frontal field (≤60°). Linear equations and goodness of fit (R^2) of the regression are stated in each panel. With individualized HRTFs at ±140° (black arrows), however, the head-turn angles significantly deviated from the regression line (Mann-Whitney test, $p<0.05$).

5.3.4 Elevational Sound Localization

The owls were stimulated at elevations of -40°, 0° and 40° from various azimuthal positions. Since the owls reacted to stimulus elevation even with individualized HRTFs only in the frontal area, I will focus on stimulus angles below ±60° in the following in order to investigate the effect of ruff removal on elevational sound localization.

In response to normal individualized HRTFs (Fig. 24A+B, black circles), the mean elevational turning angles increased significantly with stimulus elevation (Mann-Whitney test, $p<0.001$). That is, the amplitude of the elevational head-turn component was positively correlated with stimulus elevation for stimulus positions within the frontal area of about ±60° azimuth. For stimulus azimuths outside the frontal area, the elevational head-turn amplitude was not correlated with stimulus elevation. This is paralleled by a less clear relationship between ILD and elevation outside the frontal area (Fig. 35F-I).

Responses to normal non-individualized HRTFs of owl 39 often resulted in smaller mean elevational head-turn amplitudes than responses to individualized stimuli (Fig. 24A+B, black: individualized, blue: owl 39 normal). For example, owl H had a mean turning angle of -28° when it was tested with its own HRTFs at -40° elevation, whereas the mean turning angle was -23.4° when it was tested with the HRTFs of owl 39 normal at the same position (Fig. 24A). This difference was significant in a t-test ($p<0.01$).

Similar observations were made with a stimulus elevation of +40° and with the other owls, which resulted in smaller, but still significant (Mann-Whitney test, $p<0.05$) slopes of the relationship between stimulus elevation and elevational head-turn angle when individualized HRTFs were compared to non-individualized HRTFs with intact ruff (Fig. 24A: owl H, Fig. 24B: owl S). Owl P responded similar as the other owls to non-individualized HRTFs for stimulus elevations -40° and 0° (Fig. 24C, gray: HRTFs of owl H, blue: owl 39 normal). For a stimulus elevation of 40°, however, this owl located stimuli lower than those at 0° elevation (Fig. 24C).

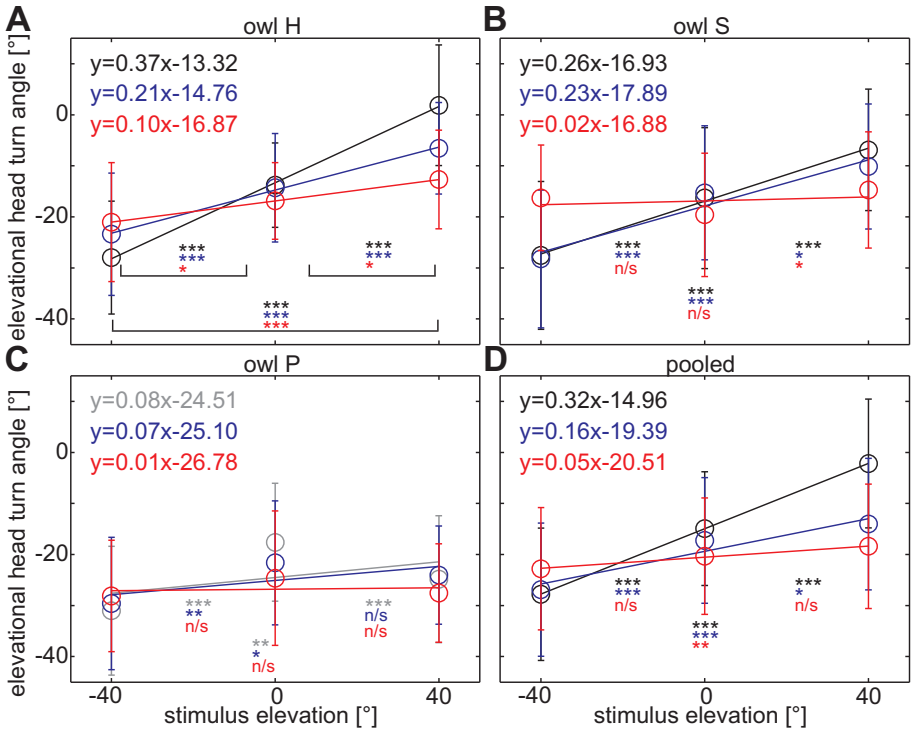

Figure 24: Elevational head-turn angles

Elevational head-turn angles (mean ± SD) are plotted against stimulus angles in the frontal hemisphere (<±60°) for **A-C**) owls H, S and P individually as well as **D**) pooled data from all owls. For each pair of stimulus angles (-40° and 0°, 0° and 40° and -40° and 40°), head-turn angles were compared with a Mann-Whitney test. Significant differences are marked with asterisks (***p<0.001, **p<0.01, *p<0.05). With individualized HRTFs (A+B, black line and circles), elevational turning angles increased significantly with stimulus elevation (Mann-Whitney test, p<0.001). The slope of this increase as given in the linear equations was lower, but still significant with non-individualized HRTFs of owl 39 normal (blue). In the ruffcut condition (red), the slope was positive for owl H, but not for owl S or owl P. Owl P reacted similar to non-individualized HRTFs (gray: owl H's HRTFs, blue: owl 39 normal) as the other two owls, but located stimuli at 40° elevation lower than those at 0° elevation. Head-turn angles increased less with stimulus elevation with ruffcut HRTFs than with normal HRTFs (D). Each data point includes at least 18 trials.

These results demonstrate that in elevation, the owls responded to normal non-individualized HRTFs slightly different than to individualized HRTFs. Differences in ILDs between individualized and normal non-individualized HRTFs were up to 8.5 dB (see above and Fig. 15C) or about 40% of the normal range (compare with Fig. 35), depending on the stimulus position. The ILD differences were increased between the stimulus condition 3 and stimulus condition 1.

In the ruffcut condition, owl H was still able to discriminate the three stimulus elevations

(Fig. 24A) meaning that the slope was significantly positive. In contrast, owl S distinguished only stimuli at 0° from those at 40° elevation, but did not discriminate between these two elevations and -40° elevation (Fig. 24B, red asterisks). For owl P, no significant differences in the elevational head-turn angles were found in the ruffcut condition for any stimulus elevation (Fig. 24C). Though owl P had difficulties in localizing stimuli at 40° elevation precisely in any stimulus condition, the general characteristics of the elevational head-turn behavior that were observed for owls H and S were preserved, in that the increase of head-turn angle with stimulus elevation was strongly reduced in the ruffcut condition compared to HRTFs recorded with intact ruff (24D).

To compare the different dependencies of the elevational head-turn amplitudes on the varying stimulus conditions, the data were pooled (Fig. 24D). The slope in the ruffcut condition (Fig. 24D, red, pooled for all owls) was clearly smaller than the slopes in the normal, individualized condition (black, pooled for owls H and S) and the non-individualized condition with intact ruff (blue, pooled for all owls). This indicated that the facial ruff provides information that helps the owl to improve localization of elevational target positions.

To test whether the changes in elevational localization were due to changes of the ILD distributions, the ILDs in the HRTFs were correlated with the amplitudes of the elevational head-turns (Fig. 25). A significant correlation was apparent for both individualized HRTFs (owls H and S, Fig. 25A) and normal non-individualized HRTFs (Fig. 25B) within the frontal area of ±60° where ILDs strongly varied with stimulus elevation (Fig. 35F-I). At more peripheral positions, where ILDs varied less systematically with elevation, ILDs were uncorrelated with the elevational head-turn angles (Fig. 25C).

In the ruffcut condition, ILDs and elevational head-turn angle were not correlated even within the frontal field (Fig. 25D). This is consistent with the observation that ILDs did not vary with elevation in this condition (Fig. 35J in the appendix).

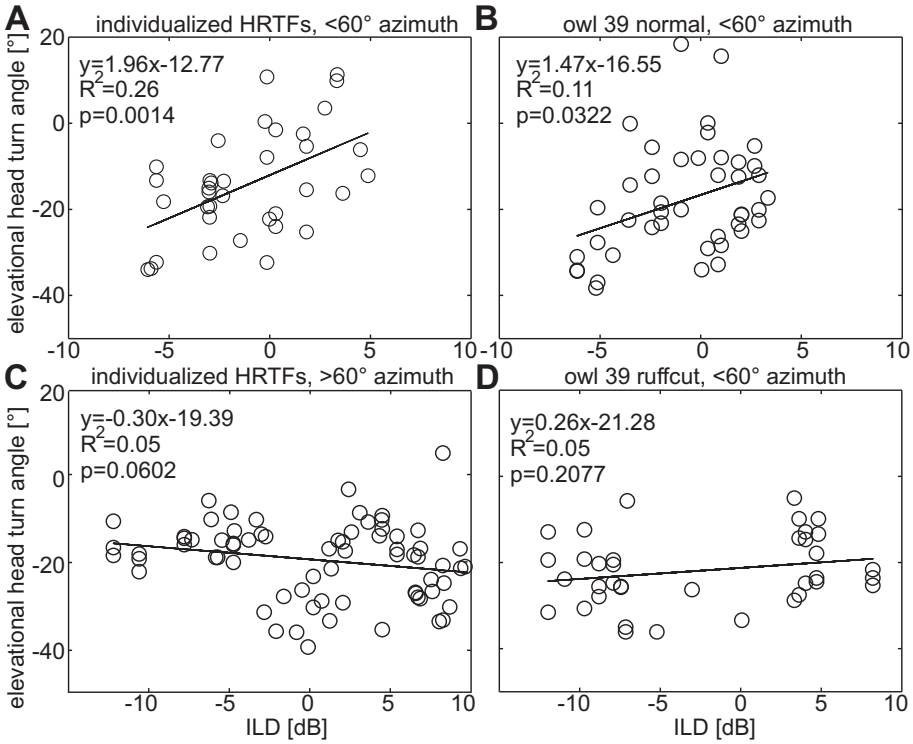

Figure 25: Elevational localization related to ILDs

For the frontal field (±60°), elevational head-turn angles were plotted against the ILDs in **A**) individualized and **B**) non-individualized HRTFs with intact ruff. Both factors were significantly correlated at the indicated level (p) within the frontal field, where ILDs strongly varied with elevation (see Fig. S4). **C**) At more peripheral positions, where ILDs did no longer vary with elevation, ILDs and elevational head-turn angles were not correlated. **D**) The same held for the ruffcut condition, where ILDs were not correlated with the elevational head-turn angle neither in the frontal field (D), nor in the periphery (data not shown).

5.4 Discussion

I simulated the removal of the barn owl's ruff in a virtual acoustic environment. Under normal virtual conditions, differences in azimuthal head-turning behavior between individualized and non-individualized HRTFs were not observed, and the owls were able to discriminate (i.e., they reacted differently to) sounds in the frontal hemisphere and targets in the rear hemisphere, respectively, even if the sounds had equal ITDs. This ability was lost after the virtual removal of the ruff.

Elevational head-turn angles were smaller with non-individualized than with individualized HRTFs. The removal of the ruff resulted in a large decrease in elevational head-turn amplitudes. In the following, I will first discuss the similarities and differences in head-turning between individualized and non-individualized HRTFs, and then turn to the ruffcut situation.

5.4.1 Sound localization with individualized and non-individualized HRTFs

The results on the equivalence of the use of individualized and non-individualized HRTFs for azimuthal sound localization in the barn owl are in accordance with findings for hu-

man listeners (Wenzel et al., 1993). Humans use both the ITD of the carrier (up to 1.5 kHz) and the ILD (at frequencies higher than 5 kHz) for azimuthal sound localization (for a review see Blauert, 1997). In the study by Wenzel et al. (1993), azimuthal localization was only marginally impaired when non-individualized HRTFs were used for stimulation. This fact suggests that the small differences in binaural cues between individualized and non-individualized HRTFs were more important for azimuthal sound localization than larger changes in monaural spectral cues.

Likewise, the observation of an increased localization error for large azimuthal or elevational values is similar to what others have observed in the barn owl (Egnor, 2001; Knudsen et al., 1979; Knudsen and Konishi, 1979; Moiseff, 1989a; Poganiatz and Wagner, 2001; Poganiatz et al., 2001), cat (May and Huang, 1996), ferret (Nodal et al., 2008), monkeys (Jay and Sparks, 1990) and humans (Populin, 2008). Nodal et al. (2008) reported that the final head bearing of the ferrets in their study before approaching a free-field sound source rarely exceeded 60° in azimuth, which is well in accordance with my results for the barn owl. Likewise, their observed head-turn latencies of about 200 ms accord with the latencies clustered around 150 ms that I measured in my experiments.

The general undershooting, i.e. a too small head-turn angle at peripheral stimulus positions, are a commonly observed phenomenon (see above). It can even occur with free-field sounds, as described by Nodal and coworkers (2008) who observed maximum head-turn angles at about ±60° for ferrets even for targets coming from the rear hemisphere. The owls in the present thesis reported all stimuli as being located in the frontal hemisphere, and therefore committed back-front errors under all conditions. However, the owls' azimuthal head-turn angles increased significantly (two-way ANOVA, $p<0.001$) with increasing stimulus azimuth under stimulation with intact ruff, and the owls localized stimuli differently even if the ITDs at two positions in the rear (140°) and front (40°) were equal (Fig. 23).

In a study by Hwang et al. (2008) and in the study by Wenzel et al. (1993), localization errors under non-individualized conditions increased in the elevational plane compared to localization with individualized HRTFs in humans, whereas azimuthal localization was barely hampered (Wenzel et al., 1988). This is what I found as well. The increased elevational localization errors in humans seem to be related to inter-individual differences in the monaural spectra. This might be the case also in the barn owl, and should be tested experimentally in this animal. The spectral notches in the HRTFs of cats (May and Huang, 1996; Tollin and Koka, 2009), rats (Koka and Tollin, 2008) or owls (Keller et al., 1998) change most prominently in the central rather than the peripheral field. Therefore, it was not surprising that vertical localization - probably also utilizing frequency-dependent cues - of the owls here was better in the frontal than the peripheral field.

In what concerns the influence of stimulus elevation on azimuthal head-turn angles (Table 4A+C), it might be difficult to understand why the stimulus elevation alone did not influence localization in the periphery (Table 4A), whereas the interaction of stimulus eleva-

tion with a given set of HRTFs (elevation*HRTF, see Table 4) influenced peripheral rather than frontal localization. However, the stimulus elevation led to a decrease head-turn angle at -40° and 40° compared to 0° elevation for any stimulus condition, which is shown in Table 4C by the significant terms for differences between the three stimulus elevations. As a consequence, the influence that stimulus elevation had on the head-turn amplitudes was similar in all owls and stimulus conditions, leading to non-significant results of the ANOVA.

However, in association with a specific set of HRTFs (intact versus removed ruff), the situation is different. In the periphery, head-turn angles strongly decrease with stimulus elevation (-40° and 40° versus 0°) when normal HRTFs are used for stimulation (Fig. 20). In contrast, when ruffcut HRTFs are used, head-turn angles in the periphery are small anyway (Fig. 21) and do not further decrease by the use of different stimulus elevations. The influence of stimulus elevation, which would normally lead to decreased azimuthal turning angles, has almost no effect here. Consequently, the stimulus elevation has a *different* effect on peripheral localization if normal HRTFs are used than when ruffcut HRTFs are used, resulting in significant terms of the ANOVA.

Interestingly, the basic features of the localization errors committed by humans and barn owls were similar, although the two species use different cues for sound localization (see Phillips (2007) for a review). For azimuthal localization errors, this may be due to the fact that ITDs depend mainly on the head diameter and sound source position, but not on frequency (for a review see (Blauert, 1997; von Campenhausen and Wagner, 2006). This is different for elevational sound localization which utilizes ILDs and monaural spectral cues and where frequency-specific peaks and notches have more influence. The monaural cues underlie stronger individual variations, but this may be overcome by frequency scaling of the directional transfer functions (Middlebrooks, 1999). Kulkarni and Colburn (1998) as well as MacPherson and Middlebrooks (2002) showed that details of the HRTF spectrum are not as important as their overall shape. This seems also to hold for the barn owl, because the owls were still able to localize the virtual sounds with non-individualized stimuli in the vertical plane, albeit with larger localization errors.

5.4.2 Localization with simulated ruff removal

In any stimulus condition, the owls reported sound stimuli - including those at stimulus angles >90° - as being in the front. Hence, all owls showed back-to-front reversals. However, under normal conditions, the owls localized targets in the periphery at larger angles than would be expected if the animals were confusing stimulus positions with identical ITDs, and were able to discriminate between targets having the same ITD (Fig. 23).

In the ruffcut condition, by contrast, the owls localized targets at ±140° azimuth at a position of about ±40° (Table 2), both positions having the same ITD (Fig. 23). They were thus apparently unable to discriminate positions on a cone of confusion, along which ITDs are identical and therefore ambiguous. Given the assumption that ITDs alone are insufficient

to distinguish between such ambiguous targets in the rear and front, these findings can only be explained if the barn owls used cues other than the ITD for the localization of the stimuli beyond some 110° in azimuth. These cues are not known at the moment. One possibility is that the owls also use ILDs, although this seems unlikely, because the owls did not discriminate well between ILDs appearing at large azimuthal values. Monaural spectral cues as observed in the high-frequency range (8-16 kHz) for humans (Langendijk and Bronkhorst, 2002) are a more likely candidate, since they allow for monaural sound localization in familiar environments (Wanrooij and Opstal, 2004) and their use to resolve front-back confusions can be specifically trained at least in human listeners (Zahorik et al., 2006). This issue needs to be further investigated in the barn owl.

Discrimination of target positions with the same ITD was not possible after the virtual removal of the ruff (Fig. 23). The removal of the ruff changed the distribution of ITDs. After the virtual removal of the ruff, the barn owls behaved as if they exclusively used the information provided by the ITD to compute the amplitude of the head-turn. In other words, ruff removal changed the important additional cues that the owl obvioulsy needs to discriminate positions having the same ITD in the frontal and rear hemispheres. After virtual ruff removal, the bird used the available information from ITDs, but this information was ambiguous and, therefore, the owls could no longer discriminate stimuli with the same ITD, but coming from different hemispheres (see Fig. 23). Ruff removal also severely hampered the owl's ability to determine stimulus elevation (Fig. 24), which can be explained by the accompanying changes in the ILD distribution (Fig. 25; von Campenhausen and Wagner, 2006; Moiseff, 1989b).

Zahorik et al. (2006) reported that human listeners stimulated with non-individualized HRTFs initially had difficulties in localizing sound sources and suffered from front-back reversals. However, their subjects learned to resolve these confusions when they received auditory, visual and vestibular feedback, so that the rate of reversals decreased. The owls in our study did not get feedback on the location of the sound source. This might explain why I did not observe any learning effects. It might be interesting to test whether additional visual feedback might also reduce back-front confusions in the barn owl.

In the present study, the use of non-individualized HRTFs in general cannot explain back-front confusions as they do in human listeners (Hill et al., 2000; Wenzel et al., 1993; Zahorik et al., 2006), since back-front reversals occurred in all conditions including individualized stimuli, and were previously observed also with free-field stimuli (Nodal et al., 2008; Poganiatz et al., 2001).

Another important question is whether in my experiments the owls could actually perceive the changes in both ITD and ILD that the simulated ruff removal caused. As Figs. 15, 36, 37 and 35 demonstrate, the ILD after ruff removal was often larger than the ILD that the owl would perceive naturally. This unnatural experience of ILDs outside the physiological range might result in confusions and hamper the localization ability. However, I think this

is unlikely, since it was shown that barn owls can not only process ITDs that are about five times larger than the physiologically occurring ITDs (Saberi et al., 2002), but also localize ILDs of up to ±25 dB (Egnor, 2001), well outside the natural range. Responses to large ILDs were observed on both the behavioral and neuronal levels (Egnor, 2001), although it has to be mentioned that the responses (the neuronal firing rate and the elevational head-turn angles, respectively) in that study reached a saturation plateau at about 10-15 dB ILD, which corresponds approximately to the maximum physiological ILD. Since the high-frequency spatial receptive fields in the auditory cortex of ferrets change depending on the use of individualized versus non-individualized virtual sound stimuli (King et al., 2001; Mrsic-Flogel et al., 2001), it would be an interesting future project to collect electrophysiological data on the neuronal responses to virtual ruffcut stimuli also in the barn owl.

Stimulation with earphones and varying stimulus parameters like ITD and ILD may be seen as the first step to create a simulated acoustic environment. Such stimulation was used to determine the importance of ITD for azimuthal sound localization (Moiseff and Konishi, 1981a; Moiseff, 1989a; Saberi et al., 1999) and the importance of ILD for elevational sound localization (Egnor, 2001; Moiseff, 1989a; Poganiatz and Wagner, 2001). In humans, presentation of ITD via headphones results in lateralization, but not in externalization (Wightman and Kistler, 1989a,b). Headphone stimulation removes the specific effects of mainly the pinna on the incoming sound. In barn owls, headphone stimulation without using HRTF-filtered sound signals also removes the effect of the ruff. This is the main effect, since the barn owl has only a small ear flap whose function is unclear.

Thus, the ruff in the barn owl is a structure which is functionally equivalent to the pinna in other animals and humans. Therefore, the virtual removal of the ruff might be expected to result in a similar influence on localization performance as plugging or removal of the pinna of other binaurally hearing species. Cats, for example, use spectral cues in the mid- and high-frequency range for elevational sound localization especially in the median plane (Huang and May, 1996; May and Huang, 1996; Populin and Yin, 1998a). In mammals, the pinna typically increases the monaural gain (in dB) and crucially influences the localization cues (Musicant et al., 1990; Tollin and Koka, 2009). Consequently, the ability to localize sound-source elevation is hampered after removal or occlusion of the pinnae in various species such as chinchillas (Heffner et al., 1996), ferrets (Parsons et al., 1999), bats (Aytekin et al., 2004; Wotton et al., 1995) or humans (Gardner and Gardner, 1973). Thus, the results from this part of the thesis underline the functional similarity of the facial ruff in the barn owl with the pinna in mammalian species, including effects on vertical and azimuthal sound localization and specifically in the discrimination of spatial positions with the same ITD.

5.4.3 Evaluation of the stationary experimental design

One could argue that pure head movements as required in the present experiments did not reflect the owl's complete natural behavior, where the saccadic head-turn usually precedes the initiation of a prey strike sequence. The present experiments were designed as a stationary behavioral task, in contrast to a free-flight paradigm where the animal has to approach or hit the target position to fulfill the task. While the former design is easier to conceive and yields more trials per day, the latter is a closer approximation of the natural striking behavior of the owl (Konishi, 1973a,b; Payne, 1962; Shifferman and Eilam, 2004; Singheiser et al., 2010).

The localization precision that the owl achieves in the stationary task should be mainly due to its sensory ability to fulfill the task, whereas the precision in the free-flight experiments include the complex motor task that is required to direct the owl's body towards the distant target. In the latter case, in addition to the sensory limitation of localizing a sound source, the motor abilities are restricted, that is, the owl cannot unlimitedly react with a turn of the body towards the target, at least not when the target position changes (Hausmann et al., 2008). This means that if the same task is repeated (for example flying towards the ground in order to strike a loudspeaker that emits 1-10 kHz broadband noise), the landing position of the owl will show a certain jitter. In addition to the influence of sensory limitations, the jitter may further increase due to restrictions in the owl's motor program while approaching the target (i.e., directing its body into the target direction, see Hausmann et al., 2008), and to the fact that the owl needs to memorize the target position without constant stimulus feedback.

The owl performs head saccades in response to a stimulus also in free-flight tasks before it leaves the perch for target strike (Ohayon et al., 2008). Thus, imprecision of head saccades are involved in both stationary and free-flight tasks, while imprecision of the flight only affects landing precision in the latter task. The difference in localization precision between both concepts is a measure for the contribution of both, sensory and motor, components to overall localization precision, and can help to assess existing stationary experimental results with respect to their relevance for natural behavior.

Sound localization precision in stationary tasks is with angular deviations from the target position of 3-10° in the frontal field similar to that found in free-flight studies (Bala et al., 2003, 2007; Knudsen et al., 1979; Konishi, 1973a,b; Poganiatz and Wagner, 2001; Poganiatz et al., 2001; Singheiser et al., 2010). From these results, it can be concluded that barn owls' localization precision is mainly influenced by sensory rather than motor restrictions, and, therefore, the results from the experiments involving only head-turn saccades towards the target should not be hampered in their validity compared to free-flight studies.

5.5 Conclusions

The results from this experimental series show that the facial ruff improves a) peripheral sound localization by increasing the ITD range and by yielding localization cues that allow discrimination of positions with equal ITD, and b) elevational sound localization in the frontal field by introducing a shift of iso-ILD lines out of the midsagittal plane, which causes ILDs to increase with increasing stimulus elevation. I also demonstrated that the changes at the behavioral level might be related to the changes in the binaural physical cues, ITD and ILD, that occur after the virtual removal of the ruff. The functional similarity of the facial ruff with that of the pinna in humans opens the possibility to use these data for autonomous agents (Calmes et al., 2007), improvement of auditory displays (Kim and Choi, 2005; Walker and Lindsay, 2006) or even in hearing aids (Dietz et al., 2009).

However, it also became clear that broadband stimulation is insufficient to resolve the role of ILDs for elevational sound localization in enough detail. For that reason, I performed a further series of behavioral experiments involving narrowband-filtered HRTFs. The results from these experiments are presented in the following section.

6 Behavioral responses to narrowband stimuli

Barn owls can localize broadband sounds with high accuracy, but localization errors increase when stimuli are narrowband noises or tones. This difference might be caused by evaluation of frequency-specific variations of ILDs or spectral cues in broadband sounds, which are present to a smaller extent in narrowband noise. It is still unclear how exactly the owls can make use of the ILDs which are present in their head-related transfer functions (HRTFs), especially in concerns of elevational sound localization. In this experimental series, HRTFs of three barn owls were 1/3 octaveband-filtered in order to create virtual acoustic stimuli. These were presented via headphones in behavioral experiments to investigate how such narrowband HRTFs influenced sound localization ability in both the horizontal and vertical planes. In a first stimulus paradigm, virtual stimuli contained the naturally occurring ILD for center frequencies from 1 to 9 kHz (native condition), or in a second stimulus paradigm, the ILD of 1/3 octaveband-filtered noise with 5 kHz center frequency was set to a mean ILD of 0 dB while preserving the native monaural spectrum (fixILD condition). I found that with native ILDs, the owls could distinguish stimulus elevations for frequencies above 2 kHz. In the fixILD condition, in contrast to native stimuli of the same frequency, the ability to determine stimulus elevation was lost. Furthermore, with fixILD stimuli, the owls turned their heads towards phantom sound sources, a phenomenon that occurs due to phase ambiguities in narrowband stimuli. Localization of phantom sources was not observed using normal 1/3 octaveband-filtered HRTFs. These findings suggest that ILDs are not only crucial for high-frequency elevational localization, but that owls might also use ILDs to resolve spatial coding ambiguities if ITD information is insufficient.

6.1 Introduction

In the previous section, I investigated the influence of the facial ruff on sound localization using broadband HRTF-filtered stimuli. The ITD is largely frequency-independent for most frequencies apart from a decrease in the 2-3 kHz band (von Campenhausen and Wagner, 2006). Barn owls as well as other animals use ITDs for localization in the horizontal plane (Carr and MacLeod, 2010, McAlpine et al., 2001, cat: Casseday and Neff, 1973, guinea pig: Shackleton et al., 2003, gerbil: Seidl and Grothe, 2005, owl: (Knudsen et al., 1979; Moiseff and Konishi, 1981a; Poganiatz et al., 2001)). ITD is computed in the brain by narrowband cross-correlation (e.g., Cai et al., 1998a,b; Colburn, 1973; Fischer et al., 2008; Goldberg and Brown, 1968, 1969; Rose et al., 1966; Yin and Kuwada, 1983) followed by across-frequency integration (Akeroyd, 2006; Shackleton et al., 1991; Stern et al., 1988; Wagner et al., 1987). While broadband stimuli yield unambiguous information about the ITD, narrowband stimuli

and specifically tonal stimuli contain phase ambiguities (for a review see Wagner, 2004). With narrowband stimuli, barn owls experience phantom sources (Saberi et al., 1998, 1999), i.e. they turn the head towards non-existing sound sources at a position that can be predicted from the signal's wavelength and the effective head diameter. The basis of this phenomenon are phase ambiguities which occur in tones or narrow frequency bands when a phase leading at one ear cannot be distinguished from its multiples leading at the opposed ear (Saberi et al., 1998, 1999). If the resulting phantom source lies outside the physiological range (i.e. if the ITD exceeds ±300 µs) or in the very far periphery, which is the case for frequencies below about 2-3 kHz, barn owls should not localize phantom sources.

When the bandwidth of the stimulus increases to about 1-2 kHz, integration across frequency channels allows for a resolution of ambiguities and phantom sources are no longer localized (Saberi et al., 1998, 1999). Interestingly, this critical bandwidth slightly differs between stimulation from free-field sound sources and stimulation via headphones (Kettler, 2010; Saberi et al., 1998). With headphone stimulation using narrowband noise centered at 5 kHz, the stimulus bandwidth had to be 2 to 3 kHz before phantom sources disappeared. In contrast, this critical stimulus bandwidth decreased to 1-2 kHz when free-field sound sources were used for stimulation (Kettler, 2010; Saberi et al., 1998). The headphone stimuli in the cited studies did not contain ILDs, since only defined ITDs were introduced to the narrowband noise stimuli. In contrast, free-field stimulation results in ILDs as long as the sound sources are not placed along the zero-ILD line (cf. von Campenhausen and Wagner, 2006 and Fig. 4). Due to the owls' asymmetrical ear placement, most sound sources produce ILDs if placed along the horizontal midline. HRTF-filtered stimuli do also contain ILDs as shown by Keller et al. (1998).

The difference in the critical bandwidth below which the owls localize phantom sources could thus be due to the use of ILDs in free-field or HRTF-filtered stimuli, but not in headphone stimulation including only ITDs.

While signal frequency and bandwidth clearly play a role in the resolution of phase ambiguities (Wagner, 2004), the involvement of other cues such as interaural level differences (ILD) remains unclear. ILDs are a consequence of the frequency-dependent, and both location-specific and ear-specific attenuation of the impinging sound by the head and body of an animal (Rayleigh, 1907).

The spatial distribution of ILDs follows a complex distribution that changes widely with frequency (Keller et al., 1998; von Campenhausen and Wagner, 2006). A characteristic feature of the frequency-specific ILD distributions is that ILDs are small and hardly vary with elevation at low frequencies, but they strongly vary with elevation and form almost horizontal iso-ILD lines at high frequencies (von Campenhausen and Wagner, 2006; Keller et al., 1998, and Figs. 4+9). Similar ILD distributions with small ILDs at low frequencies and large ILDs at high frequencies are also present in humans (Wightman and Kistler, 1989a), monkeys (Spezio et al., 2000) or rats (Koka and Tollin, 2008).

Poganiatz and Wagner (2001) investigated the influence of broadband ILDs (4-10 kHz) on elevational sound localization behavior. These frequencies cover the range most important for sound localization in the barn owl (Konishi, 1973a,b; Singheiser et al., 2010). Poganiatz and Wagner (2001) manipulated the virtual stimuli by setting the mean ILD to either -6 dB (left ear louder) or to +6 dB (right ear louder) independent of stimulus location while preserving all other location cues. The owls' elevational head-turn angles in response to those manipulated stimuli were directed to the elevation that was coded by the fixed ILD for most, but not for all stimulus positions. Hence, the use of broadband ILD could only partly explain the elevational head-turn behaviour. These authors already speculated that the frequency-specific ILDs may improve elevational sound localization. This hypothesis is followed up with the experiments outlined here.

If the owl uses ILDs, then the question arises of whether it can use ILD cues in single frequency bands, or if integration across frequencies is needed for accurate localization. Current evidence implies extraction of sound localization cues in single frequency bands, with subsequent integration of binaural and spectral cues in the external nucleus of the inferior colliculus (ICx) and in the optic tectum, where the information is combined in a spatial map (Knudsen and Konishi, 1978).

In this chapter of the thesis, I tested the assumption that barn owls could use ILDs in narrowband HRTF-filtered stimuli for elevational localization as well as for the identification of phantom sources. For this purpose, I used the same behavioral paradigm introduced in section 5.2 to stimulate barn owls with 1/3 octaveband-filtered HRTFs centered at frequencies between 1 and 9 kHz. Hence, it could be analyzed at which frequencies and to what extent the owls can determine stimulus elevation.

In an additional stimulus condition, I fixed octaveband HRTFs with 5 kHz center frequency at a mean ILD of 0 dB, meaning that only minor residual ILDs were present between the stimuli for the left and right ear, respectively. Comparison of this "fixILD" condition with reactions to the HRTFs containing the natural ("native") ILD that usually occurs in free-field stimuli served to answer the question of whether the ILD was indeed the crucial cue for the owl to resolve stimulus elevation and to distinguish phantom sources from the correct sound source.

6.2 Methods

Throughout this chapter, the term "real" sound source refers to a virtual stimulus replayed via headphones, providing the same amplitude of localization cues (ITD, ILD, monaural spectra) that would also be present in a free-field sound from the same spatial position. In contrast, the position of a "phantom source" is calculated from the phase equivalents of a given stimulus as described in the Introduction.

6.2.1 Animals and Handling

For this part of the thesis, I used the three barn owls (owls H, S and P) that had already participated in the experiments described in section 5. Care and treatment of the owls were in accordance with the guidelines for animal experiments as approved by the Landespräsidium für Natur, Umwelt und Verbraucherschutz Nordrhein Westfalen, Recklinghausen, Germany, and complied with the NIH Guide for the use and care of laboratory animals.

For the calculation of stimuli for the behavioral experiments, the three sets of individualized HRTFs measured as described in section 5.2 were re-used.

6.2.2 Creation of 1/3 octaveband-filtered stimuli

For a closer investigation of the role of frequency-specific localization cues, I calculated 1/3 octaveband filters from the owls' individualized HRTFs, with center frequencies of 1, 2, 3, 5, 7 and 9 kHz as described in section 4.2.3. Filtering of broadband noise (300 Hz to 15 kHz) with these octaveband filters resulted in narrowband signals (head-related impulse responses, HRIRs). The corresponding HRIRs for -40° and 40° azimuth and either -40°, 0° or 40° elevation were used for stimulation of the owl. Apart from the stimuli, the behavioral testing paradigm was identical to the simulation of ruff removal described in section 5.2.

The filter bandwidth of 1/3 octave was chosen because the basilar membrane of the cochlea acts as a filter where incoming sound is processed in frequency "channels" having a width of approximately one third of an octave, with an overrepresentation of high frequencies from 5-10 kHz (Köppl, 1997). Critical bands in barn owls approximate 1/3 octave bandwidth (Quine and Konishi, 1974), similar to the cat (Ehret and Schreiner, 1997; Nienhuys and Clark, 1979). Thresholds increase by about 15 dB per octave for frequencies below 1 kHz and by about 40 dB per octave at frequencies above 3 kHz (Dyson et al., 1998).

Each of these HRTF-filtered stimuli contained a naturally occurring ("native") ITD, ILD and monaural spectrum, meaning that the amplitude of these cues reflected the situation in free-field sounds. Therefore, I will call this first stimulus condition the "native" or natural condition. On the other hand, I also calculated stimuli whose mean ILD was set to 0 dB, similar to the approach described in Poganiatz and Wagner (2001). This was the so-called "fixILD" condition, or stimulus condition 2. For this stimulus condition, I first calculated the average energy (intensity) of each ear's signal by squaring the sum of the signal in the

time domain within the 5 kHz octaveband, and then calculated the average energy in decibel using the common logarithm following equation 5:

$$intensity[dB] = 10 * log10(energy) \tag{5}$$

Since the ILD is by the factor 2 smaller than the interaural intensity (IID), an IID of zero also results in an ILD of zero dB. In the following, I will use the term "fixILD" to refer to stimuli with a mean ILD (and IID) of zero dB corresponding to equation 6:

$$level[dB] = 20 * log10(energy) \tag{6}$$

The average binaural level (ABL) was calculated as the mean sum of the right and left ear's levels:

$$ABL[dB] = \frac{(level\,right\,ear + level\,left\,ear)}{2} \tag{7}$$

The interaural level difference (ILD) was defined as the difference between the levels from the right and left ears:

$$ILD[dB] = levelrightear–levelleftear \tag{8}$$

For the calculation of stimuli, the difference of each ear's signal to the average amplitude of both ears was added to the signals for the left and right ear, respectively, in order to set the ILD to 0 dB while keeping the average amplitude constant. For example, if the level of the right ear's signal in the 5 kHz-octaveband was 10 dB (right ear louder) and that of the left ear was 2 dB (left ear louder), then the right ear's signal was reduced by 4 dB and the left ear's signal was amplified by 4 dB in order to preserve the ABL of 6 dB (Fig. 26). Note that since the native monaural spectra of the stimuli were preserved, only the mean ILD was set to zero dB. This resulted in small residual ILDs of about ±2 dB in the stimuli after manipulation (Fig. 26G, gray). The stimuli were presented at 33.2 ± 2.7 dB SPL, approximately 20 dB above the owl's hearing threshold, via headphones that were calibrated for their influence on the signals. Level of the background noise in the experimental chamber was at 23 dB SPL.

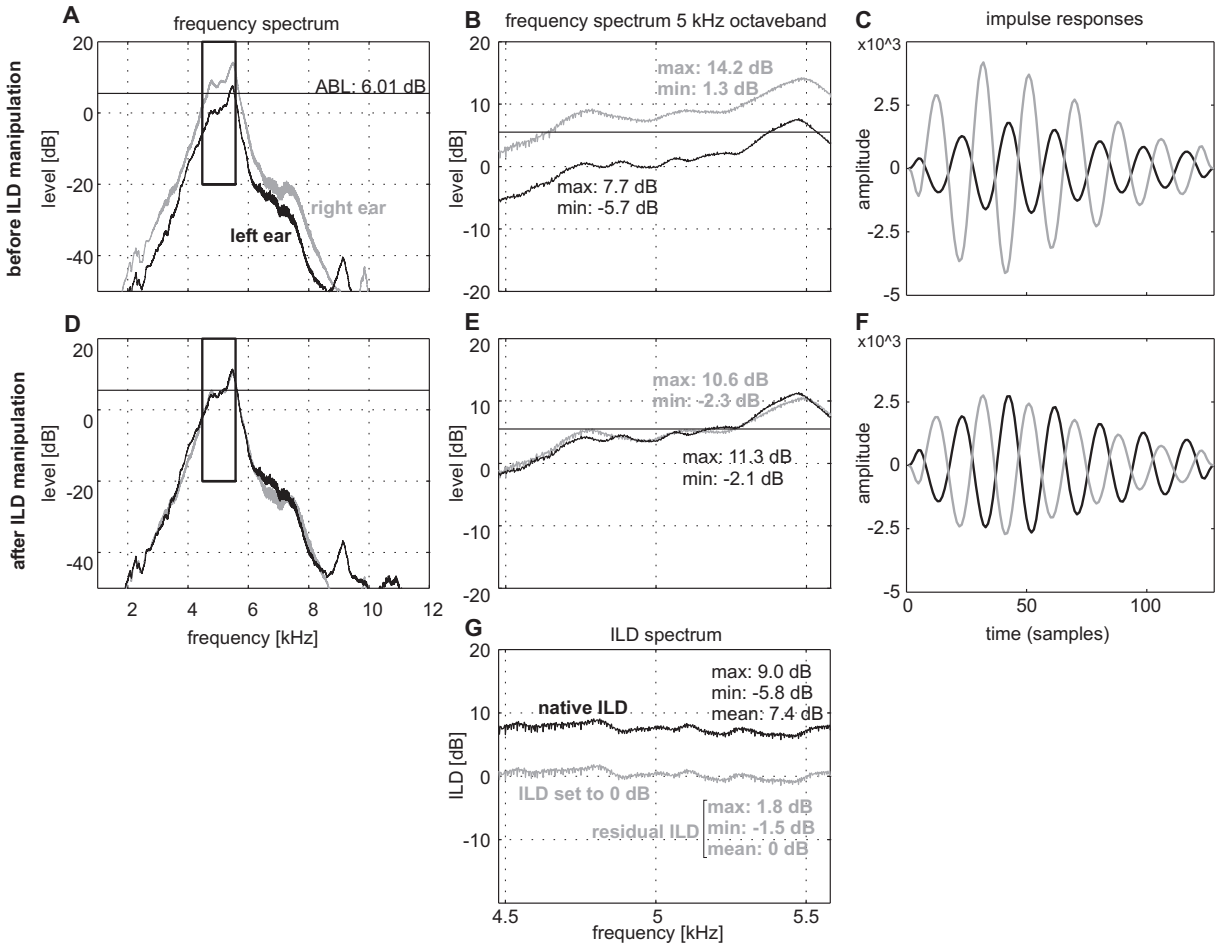

Figure 26: Calculation of stimuli with fixed ILD

A) For the stimulus condition where the ILD was set to 0 dB, the level for each ear's signal (black = left ear, gray = right ear) was calculated in the 1/3 octaveband centered at 5 kHz. Exemplary shown are the levels for 40° stimulus azimuth and 0° elevation. The black frame shows the borders of the 5 kHz octaveband and is enlarged in panel **B**). **C**) Impulse responses for the left (black) and right (gray) ear for the corresponding stimulus position. Maximum (max) and minimum (min) amplitudes are indicated in dB. **D-F**) Analogously to panels A-C), the same signal is shown after the ILD was set to 0 dB. The left and right ear's signals were then shifted by the absolute value needed to achieve an ILD of 0 dB while keeping the average binaural level (ABL) constant. Small residual ILDs (±2 dB) remained, which was due to the preserved monaural spectra. **G**) ILD spectra for the unmanipulated signal (black) and after the mean ILD was set to 0 dB (gray). The minimum, maximum and mean ILD in dB are indicated for each signal.

6.2.3 Experimental Procedure

The experimental procedure during this experimental series was identical to that of the previous behavioral experiments described in section 5. The behaving owl was placed in the same sound-attenuating chamber where also the HRTFs were recorded. HRTF-filtered stimuli were replayed through headphones (Sony MDR-E831LP) that were attached to a metal plate in the owl's skull. The same metal plate also held the sensor of a real-time head-tracker (MiniBird, Ascension Technology Corporation, Burlington, Vermont, USA) which allowed to record the position of the owl's head constantly at 80 Hz sample rate. The owl was trained to fixate a frontally mounted red light diode. When the owl's head position deviated by less than 5° of azimuth and less than 7° of elevation from this position that was defined as 0° azimuth and 0° elevation, a stimulus was triggered.

The owl's head saccades were counted as valid trial if it exceeded a velocity of 20 °/s and occurred within 50 to 500 ms after a stimulus was provided. Otherwise, the trial was defined as incorrect trial or error, as was a trial in which the owl did not move its head at all (no-reaction trial). The time between stimulus onset and the owl's head-turn was defined as latency.

Each owl was stimulated at ±40° azimuth and -40, 0 and 40° elevation at least 20 times. Stimulus duration was 100 ms. Spatial positions were presented in pseudo-randomized order in the course of daily experimental sessions, each lasting between 20 and 60 minutes. The owl received a food reward in 60 % of all trials. The animals were rewarded randomly and not based on deviation from the expected target, because I did not know in advance how the owls would perceive the narrowband stimuli. Random rewarding prevented selective rewarding of specific spatial positions, which may occur if the spatial position that the owl perceives strongly deviates from the expected position.

Throughout this chapter the term "real" sound source refers to a virtual stimulus replayed via headphones, providing the same amplitude of localization cues (ITD, ILD, monaural spectra) that would also be present in a free-field sound from the same spatial position. In contrast, the position of a "phantom source" is calculated from the phase equivalents of a given stimulus. In the barn owl, the ITD changes by 2.5 µs per degree in azimuth (von Campenhausen and Wagner, 2006). For example, for 5 kHz tone with a period duration of 200 µs a signal with left-side leading of 50 µs would be located at -20° azimuth, while the phantom source, occurring at +150 µs (right ear leading), would be located at 60° azimuth.

6.3 Results

For all three owls (owls H, S and P) that participated in this experimental series, the spatial distribution of ILDs in the various frequency bands was characteristic as measured by Keller et al. (1998) or von Campenhausen and Wagner (2006), meaning that ILDs were small and mainly varied with azimuth for frequencies below 3 kHz, whereas their amplitude was large and strongly varied with elevation for higher frequencies (Fig. 27).

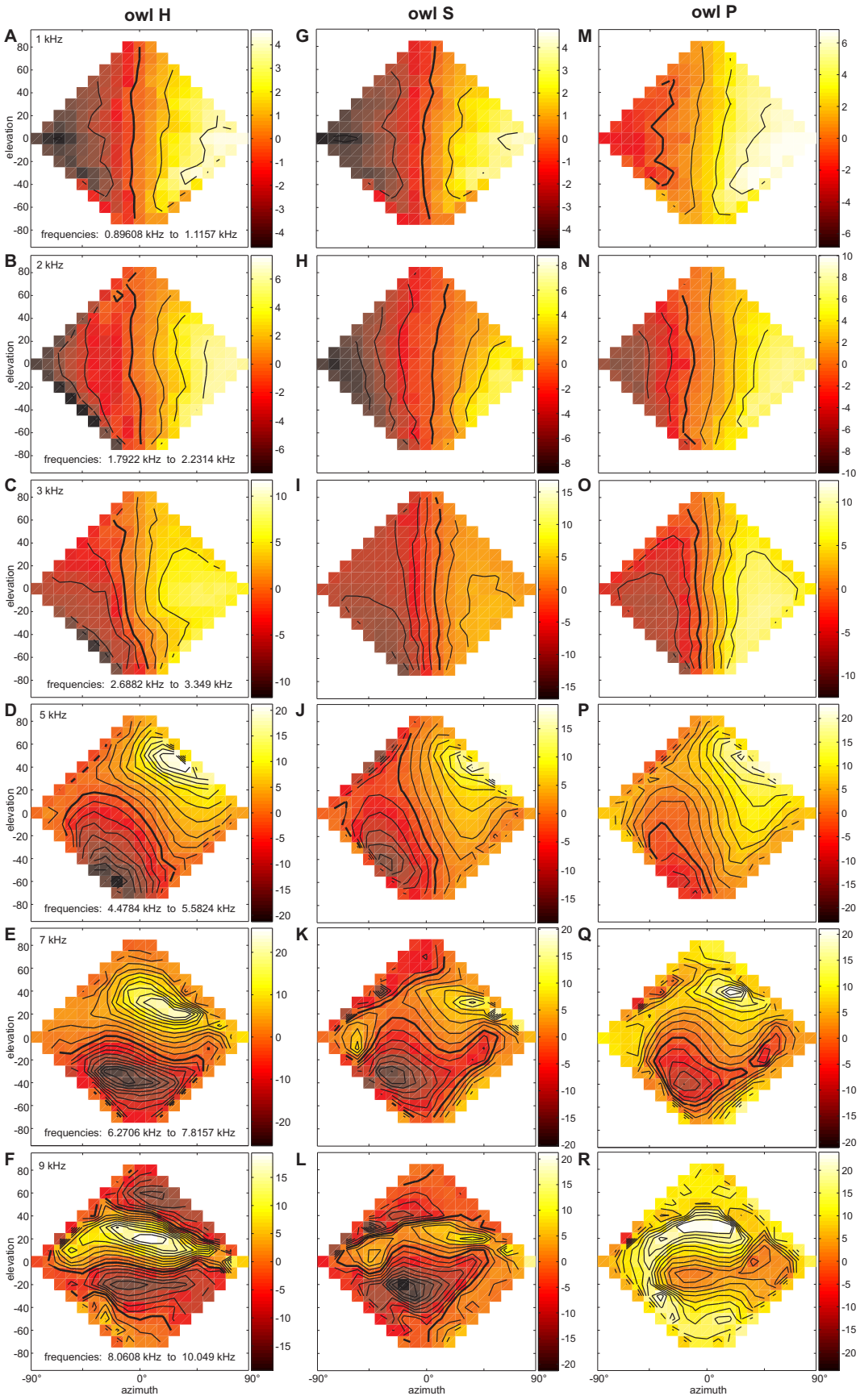

Figure 27: 1/3 octaveband-filtered HRTFs at various center frequencies.

HRTFs of the three behaving owls (**A-F**) owl H; **G-L**) owl S and **M-R**) owl P) were 1/3 octaveband-filtered, resulting in ILD patterns of increasing complexity with increasing center frequency (given in the upper left corner, in kHz). At low frequencies, ILDs were small and hardly varied with elevation, whereas they strongly varied with elevation at frequencies >3 kHz.

The owls were stimulated with 1/3 octaveband-filtered HRTFs at either -40 or +40° azimuth and three different elevations (-40°, 0° and 40°). There were two stimulus paradigms: first, the ability of the owls to localize octaveband-filtered noise bursts containing the natural localization cues was tested for center frequencies from 1 to 9 kHz. In the second condition, the ILD of stimuli with 5 kHz center frequency was set to zero dB ILD to see whether the owls might use ILDs for elevational localization and/or for the detection of phantom sound sources.

Over a period of several months, a total of 3999 trials were collected for the three owls. For owl H, 1342 trials were recorded, among which 229 trials did not meet the criteria for correct head-turn responses as defined in section 6.2.3. For owl S, 1412 trials were recorded among which 218 were invalid as defined by the error criteria, and for owl P, 178 of 1245 trials were invalid. The occurrence of invalid trials was evenly distributed across center frequencies and stimulus elevations.

6.3.1 Localization of 1/3 octaveband-filtered noise

All owls localized 1/3 octaveband-filtered broadband noise quite accurately in azimuth for each of the center frequencies from 1 to 9 kHz (Fig. 28).

For example, Fig. 28A shows the mean head-turn angles of owl H in response to the two stimulus azimuths (-40° in black, +40° in white) and three stimulus elevations (-40, 0 and 40°). When the stimulus angle was -40°, the owl always turned its head towards about -40° azimuth as shown on the x-axis. The y-axis denotes elevational head-turn angles. At 1 kHz, owl H turned the head towards an elevation slightly below the horizontal plane irrespective of the stimulus elevation (black circles and triangles in Fig. 28A for -40, 0 and 40° elevation, respectively). Thus, at 1 kHz center frequency and -40° stimulus azimuth, the owl was unable to discriminate between the three stimulus elevations. The same held for positive stimulus angles (white circle and triangles in Fig. 28A), where the owl localized stimulus azimuth correctly near 40° with an undershooting (i.e., too small head-turn angle) of about 10°. This time, head-turn elevations were slightly positive.

With increasing frequency (top to bottom, Fig. 28A-F), elevational head-turning components in owl H increased and were directed more towards the elevation represented by the stimuli. In other words, when stimulus elevation was -40° at 3 kHz frequency, the head-turn angle of owl H was about -15 to -20° for 40° and -40° stimulus azimuth, respectively (leftwards triangles, Fig. 28C). For 40° stimulus elevation (rightward directed triangles), elevational head-turns were directed towards positive elevations, even though the absolute head-turn angles were far too small.

Elevational localization was best for stimuli having a center frequency of 5 kHz, meaning that the elevational head-turn angles were closest to the stimulus position (Fig. 28D). For the other two owls, the general extent of azimuthal and elevational head-turn amplitudes was similar to owl H (Fig. 28G-L for owl S, M-R for owl P). Mean localization errors for all

owls are also given in Table 6.

In summary, the three barn owls exhibited almost normal azimuthal sound-localization behavior, as compared to broadband sound localization, in response to native 1/3 octaveband-filtered stimuli. By contrast, only stimuli having center frequencies above 3 kHz elicited head turns with elevational components different for stimuli originating from below and above the horizontal plane.

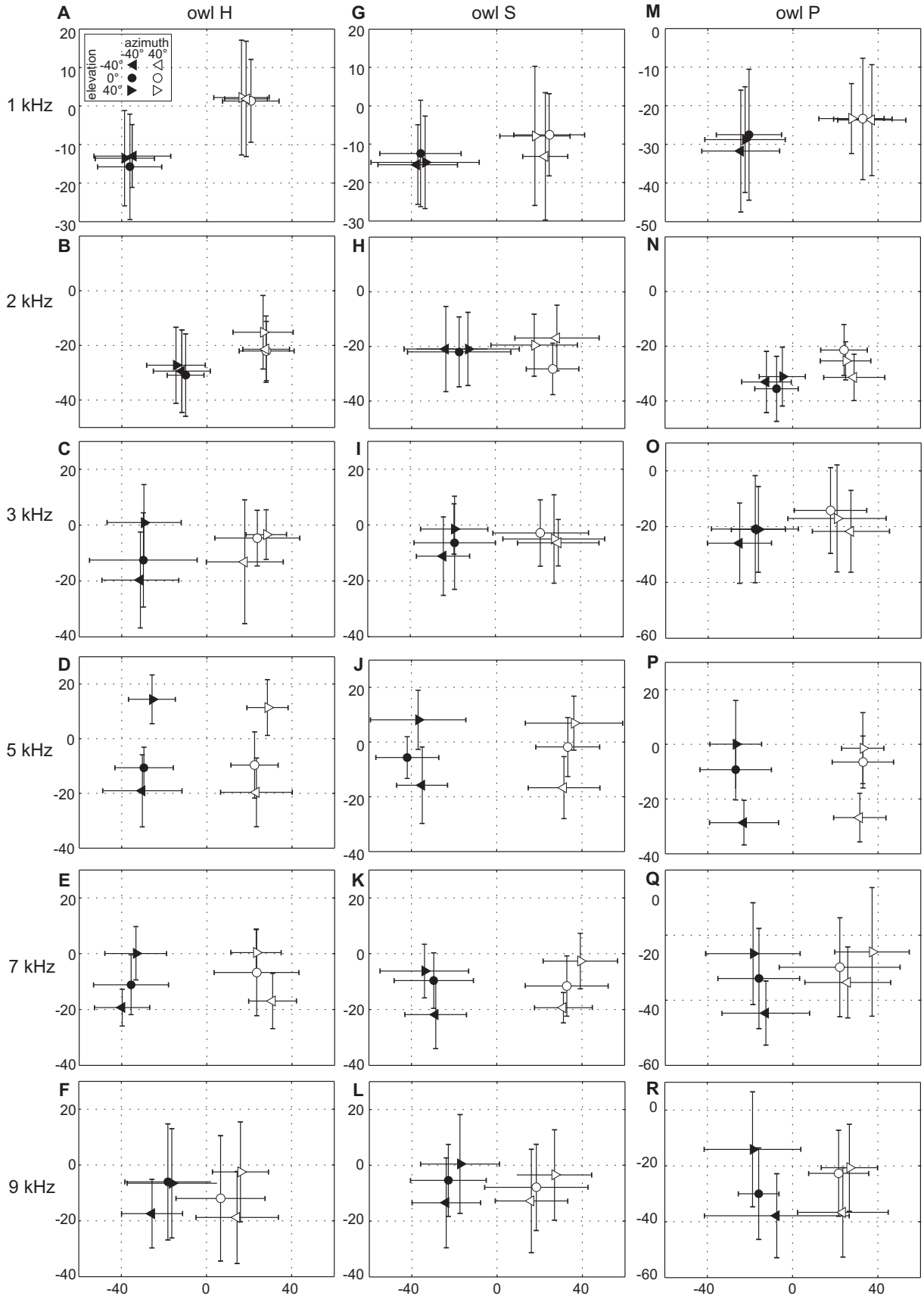

Figure 28: Reactions to 1/3 octaveband-filtered stimuli

For the center frequencies denoted left to each row, the mean azimuthal head turn angle is plotted against the mean elevational angle for each owl (**A-F**) owl H, **G-L**) owl S, **M-R**) owl P).

For all three owls, an ANOVA analysis of variance with Scheffé post-hoc test was performed to test whether the owls could localize virtual sound source elevation at the different stimulus frequencies (Table 5).

Table 5: Influence of stimulus frequency on head-turn elevation
For each of the owls as well as for the pooled data, an ANOVA with Scheffé post-hoc test (p values are given in each column) revealed a signifcant influence of frequency on head-turn elvation for frequencies above, but not below 3 kHz. With stimuli of 5 kHz where the ILD was set to 0 dB (fixILD), two of the owls were not able to determine stimulus elevation.

frequency [kHz]	Owl H	Owl S	Owl P	pooled, all owls
1	0.962	0.370	0.720	0.944
2	0.351	0.036	0.024	0.372
3	0.000	0.303	0.131	0.001
5	0.000	0.000	0.000	0.000
7	0.000	0.000	0.012	0.000
9	0.001	0.003	0.000	0.000
broadband	0.000	0.000	0.082	0.000
fixILD	0.961	0.000	0.291	0.012

The influence of the stimulus frequency on the elevational head-turn angle was not signficant for 1 and 2 kHz for all owls. In other words, none of the owls could discriminate stimulus elevations at those frequencies. For owls S and P, it was also not significant at 3 kHz. At frequencies above 3 kHz, however, all owls were able to discriminate stimulus elevation ($p<0.001$). This can also be seen in Fig. 29A, in that the mean elevational head-turn angles are equal for all three stimulus elevations at 1 and 2 kHz frequency, but the owls start to exhibit different elevational head-turn angles at 3 kHz and higher frequencies.

For all stimulus angles, azimuthal accuracy exceeded elevational accuracy in terms of the localization error, i.e. the mean deviation between stimulus angle and head-turn angle (Fig. 29B, Table 6).

Table 6: Mean localization errors with octaveband stimuli
The first column gives the centre frequency of the respective 1/3 octaveband. The second column gives the azimuthal localization error, the third column the elevational localization error in degree for pooled data of all owls.

frequency [kHz]	azimuthal error [°]	SD azimuth [°]	elevational error [°]	SD elevation [°]
1	13.78	3.09	31.65	19.07
2	21.10	7.89	34.76	23.83
3	17.56	3.10	27.28	16.97
5	10.32	2.19	19.99	12.15
7	11.52	3.62	27.35	18.13
9	22.01	2.69	25.73	16.18
broadband	7.03	2.99	28.68	21.43
fixILD	36.56	5.74	34.34	21.54

The respective localization error that the owls committed with broadband noise is indicated by the black line for the azimuthal deviation to the stimulus angle, and by the dotted

line for the elevational deviation (Fig. 29B). That is, in response to native HRTFs, the owls discriminated stimulus azimuth accurately with mean localization errors between 7° (broadband) and 22° (9 kHz, see Table 6). Elevational errors were with 20° (5 kHz) to 35° (2 kHz) higher (Table 6), which was mainly due to a small elevational head-turn angle at 40° stimulus elevation (Fig. 29A). The respective localization error that the owls committed with broadband noise is indicated by the black line for the azimuthal deviation to the stimulus angle, and by the dotted line for the elevational deviation (Fig. 29B).

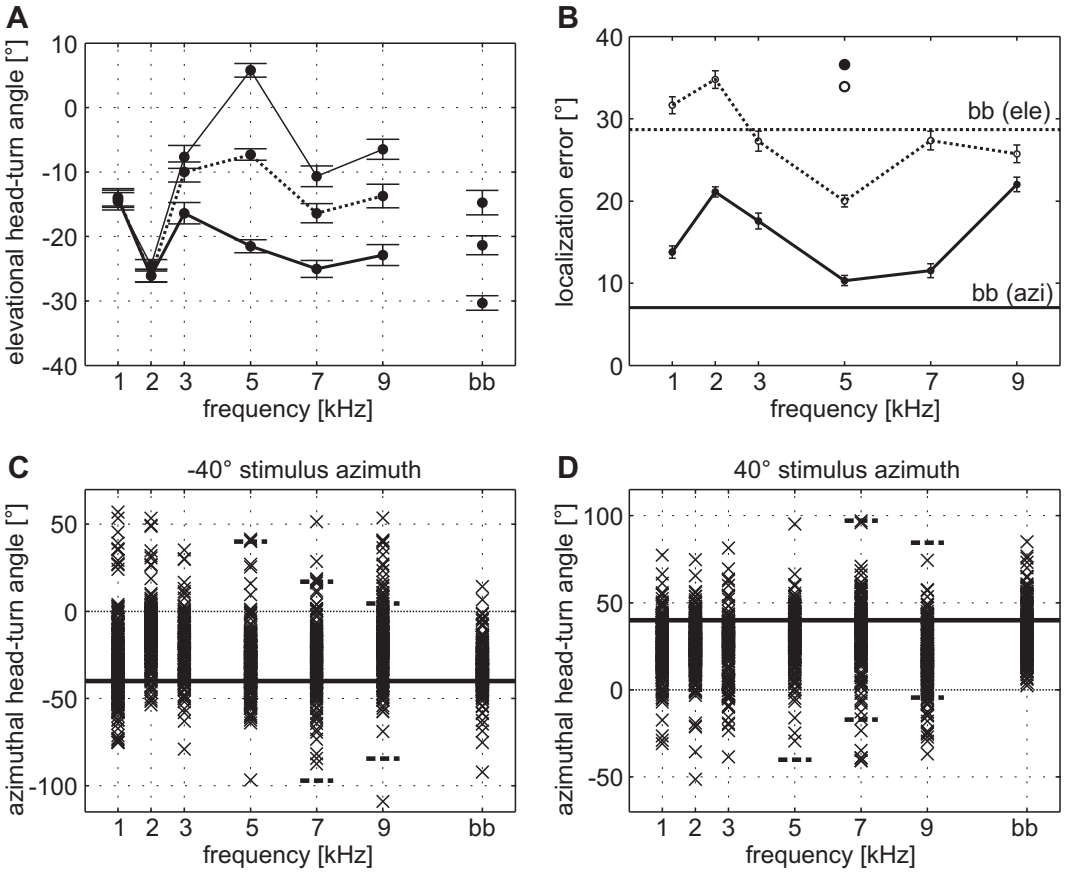

Figure 29: Azimuthal and elevational head-turn responses

A) Mean elevational head-turn angles are plotted for each stimulus elevation (-40, 0 and 40°) separately, for each 1/3 octaveband with center frequency 1-9 kHz as well as for broadband (bb) stimuli. The owls were able to discriminate stimulus elevation for frequencies >3 kHz. B) Azimuthal (black lines, mean ± SEM) and elevational (dotted lines) localization errors, i.e. mean deviation in degree of the head-turn angle from the stimulus position, are shown for each stimulus frequency for pooled data of all owls. Elevational errors exceeded azimuthal errors for any frequency as well as for broadband stimulation (bb). Gray lines show the mean localization error for stimuli with ILD = 0 dB at 5 kHz center frequency (solid line: azimuthal error, dashed line: elevational error). Each datapoint includes 39 to 120 trials. Azimuthal head-turn angles were plotted for C) -40° stimulus azimuth and D) 40° stimulus angle for each frequency. The position of the phantom sources adjacent to the stimulus azimuth are indicated by dashed lines.

For a more detailed analysis of the owls' reactions to virtual stimuli of various center frequencies, azimuthal head turn angles were plotted separately for each stimulus angle (Fig. 29C+D). Since one of my goals was the analysis of azimuthal ambiguities known as phantom sources, I calculated the position of phantom sources for each 1/3 octaveband (indicated by dashed lines in Fig. 29C+D) from the wavelength of the corresponding frequency and the ITD of about ±100 µs at ±40° stimulus azimuth (von Campenhausen and Wagner, 2006).

Table 7: Calculation of phantom source positions

From the period duration for each frequency (first and second columns), the position of phantom sound sources was predicted for stimulus azimuths of -40° or 40°, respectively. Calculation was based on an ITD change of 2.5 µs per degree, i.e. 100 µs ITD corresponds to a sound source at 40° azimuth. Phantom sources corresponding to an ITD of more than ±300 µs lie outside the owl's physiological range.

		stimulus azimuth: -40°	stimulus azimuth: 40°
frequency [kHz]	**period [µs]**	**phantom source position [azimuth]**	**phantom source position [azimuth]**
1	1000	beyond physiological range	beyond physiological range
2	500	beyond physiological range	beyond physiological range
3	333	beyond physiological range	beyond physiological range
5	200	40°	-40°
7	143	17°	-17°
9	111	4°	-4°

For example, at 5 kHz, the period duration is 200 µs. At 40° stimulus azimuth, a phantom source would occur at -40°, corresponding to -100 µs ITD. The position of phantom sources was calculated for all other frequencies in the same way (Table 7).

The observed azimuthal head turn angles (crosses in Fig. 29C+D) corresponded to the real sound source (bold line) rather than to any of the phantom sources. The only possible exception is at 9 kHz stimulus frequency, where the phantom source lies close to zero degree azimuth and a reaction to this phantom source cannot be discriminated from a no-reaction trial (cf. Methods).

Thus, in response to native narrowband stimuli (stimulus condition 1), head turns were only directed to the real sources and not to phantom sources despite the fact that spectral information was limited.

6.3.2 Localization of 1/3 octaveband-filtered stimuli with fixed ILD

The results presented so far prompted me to reason that the ILD contained in the native stimuli might help to remove ambiguities in azimuth occurring in the naroowband stimuli. Narrowband ILDs might also influence elevational localization. If that is correct, the owls should no longer be able to determine stimulus elevation and should exhibit phase ambiguities if the animals were stimulated with 1/3 octaveband-filtered noise whose ILD was artificially set to 0 dB for all tested stimulus locations.

When such stimuli were presented to the owls, the ability to distinguish various stimulus elevations degraded completely for two of the owls (Table 5). The third animal, owl S, was still able to distinguish the various stimulus elevations in stimulus paradigm 2. However, discrimination was impaired when compared with natural stimuli of the same center frequency and spectral content (compare Fig. 28J to Fig 30B, see Table 5).

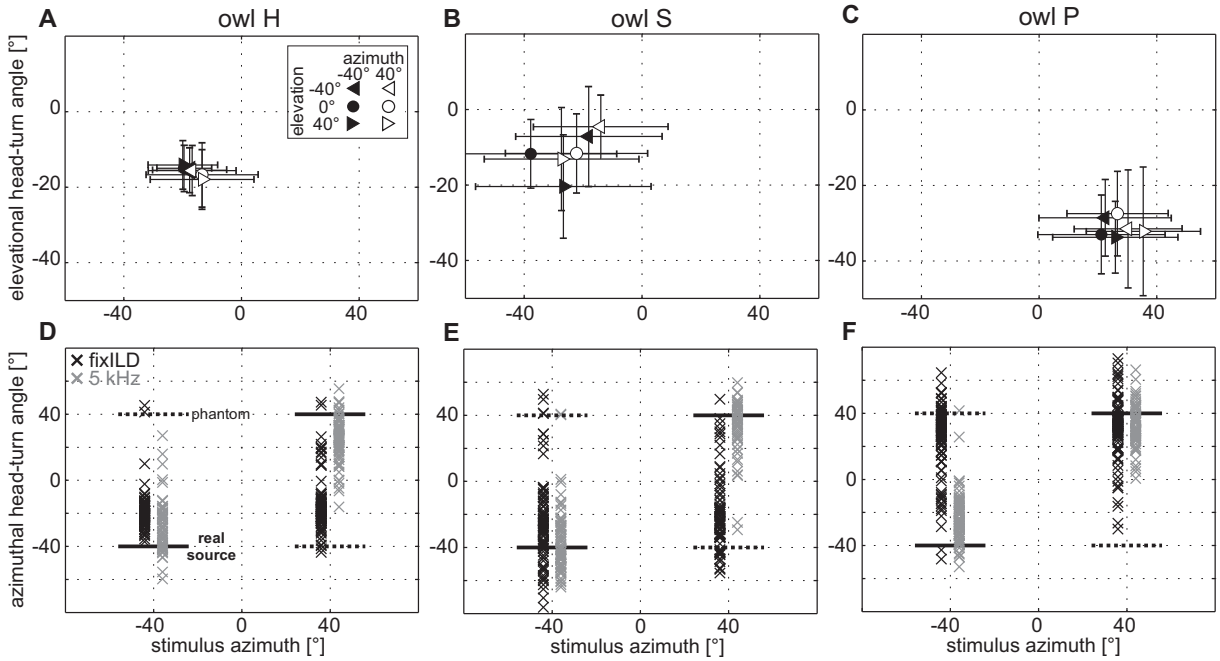

Figure 30: Reactions to stimuli with fixed ILD

When stimulated with 1/3 octaveband-filtered fixILD stimuli with 5 kHz center frequency, the owls showed similar elevational head-turn angles in response to different stimulus elevations. This stood in contrast to responses to native stimuli with 5 kHz center frequency (cf. Fig. 28D,J,P), where the owls responded with a head-turn to the stimulus elevation angle. With fixILD stimuli, the owls also localized stimuli preferentially in one hemisphere (A+B: owls H and S, left hemisphere, C) owl P, right hemisphere). Plotting is analogous to Fig.28.

Furthermore, two of the owls (owls H and S, Fig. 30A+B) always turned their heads to the left, irrespective of whether the stimulus azimuth was -40 or 40°. By contrast, the third owl (owl P) preferentially turned its head to the right. By contrast, the third owl (owl P) preferentially turned its head to the right (Fig. 30C). For 5 kHz center frequency, the phantom sound source corresponding to -40° stimulus azimuth is at 40° azimuth and vice versa for a virtual source at 40° azimuth. Hence, the owls exhibited a bias towards one hemisphere irrespective of stimulus azimuth.

Azimuthal (gray line in Fig. 29B) and elevational localization errors committed with fixILD stimuli at 5 kHz usually (dashed gray line in Fig. 29B) exceeded the errors made with normal, unmanipulated virtual stimuli, with the exception of a smaller elevational error for normal stimuli at 2 kHz center frequency.

The occurrence of phantom sources in stimulus paradigm 2, but not in stimulus paradigm 1, also becomes obvious from Fig. 30D-F. Reactions in both stimulus paradigms are plotted as a function of stimulus azimuth. The owls localized the real sound source in the natural condition. By contrast, they localized stimuli at an azimuthal angle corresponding to the phantom source position in the fixILD condition. The phantom sound source that corresponds to 5 kHz frequency lies at 40° azimuth for -40° stimulus azimuth, and vice versa for 40° stimulus azimuth. In other words, the owls exhibited a bias towards one side in the fixILD condition, that is, they located stimuli always at -40° (owls H and S, Fig. 30D+E) or at +40° (owl P, Fig. 30F).

6.3.3 Latencies

The time between stimulus onset and the beginning of a head turn (a head saccade with a velocity of >20 °/s) was recorded during the experiments as an indicator for the owl's motivation and the task difficulty. These latencies, shown for each frequency in Fig. 31A-C, were not normally distributed as tested with a Kolmogorov-Smirnov test (p>0.05). The latencies exhibited a right-side tilted rather than a Gaussian distribution, which is also visible in Fig. 32. This also resulted in a large number of outliers (data points exceeding 1.5 times the interquartile range) when the latencies were displayed as box plots (Fig. 31A-C). Therefore, median rather than mean latencies were compared with a non-parametric Mann-Whitney test for the various stimulus conditions.

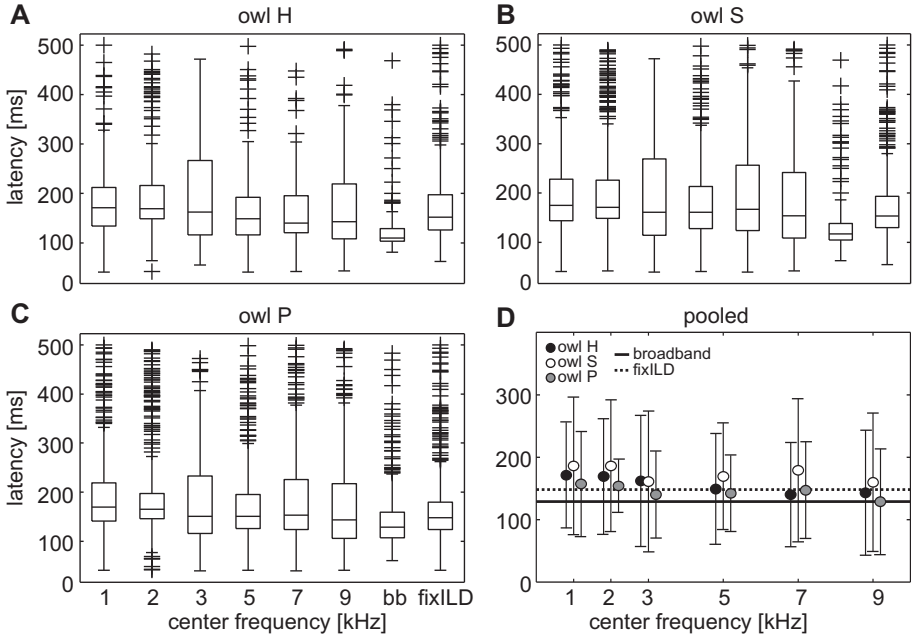

Figure 31: Latencies in response to 1/3 octaveband-filtered stimuli

A-C) The latencies of the three owls are shown as box-and-whiskers plots for each of the owls. Lower and upper boundaries of the box designate the lower and upper quartiles, respectively. The median is indicated by the horizontal line in each box. Whiskers show the extent of the remaining data and are restricted to 1.5 times the interquartile range. Data points beyond the whiskers are defined as outliers and marked by a cross. The large number of outliers results from the right-tilted distribution of latencies. **D**) Median latencies, pooled for the three owls, tend to decrease with increasing center frequency in kHz. However, the correlation was not significant (linear regression, p = 0.0571, goodness of fit: R2 = 0.6367). Reactions to stimuli with fixated ILD (fixILD, dotted line) were not different from those to normal stimuli of the same frequency, whereas reactions to broadband stimuli (bb, black line) were significantly faster for any owl (Mann-Whitney test, p<0.05).

In general, the latencies were clustered between 150 and 200 ms for the 1/3 octaveband stimuli (Fig. 31A-C), with minor differences in the reaction times to stimuli with various center frequencies. When the latencies for each of the three owls were plotted against stimulus frequency (Fig. 31D), a trend of decreasing latencies with increasing center frequency became apparent. An influence of the frequency on latencies was confirmed by a one-way ANOVA (p = 0.0019). That is, at 1 kHz the latencies had a median of 170 ms and decreased to 151 ms at 5 kHz where they remained relatively stable (Table 8). The relationship between center frequency and median latency was described by the linear equation y = -2.6947x + 167.79 (goodness of fit: R^2 = 0.7196). However, the trend was not significant (Spearman Rank

correlation, $p = 0.05833$).

Table 8: Latencies for 1/3 octaveband-filtered noise

For each center frequency, the median and mean latencies as well as standard deviations (SD) are given in ms for pooled data from all owls.

center frequency [kHz]	median [ms]	mean [ms]	SD [ms]
1	170	192.9	93.9
2	165	190.4	84.7
3	151	179.9	98.2
5	151	172.5	79.4
7	153	187.3	99.3
9	144	173.9	100.7
broadband	129	148.5	67.0
fixILD	148	165.8	71.5

Latencies for broadband stimuli (black line in Fig. 31D and light gray line in Fig. 32) were shorter than those for narrowband stimuli (Table 8). In Fig. 32 this is obvious in that the median latency for narrowband stimuli (vertical black line) was 157 ms compared to 129 ms for broadband stimuli (light gray line).

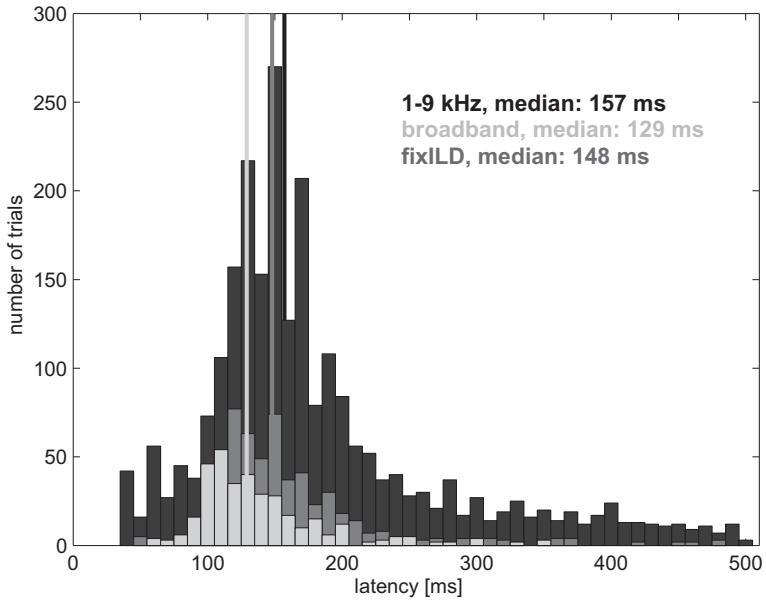

Figure 32: Histogram of latencies for 1/3 octaveband stimuli

For the three owls, pooled median latencies in reaction to 1/3 octaveband-filtered noise with center frequencies from 1 to 9 kHz (dark gray) as well as to fixILD stimuli (medium gray) and broadband (light gray) are shown in a histogram. Reactions to broadband stimuli were faster than to 1/3 octaveband stimuli.

Reactions to fixILD stimuli with 5 kHz center frequency, in contrast, were not significantly different from unmanipulated stimuli of the same frequency (Fig. 31D, Mann-Whitney test, $p \leq 0.1516$). In sum, latencies for 1/3 octaveband-filtered stimuli, whether normal or manipulated, were slightly longer than for broadband stimuli.

6.4 Discussion

In the present experimental series, I stimulated barn owls with 1/3 octaveband-filtered, individualized HRTFs at center frequencies from 1 to 9 kHz. Two stimulus conditions were created, either the naturally occurring ITDs, ILDs and monaural spectra in the respective frequency band were preserved ("native", stimulus condition 1), or the ILD was set to 0 dB at a center frequency of 5 kHz ("fixILD", stimulus condition 2).

The owls showed reduced elevational localization accuracy in stimulus paradigm 1 and azimuthal localization biases in stimulus paradigm 2. In the following I will first discuss and compare my findings with respect to general observations made in behavioral sound-localization experiments across different species. I will then turn to the relevance of the presented results for mechanisms of underlying azimuthal and elevational sound localization. Finally, I will speculate about a possible dominance of ITDs over other cues in barn-owl sound localization.

6.4.1 General behavioral observations

Most species localize noise stimuli more accurately than narrowband noise or tones (Bala et al., 2003, 2007; Brown et al., 1978; Casseday and Neff, 1973; Ehret and Dreyer, 1984; Gatehouse and Shelton, 1978; Heffner and Heffner, 1988; King and Carlile, 1994; Konishi, 1973a,b; Martin and Webster, 1987; Populin and Yin, 1998a). Part of this improvement in performance may be explained by across-frequency integration removing ambiguous cyclic neuronal responses to tones.

In response to the 1/3 octaveband-filtered stimuli, all owls undershot the target, i.e. exhibited too small turning angles, in both azimuthal and elevational planes (Table 6). This undershooting is a commonly observed phenomenon not only in barn owls (Hausmann et al., 2009; Knudsen and Konishi, 1979; Knudsen, 1981; Poganiatz and Wagner, 2001; Poganiatz et al., 2001), but also in other species such as the ferret (Nodal et al., 2008) or the cat (May and Huang, 1996). It might be explained by Bayesian inference mechanisms (Fischer, 2007).

The owls in my study showed a bias in azimuthal localization for stimulation with fixILD where the mean ILD was set to zero. In a similar stimulus paradigm, Saberi et al. (1999) observed a bias in two owls, one of which always turned its head towards the more central sound source, be it a real or a phantom source, whereas the second owl preferred the more lateral source.

In my study, the position of real and phantom sources were symmetrical along the midline (at -40 and 40° azimuth, respectively). The owls localized either the source at -40° or that at 40° azimuth, irrespective of the stimulus azimuth. This suggests that the owls experienced phantom sources in the fixILD condition, and responded with a head-turn to their preferred side (left in two owls, right in one owl), similar to the bias for central versus peripheral sound sources reported by Saberi et al. (1999).

All owls tended to turn more towards stimuli in the lower than the upper hemisphere as has already been described earlier (Knudsen et al., 1979). Elevational localization errors measured in my study exceeded azimuthal localization errors (Fig. 29D), also in accordance with earlier studies (Bala et al., 2003, 2007; Hausmann et al., 2009; Knudsen et al., 1979; Knudsen, 1981).

Knudsen and Konishi (1979) stimulated barn owls with pure tones. Azimuthal and elevational localization errors in that study were with total errors of 6.2° to 22.6° in the range of those measured in my study (7° to 35°, see Table 6). When compared to localization errors measured for pure tones in the barn owl (Knudsen and Konishi, 1979), it became obvious that the owls in my experiments committed larger localization errors in both azimuthal and elevational planes than the owls in the cited study (Fig. 33).

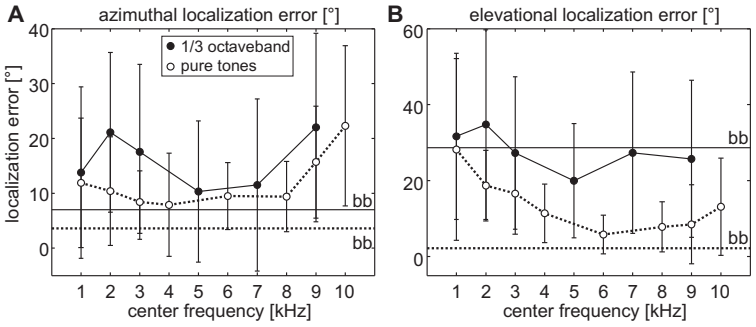

Figure 33: Localization errors for pure-tone versus 1/3 octaveband stimulation

For comparison, **A**) azimuthal and **B**) elevational localization errors (mean ± SD) in response to 1/3 octaveband-filtered noise (black) and pure tones (dotted) are plotted against stimulus frequency in kHz. Localization errors for broadband stimuli (bb) are indicated by the black lines for octaveband stimuli and the dotted lines for pure tones. Data for pure tone localization is taken from (Knudsen and Konishi, 1979). All data points include pooled results for all stimulus positions and owls.

Broadband localization errors fell below narrowband localization errors in all cases with the exception of elevational localization under 1/3 octaveband stimulation (Fig. 33B, black line), which is generally explained by the integration of information across all frequencies, making sound localization easier.

It was expected that the owls committed smaller errors for octaveband stimuli with their larger bandwidth and, therefore, higher informational content than for pure tones, even though the latter stimulus condition involved ongoing (closed-loop) stimulation. This is, however, not what I found. Nevertheless, it is likely that the larger localization errors in my study were due to the owls' difficulties in localizing positively elevated sound sources (Fig. 29C) rather than by some easier locatability of pure tones.

This is further supported because the owls used in the present experiments likewise had difficulties in localizing broadband stimuli at positive elevations (chapter 5.3.4). Small differences in localization performance can also be due to individual differences in localization ability or motivation of the animals, as well as to slight misalignments of the owl during HRTF measurement, i.e., a too small elevation of the owl's head. However, one would be expected the owl to exhibit a systematic shift of all localized positions towards lower elevations, rather than a selective impairment of the ability to locate positively elevated sounds (Fig. 29C).

In any case, the general course of both horizontal and vertical localization errors for

octaveband stimuli with stimulus frequency as measured here followed closely that measured for pure tones measured by Knudsen and Konishi (1979) apart from a slight deviation in azimuthal errors in the 2-3 kHz band (Fig. 33A).

That is, deviations to the target position were usually larger at very low ($\leq$2 kHz) and very high (>7 kHz) frequencies than for the intermediate frequency range, and localization errors were lowest for 5 kHz for both octaveband stimuli and pure tones (compare results presented in section 6.3 with Knudsen and Konishi, 1979).

Localization errors measured for barn owls in behavioral tasks for the frontal field (Hausmann et al., 2009; Knudsen et al., 1979; Poganiatz and Wagner, 2001; Poganiatz et al., 2001; Singheiser et al., 2010, present thesis) usually exceed by far the maximum accuracy of 1-3° in both azimuth and elevation that have been reported by Bala and coworkers(2003; 2007) using conditioned pupillary reflexes. Under such conditions, best localization performance in the owl falls short of the maximum accuracy of about 1° measured in humans (Mills, 1972).

Of course, it has to be regarded that reflexive responses such as the pupillary reflex are not subject to the additional error introduced by the motor response, i.e., the actual head-turn towards a sound target (Hausmann et al., 2009; Knudsen et al., 1979; Poganiatz and Wagner, 2001; Poganiatz et al., 2001) or even the flight towards it (Hausmann et al., 2008; Konishi, 1973a,b; Payne, 1962, 1971; Singheiser et al., 2010). Also motivational effects might impair the head-turn response and thereby reduce the measured localization accuracy. When similar tasks and setups are compared between owls and humans, localization accuracy is similar in both species (Bronkhorst, 1995; Carlile et al., 1997; Makous and Middlebrooks, 1990), also emphasizing how localization performance may depend on the experimental setup.

In the following, the relevance of my observations for azimuthal and elevational sound localization will be regarded separately in more detail.

6.4.2 Azimuthal localization of narrowband sounds

It is generally agreed that azimuthal information is computed by narrowband cross-correlation of temporal signals in both mammals and birds although the underlying neural mechanisms seem to be different (Leibold, 2010; Wagner et al., 2007).

Narrowband cross-correlation results in phase ambiguities that are present in the barn owl for frequencies above 3 kHz. Consequently, no response ambiguities occurred for narrowband stimuli having center frequencies of 1 or 2 kHz in this and other studies (Knudsen et al., 1979).

In the high-frequency range, ambiguities are removed by across-frequency integration (Mazer, 1998; Wagner et al., 1987). This happens in the projection from the lateral shell of the central nucleus of the inferior colliculus (ICls) to the ICx. In this step, low frequencies information is lost as well (Wagner et al., 2007). Since sound localization is mediated by pathways containing broadband neurons like those in ICx (Wagner, 1993) or in the forebrain (Vonderschen and Wagner, 2009), all information reaching the motor center is processed through broadband neurons.

The question that I cannot answer based on my findings is how broad a signal needs to be to remove the ambiguity. Obviously, the 1/3 octaveband stimuli were broad enough as long they contained native ILDs. It will be a task for future investigations to find the threshold bandwidth that does not result in localization ambiguities.

Comparisons with other animals and humans are difficult because in mammals, the effective cues are most likely ILDs and ITDs derived from envelopes, whereas barn owls use ITDs derived from the carrier. Tollin and Yin (2002) used virtual acoustic stimuli with fixed ITD to show for the cat's lateral superior olive (LSO), a nucleus processing ILD information, that azimuthal spatial receptive fields were determined mainly by narrowband ILDs. Localization of narrowband noise in the cat is accurate only in azimuth, but not in elevation, as shown by (Ruhland and Yin, 2008). Although I used 1/3 octaveband filtered signals, azimuthal sound localization was close to normal when the owls were stimulation with stimuli containing the native localization cues. By contrast, the owls showed response biases in stimulus paradigm 2 with the fixILD stimuli. This finding is similar to what Saberi et al. (1998) have observed and implies that ILD information helps in separating left and right hemispheres.

Free-field stimulation results in ILDs as long as the sound sources are not placed along the zero-ILD line (cf. von Campenhausen and Wagner, 2006). Due to the owls' asymmetrical ear arrangement, most sound sources produce ILDs if placed along the horizontal midline. HRTF-filtered stimuli do also contain ILDs as shown by Keller et al. (1998) or Hausmann et al. (2009). The HRTF-filtered stimuli used for the present study provided ILD information (Fig. 27) just as do free-field sounds.

Therefore, the owl should be able to resolve coding ambiguities by extracting this ILD. If the sound source is positioned, for example, in the right hemisphere and the signal frequency exceeds 2-3 kHz, the ILD is positive (i.e., the signal is louder at the right ear), and vice versa for sounds coming from the left hemisphere (cf. Fig. 27, see also Moiseff, 1989a). For lower frequencies, the ILD varies with azimuth, but not with elevation. That is, within the high-frequency range, the positive ILD in free-field and HRTF-filtered sounds should hint at the hemisphere the sound originates from. The reason for that is that positive ILDs (right ear louder), for example, occur in the upper right hemisphere (Fig. 27), whereas negative ILDs (left ear louder) occur in the lower left hemisphere, but not vice versa. Thus, ILD amplitude would be a sufficient cue to the hemisphere where the sound originates from. This coincides with what I observed in my experiments, since the owls did not localize phantom sources when stimulated with native narrowband stimuli, but they did so when the ILD was set to 0 dB (Figs. 28+30).

It thus seems that the owls can use this high-frequency ILD information to resolve coding ambiguities. Since ICx neurons combine ITD and ILD information in a multiplicative way (Pena and Konishi, 2001), the midbrain pathway is not suited for this disambiguation. The resolution of ambiguities may be achieved in the forebrain pathway. Although broadband ILDs did not influence ITD tuning in this nucleus (Vonderschen and Wagner, 2009), the

situation for narrowband ILDs needs further investigation.

6.4.3 Elevational localization of narrowband sounds

With narrowband stimuli, elevational sound-localization precision was degraded compared to broadband stimulation (Keller et al., 1998; Poganiatz and Wagner, 2001).

Mean elevational errors were about 30-35° for 1 kHz frequency and tended to strongly decrease with increasing frequency up to about 7 kHz for both responses to 1/3 octaveband-filtered noise (section 6.3 and comparative data for pure tones, Knudsen et al., 1979, see Fig. 33B). When higher frequencies were present, the owls distinguished between stimulus elevations by making head-turns of different amplitudes and signs. For higher frequencies, mean elevational errors slightly increased again to values of 13.1° for pure tones (Knudsen and Konishi, 1979, their Table 1) respectively 25° for 1/3 octaveband stimuli. As for azimuthal errors, the change of localization errors with frequency was alike for both stimulus conditions, apart from the systematically larger elevational errors observed in my experiments.

Elevational accuracy was especially low for frequencies below 3 kHz, which can be explained because barn owls use mainly ILDs for elevational localization, even though ITDs may play an additional role (Poganiatz and Wagner, 2001). In the owls' HRTFs, ILDs at frequencies below 3 kHz barely exceed ±5 dB and do not vary with stimulus elevation (Figs. 4+27, see also Hausmann et al., 2010). Therefore, it is not surprising that the owls were barely able to determine stimulus elevation at 1 or 2 kHz.

The difficulties in localizing low-frequency sound sources accurately in elevation matches observations made in humans (Algazi et al., 2000; Carlile et al., 1999). The subjects in the latter study committed large errors when pointing their faces to an elevated sound source with low-pass filtered noise (<2 kHz), particularly including reversals along the cones of confusion (see Blauert, 1997). In contrast, they had no problems in localizing the sound source when frequencies below 2 kHz were removed from the signals so that only high frequencies remained.

Similar difficulties in localizing low-frequency tones were observed in other animals (cat: Martin and Webster, 1987; Populin and Yin, 1998a, monkey: Brown et al., 1978, bat: Koay et al., 1998, pigeon: Lewald, 1987, bobwhite quail: Gatehouse and Shelton, 1978).

Close to what I observed for the owl in the low-frequency range (Fig. 28A+B), cats respond with a "default elevation" if they cannot localize elevational sound sources (Ruhland and Yin, 2008). In contrast to the cats, our owls responded to some degree to stimulus elevation in the high-frequency range (Fig. 28), consistent with the use of ILD information for elevational localization in owls, but not in mammals. The fact that the owls could not distinguish stimulus elevations with either low-frequency sounds or fixILD stimuli suggests that these stimuli did not contain enough elevational information. Specifically the residual ILDs (see Methods and Fig. 26) that were present in the fixILD stimuli were insufficient to elicit marked elevational head-turn angles in the owls.

Dichotic stimulation of barn owls with noise of varying interaural correlation (Egnor, 2001) resulted in increasing elevational head-turn angles with increasing ILD amplitude up to about 10 dB, but then the elevational head-turn angle reached a plateau at 20° where it did no longer increase with increasing ILD. This implies that either elevations >20° are encoded by cues other than the ILD, or that owls do not localize more elevated sounds. The influence of ILDs may depend on the stimulus position. Moiseff (1989a) showed that owls responded to stimuli with varying ITD, but an ILD of zero dB, with a head-turn towards the lower hemisphere if the ITD was positive (right ear leading).

In contrast, elevational head-turn angles were close to 0° for negative ITDs (left ear leading). Poganiatz and Wagner (2001) reported almost identical results. These studies indicate that the coding of sound source elevation in the barn owl depends not exclusively on ILDs. Our results argue against a contribution of narrowband monaural spectral cues, similar to what Poganiatz and Wagner (2001) concluded.

This suggests a role of ITD also for elevational sound localization as indicated by Euston and Takahashi (2002) from electrophysiological experiments. These authors measured spatial receptive fields in the barn owl's ICx by keeping ITDs at a fixed value while systematically varying ILDs according to their natural amplitude at a given spatial position. The derived "ILD alone" spatial receptive fields revealed horizontal bands of ambiguous (equal) ILDs, very similar to the narrowband ILD distributions measured in barn owl HRTFs (Fig. 27). The "ILD alone" receptive fields differed from the receptive fields measured for virtual stimuli that contained both the native ILD and ITD, the latter being restricted to a narrow spatial position. The same held true for the reverse stimulus configuration, with fixed ILD and varied ITD (Euston and Takahashi, 2002; Keller and Takahashi, 2005). That is, only the combination of ILDs with a specific ITD leads to the spatially restricted receptive fields observed in the ICx.

In my study, the removal of narrowband ILDs in stimulus condition 2 apparently resulted in regions with ambiguous elevational cues, leading to "default" head-turn responses as reported by Ruhland and Yin (2008) for cats. Hence, spatial representations of either ITD or ILD alone are insufficient to resolve all spatial coding ambiguities in both mammals and owls. My results reveal another important aspect, namely that stimulus elevation does not seem to be represented within each separate frequency channel. If that was the case, then the ILDs at frequencies below 3 kHz would still encode the correct elevation, even though they are small (see Fig. 27). The owls should respond with a head-turn towards the stimulus elevation even for frequencies below 3 kHz, which we did not observe. Furthermore, the elevational accuracy decreased for frequencies above 7 kHz (Fig. 27E,F). It was best for frequencies from 5-7 kHz, where the ILD pattern closely resembles the broadband distribution (see von Campenhausen and Wagner, 2006). Note that this does not mean that owls could not use ILD information from narrow frequency bands. Obviously, high-frequency narrowband ILDs provoque elevational head turns and the owls can distinguish stimulus elevations presumably

based on these ILDs (Fig. 27). It only means that the correct representation of stimulus elevation may require both ITD and at least high-frequency ILDs, whereas narrowband ILDs alone provoqued elevational head-turns whose amplitude was not frequency-independent, as would be expected for representation of elevation within each single frequency channel.

6.4.4 The role of higher-order brain regions

The results discussed so far imply that broadband ILD and ITD are sufficient to a) encode both stimulus azimuth and elevation, and b) distinguish the real source from illusory sources. If broadband ITD and ILD are present and integrated already at the level of the ICX (see above), what then may be the role of higher-order regions such as the forebrain?

In the owl's AAr, tuning curves differ from those in the IC (Vonderschen and Wagner, 2009), which suggests a differential way of neuronal processing in both brain regions. Similarly, Bizley and coworkers (2005) discovered distinct regions in the ferret auditory cortex that differed in their response latencies, tonotopic organisation and frequency selectivity. Ferrets exhibit a good plasticity for auditory learning, that is, after ear plugging they can learn to localize sound sources accurately again, even without visual feedback (Kacelnik et al., 2006), a finding that would not be achieved if only the physical cues were evaluated without learning or processing in higher-order brain regions. Sound localization also depends on the time course of incoming sounds, as demonstrated by Spitzer and Takahashi (2006) who showed that owls localize leading sounds when a second sound follows with less than 10 ms delay, but they localize lagging sounds with longer delays.

That is, even the combination of ITD and ILD information alone as present in the ICx would be insufficient to localize sound sources unambiguously under all circumstances. Resolution of ambiguities may take place in the ascending pathway higher than the ICx. In such higher regions, binaural information might for example be combined with monaural spectral cues as a further indicator for sound location. The role of monaural cues is not yet clarified in the owl, due to the fact that ITDs and ILDs alone should principally suffice to encode spatial positions in both azimuth and elevation.

Additional top-down control might help to weigh conflicting cues. Since the response delays for conflicting cues tend to exceed that for single or natural sources (Johnen et al., 2001; Poganiatz and Wagner, 2001; Spitzer and Takahashi, 2006), it is likely that in those cases, further processing of the localization cues takes place. The main duty of forebrain regions may be to evaluate the relative importance of localization cues and to direct attention towards salient positions in space when conflicting cues are present (Johnen et al., 2001; Winkowski and Knudsen, 2006; Witten et al., 2010). In the following, I will discuss the potential impact of conflicting cues on the owls' localization behavior.

6.4.5 Localization dominance in azimuthal sound localization in barn owls?

Localization dominance, a phenomenon known from human sound localization, refers to the observation that one localization cue might dominate the behaviour and that the information in other cues seems to be neglected (Wightman and Kistler, 1992). In barn owls, Poganiatz et al. (2001) reported that the barn owls stimulated with broadband noise used only ITDs to compute the amplitude of the azimuthal head turn. By contrast, I observed changes in azimuthal head turning when ILDs were removed from narrowband stimuli. This indicated that not only ITDs but also ILDs may be used when the stimulus has a narrow bandwidth. It may thus be that the ITD dominates behaviour as long as ITDs contain sufficient information to resolve sound source azimuth.

However, if spatial coding ambiguities arise, other cues such as frequency-specific ILDs may come into play. This speculation is supported by the finding that if ambiguous spatial positions are encoded by the same ITD, the owl seems to use further cues to resolve such ambiguities (Hausmann et al., 2009). In other words, ITDs might dominate ILD cues. A dominance hierarchy of localization cues was also reported by Witten et al. (2010) who stimulated barn owls with synchronous sounds, either separated in azimuth or in elevation. One of the sounds contained frequencies from 3 to 5 kHz and the other from 7 to 9 kHz. Interestingly, when the sound sources were separated in azimuth, the owls followed the low-frequency cue, and when the sources were separated in elevation, the owls located the high-frequency sound.

Those results support the speculation that the owl may weigh localization cues according to their frequency and spatial origin. It is beyond doubt that ITDs are sufficient to elicit azimuthal head-turns. Still, my findings question whether the ITD is really the only cue that is used for azimuthal sound localization, as suggested by Poganiatz and coworkers(2001), or if it might just be the dominant cue, supported by a combination with frequency-specific ILDs if coding ambiguities occur.

6.4.6 Latencies

The latencies measured for reactions to 1/3 octaveband-filtered respectively broadband noise (Figs. 31 and 32) were distributed around medians of 130 to 170 ms and means of 150 to 190 ms (Table 8), well in accordance with head-turn latency measurements in previous studies in the barn owl (Knudsen et al., 1979; Poganiatz et al., 2001; Hausmann et al., 2009, 2008), but also in mammalian species such as the monkey with 120 to 170 ms depending on the animal (Whittington et al., 1981) or the ferret with approximately 200 ms (Nodal et al., 2008).

Latencies measured in the present study tended to slightly decrease with increasing stimulus frequency, from about 170 ms at 1 kHz center frequency up to 5 kHz, where it remained relatively stable at a median of about 150 ms (Fig. 31D, Table 8). Latencies for broadband

stimulation were with about 130 ms constantly smaller than for any of the 1/3 octaveband-filtered noises, almost identical to the latencies measured in the previous experimental series using normal individualized and ruffcut stimuli (Fig. 16). Since the two experimental series (chapters 5 and 6) were separated by several months, the closely matching latencies measured for broadband stimuli in both series prove that the owls indeed responded with a stereotyped, reliable head saccade.

One could question if the head-turn responses to the octaveband stimuli were saccadic because the median latencies measured for those stimuli exceeded those for broadband noise by several tens of milliseconds. This would not necessarily be expected from a stereotyped, inborn response to sound stimuli. However, the response latency is generally considered to be a measure for the animal's motivational status as well as for task difficulty. Task difficulty may include ambiguity of sound signals, or the requirement to choose between two concurrent spatial cues (Johnen et al., 2001).

Poganiatz and coworkers(2001) found the latency to be higher when the ITD of virtual stimuli was manipulated so that it corresponded to one hemisphere while all other localization cues hinted at the opposed hemisphere. This stimulus configuration led to increased reaction times, likely due to confusion of the owls in making their decision of which target to look at. Consequently, one can conclude from the increased latency for narrowband stimuli used in the present experimental series that the owls might find such stimuli more difficult to locate. This, in turn, might lead to an additional neuronal processing step, namely the decision of where the virtual sound source is located.

Saberi and coworkers (1999) were able to show with electrophysiological recordings in the optic tectum, where auditory and visual information are integrated, that the neuronal representations of a virtual sound source and its corresponding phantom source were equally weighted in terms of neuronal spiking rate when the stimuli were narrowband ($<$3 kHz bandwidth). In contrast, when the stimulus bandwidth exceeded 3 kHz, the weight shifted towards the real sound source, making the neuronal representation of the source position unambiguous. Consequently, regardless of the fact that the motor response itself (i.e., the head saccade) may be stereotyped, the preceding decision of where the saccade should be directed to is not.

6.5 Conclusions

The results presented in this section show that barn owls may extract and use ILDs within narrow frequency bands a) to determine stimulus elevation for frequencies above 2 kHz, and b) to resolve azimuthal coding ambiguities, i.e., prevent side reversals that usually occur with narrowband stimulation. Monaural spectral characteristics in 1/3 octavebands in contrast played a minor role for the owls' localization ability at least in the presented behavioral task. This can be concluded from the fact that the owls localized phantom sound sources when the ILD of virtual stimuli was set to zero, even though the monaural frequency spectra were preserved (Fig. 26).

The owls were furthermore unable to discriminate stimulus elevations in the fixILD condition. Consequently, the findings presented in this section support the speculation of Poganiatz et al. (2001) and Poganiatz and Wagner (2001) that monaural spectra, in contrast to ILDs, were not crucial for barn owls' localization performance. Additionally, my results clearly suggest that the owls cannot use narrowband spectra to resolve azimuthal coding ambiguities, while ILDs are indispensable.

7 General Discussion

In the present thesis, I calculated and analyzed head-related transfer functions of American barn owls as a basis for the computation of virtual acoustic stimuli. These were used, either manipulated or unmanipulated, to determine the influence of frequency-specific transfer characteristics of the facial ruff on the owls' localization performance in a behavioral task.

In the following, the main results presented in this thesis will be summarized and reviewed in the context of existing studies in the owl as well as in other species. Furthermore, the implications of the presented results for future research will be discussed.

7.1 Relevance of HRTF properties for sound localization

The barn owls' adaptations to auditory localization have been further elucidated by the results of the present thesis. For instance, the barn owls' facial ruff allows them not only to locate sound sources with high accuracy in the frontal field of sight (Bala et al., 2007; Knudsen et al., 1979; Konishi, 1973b), but also to resolve spatial coding ambiguities in the periphery. If the facial ruff is virtually removed (see section 5), the owls' ability to locate sounds in both the azimuthal and elevational periphery decreases dramatically, and the owls are no longer able to distinguish positions with equal ITD. The impact of binaural cues on sound localization behavior can be predicted from the physical cues (ITD, ILD, monaural gains) contained in the owls' HRTFs as presented in sections 4 and 5.

In particular, removal of the facial ruff feathers changed the spatial distribution of ITDs and ILDs especially in the periphery for angles exceeding ±60° azimuth. Correspondingly, virtual ruff removal resulted in reduced azimuthal head-turn angles at peripheral stimulus angles, an inability to discriminate spatial positions with equal ITDs, and an inability to determine stimulus elevation even within the frontal field. Those findings accord to established models of sound localization, which predict an approximately linear increase of azimuthal head-turn angle with increasing ITDs in the frontal field, and confusion of positions with equal ITDs (see Blauert, 1997 for a review).

The previous findings that barn owls relied exclusively on the ITD for azimuthal localization (Knudsen et al., 1979; Poganiatz et al., 2001) are only partly supported by the findings from the present thesis. Although the owls' azimuthal head-turn angles increased with increasing ITD respectively stimulus azimuth as reported by the above cited studies, the owls in my experiments apparently used additional cues for localization in the periphery. As a consequence, they confused positions with the same ITD, but lying in different hemispheres, when the facial ruff was virtually removed (section 5).

Localization in the auditory periphery has rarely been investigated. Poganiatz et al. (2001) found that owls located stimuli whose ITD was set to -100 µs (left ear leading) respectively 100 µs (right ear leading) at -40° azimuth respectively +40° azimuth. The authors concluded from their results that ITD was the only relevant cue for azimuthal localization. However,

their observation may also be explained by a localization dominance as discussed in section 6.4.5. The stimulus configuration of Poganiatz et al. (2001) was not the natural stimulus condition, since the fixed ITD of ±100 µs was combined with the ILD and monaural spectra of a stimulus from ±140° azimuth. In that case, the owl may have experienced an unnatural stimulus and hence located the position of the presumably dominant ITD.

Nevertheless, that does not necessarily imply that ILDs or monaural spectra do not play any role in azimuthal localization, as the owls could distinguish frontal and rear positions having the same ITD before, but not after simulated ruff removal (section 5). This implies a use of further cues, presumably ILD or monaural cues, to resolve front-back ambiguities.

In sum, it became clear that barn owls need additional cues to distinguish positions with equal ITD. It is still to be evaluated what cues are needed specifically, i.e., ILDs or monaural spectral cues. This might be done by stimulating owls with "ruffcut" stimuli from rear positions, and artificially setting the ILD of those stimuli to the ILD that would naturally occur at the corresponding position in the rear, i.e., along the cone of confusion. If in response to such stimuli the owls localized the position significantly more peripherally, corresponding to the position that is localized in response to unmanipulated virtual stimuli, then one could conclude that ILDs are needed to resolve front-back confusions. Alternatively, the "ruffcut" ILD could be preserved but the monaural spectrum could correspond to that at the rear position. In case of a change in the localized position, the resolution of front-back confusion would rely on monaural spectral cues.

Up to date, the exclusive role of ITDs for azimuthal localization has rarely been questioned, although my findings imply that this may not hold for resolution of coding ambiguities, as discussed above. My findings support the observation of Witten et al. (2010) that ITD is the *dominant* factor for azimuthal localization, since the owls' azimuthal head-turn angle correlates with the ITD amplitude in the frontal field. Hence, the role of additional cues other than the ITD may be restricted to the resolution of coding ambiguities that mainly occur between rear and frontal hemispheres, as well as along the frontal and midsagittal planes at least in mammals (Gardner and Gardner, 1973; Searle et al., 1975; Wenzel et al., 1993; Zahorik et al., 2006).

The results from the simulation of ruff removal as described in section 5 raised the question of how the owl can resolve coding ambiguities that arise from equal ITDs or ILDs. Azimuthal coding ambiguities also occurred with narrowband stimulation in my experiments (section 6) as well as in other studies on a behavioral and electrophysiological level (Mazer, 1998; Saberi et al., 1998, 1999). The results I presented in section 6 imply that owls use ILDs to resolve coding ambiguities, and also that ITD information alone does not elicit elevational head-turns.

The former observation is a challenge for the role of the midbrain pathway for the resolution of spatial coding ambiguities. It is beyond doubt that processing of ITD and ILD cues including across-frequency integration is performed in the ICx (Knudsen and Konishi, 1978;

Takahashi et al., 1984; Takahashi and Konishi, 1986). Consequently, lesion of ICx regions leads to selective localization deficits in the owl (Wagner, 1993).

However, it is also known that the ICx acts in a multiplicative way (Pena and Konishi, 2001). ICx neurons are selective for a specific combination of ITD and ILD, both of which are independent inputs. The same space specific neuron yields an output of zero, that is, generates no action potentials, when stimulated with another than its preferred ITD and ILD combination. Changes in input ILD do not change the ITD tuning and vice versa. Multiplicative interaction also implies that azimuthal coding ambiguities as occurring in my experiments (section 6) is not resolved by means of ILD on the level of the ICx. Since the fixILD stimuli elicited an azimuthal head-turn angle, it seems likely that the owl still had the ITD information available, but that this ITD information did no longer code for a specific hemisphere. This in turn suggests that additionally to the multiplicative output of the midbrain pathway, binaural information is mediated to the motor cortex via a different pathway. When localization cues interact, for example, additively, ITD as well as monaural cues could be preserved even with an ILD input of zero, and vice versa. As explained above, the midbrain ICx is no suitable candidate for such an additive interaction.

However, there is a second pathway for ITD and ILD processing in the owl's brain, the role of which is still unclear. This forebrain pathway projects from the nucleus ovoidalis to the auditory arcopallium (AAr) (Takahashi and Konishi, 1986). Vonderschen and Wagner (2009) demonstrated that the neuronal tuning curves in ICx and AAr differ from each other and are presumably allocated to different tasks. One of those tasks may be to combine binaural localization cues with each other as well as with monaural spectral cues, if ambiguities arise. This may explain how ILD information might help the owl to determine the hemisphere a sound originates from. The owls' midbrain pathway may be important for quick localization in the central field, while the forebrain pathway may mediate the evaluation of ambiguous cues in a top-down control or direct spatial attention towards salient targets, as discussed in section 6.4 or help with discrimination and lateralization of ITD cues as proposed by Vonderschen and Wagner (2009).

Precise localization is not only an issue in the azimuthal plane, but also in elevation. Due to the complex changes of ILDs and spectral cues with stimulus elevation in barn owl HRTFs, assessing the individual contribution of ITDs, ILDs and monaural cues to elevational localization is difficult. Poganiatz and Wagner (2001) reported an influence of factors other than the ILD on elevational head-turn amplitude, and Egnor (2001) found a sigmoidal rather than strictly linear relationship between increasing ILDs and head-turn elevation, which additionally depended on the interaural correlation of dichotic stimuli.

In barn owls' HRTFs, the spatial changes of ILDs are highly sensitive to frequency changes, with small changes of ILDs with azimuth for low frequencies and dramatic changes of ILDs with elevation for high frequencies (Fig. 27). Elevational localization errors change, as do azimuthal errors, with sound frequency (Knudsen and Konishi, 1979, Fig. 33). The findings

presented in section 6 confirm earlier findings that frequencies above 3 kHz are needed for precise localization especially in the vertical plane (Konishi, 1973a; Singheiser et al., 2010). For lower frequencies, the owls did not discriminate different stimulus elevations.

As I showed in section 6, narrowband stimuli with 1/3 octave bandwidth elicited elevational head-turns in owls when the center frequency exceeded 2 kHz. Such stimuli are assumed to activate single frequency channels, because these have a critical bandwidth of approximately 1/3 octave (Quine and Konishi, 1974). Obviously, the owls were not only able to extract localization cues from those stimuli, but these cues were also lost when the ILD of 1/3 octaveband stimuli (5 kHz center frequency, fixILD stimuli) was set to zero.

Thus, neither the ITD alone nor narrowband spectral cues alone, both being preserved in the fixILD stimuli, were sufficient for elevational localization, while an influence of ILDs on elevational head-turn behavior is obvious. On the other hand, the fact that elevational localization behavior cannot be explained by the use of ILDs alone (Egnor, 2001; Moiseff, 1989a; Poganiatz and Wagner, 2001) leads to the conclusion that ILDs have to be combined with either ITD or monaural spectral cues in order to determine stimulus elevation.

A combination of ILD and ITD is a likely candidate as an indicator for target elevation, because their combination results in sharply restricted spatial receptive fields in the external nucleus of the inferior colliculus (ICx) (Euston and Takahashi, 2002; Knudsen and Konishi, 1978; Mazer, 1998). Up to the level of the ICx, ITD and ILD information is processed separately and within single frequency channels, as supported by a large amount of both behavioral and electrophysiological studies that tested neuronal responses to tones or passband-filtered stimuli in the auditory nuclei of the owl's brain (Carr and Konishi, 1988; Euston and Takahashi, 2002; Knudsen and Konishi, 1978; Manley et al., 1988; Moiseff and Konishi, 1981a; Moiseff, 1989b; Saberi et al., 1998, 2002; Spitzer and Semple, 1991; Takahashi et al., 1984, 2003; Vonderschen and Wagner, 2009; Wagner, 1993; Wagner et al., 2007). Frequency information is integrated to form the unambiguous representation of auditory space observed in the ICx, which then projects to the optic tectum (Knudsen and Konishi, 1978; Konishi, 2003; Olsen et al., 1989; Wagner, 1993).

An open question is whether this integration across frequency is a prerequisite for elevational localization, or if information from narrow frequency bands may already yield sufficient cues to elevation. In the view of current scientific evidence including the results presented in section 6, it is unlikely that integration across wideband frequency channels is mandatory for barn owls, i.e., that they could only use broadband ILDs to determine stimulus elevation rather than extracting frequency-specific ILDs. The difference between both models is illustrated in Fig. 34.

Nevertheless, it is also clear that the ILD information present in each frequency channel alone does not yield sufficient cues to determine stimulus elevation unambiguously, because receptive fields of ICx neurons contain large regions of equal, hence ambiguous, ILDs when the ITD is kept fixed (Euston and Takahashi, 2002). Only the combination with ITDs

creates, at least in the frontal hemisphere, the spatially restricted unambiguous receptive fields seen in the ICx.

Indeed, the influence of other cues than the ILD alone on elevational head-turn angles measured by Poganiatz and Wagner (2001) for such a stimulus configuration could be explained because the owls had to localize virtual sound sources within "ITD alone" receptive fields given that the ILD was set to a fix value. For such a stimulus configuration, the owl might derive the correct stimulus position for some spatial regions, if the ITD and ILD coincide with their natural amplitude at that position. In contrast, certain other ITD-ILD combinations might result in invalid combinations that would usually not occur. One could evaluate this hypothesis by systematically measuring the neuronal representation of virtual sounds with fixed ILD, thus the "ITD alone" receptive fields. The position that the owls localize with fixILD stimuli should then lie along iso-ITD lines. Keller and Takahashi (2005) measured such ITD alone receptive fields in the ICx, but they did not test these stimuli behaviorally.

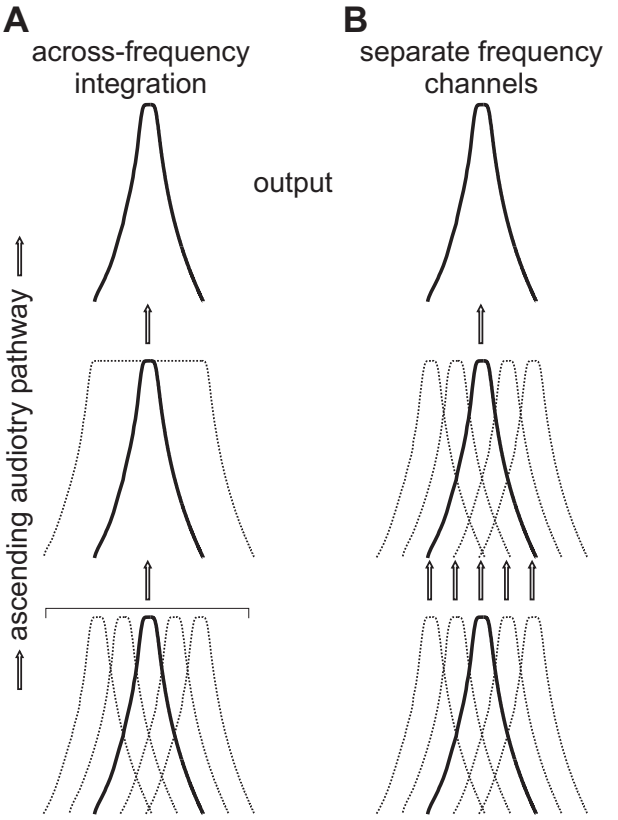

Figure 34: Preservation versus integration across frequency channels

Representation of spatial information across frequencies is possible through alternative ways. Either, as shown in **A**), across-frequency integration may be performed before information is evaluated in the forebrain. Such across-frequency integration is achieved in the ICX, but it is unknown if information is preserved in separate frequency channels along a different neuronal pathway to the forebrain. **B**) Additionally to the frequency-integrated information from the ICx as shown in A), information may be preserved and transduced to the forebrain along a separate neuronal pathway. The output information (top row in A) and B)) would be the same in both cases.

While the ICx combines and integrates ITD and ILD in a multiplicative way rather than preserving individual frequency channels (Pena and Konishi, 2001), it is so far unknown if information is preserved within frequency channels in the above described forebrain pathway or not. My results do not allow to draw conclusions on frequency integration versus preservation in the forebrain pathway, since the final motor (behavioral) output would be the same in both cases, as illustrated in Fig. 34. At least, the owls' ability to discriminate varying stimulus elevations to a good extent even with 1/3 octaveband-filtered noise (chapter 6) or pure tones (Knudsen and Konishi, 1979) favorizes that elevational localization cues are available within narrow frequency bands. However, the amplitude of the elevational head-turn angles that these narrowband cues elicit (see Fig. 28) do not reflect the actual stimulus elevation. That is, positive ILDs elicit more positive head-turn elevations than negative ILDs, which in turn elicit negative head-turn elevations. Still, in most frequency bands, the

head-turn elevation does not correspond to the stimulus elevation, and no representation of stimulus elevation seems to be present at frequencies below 3 kHz. This indicates that ILD may yield some cue to stimulus elevation, but be insufficient for accurate localization of elevated sound targets.

Integration across frequencies tends to improve localization performance as shown by the smaller mean localization errors in response to broadband noise (discussed in chapter 6.4). That means, narrowband information to target elevation is obviously available to the owl, but generally does not seem to be unambiguously enough to match broadband performance.

Considering the results discussed above, it seems obvious that the owl must suffer from confusions, presumably in both azimuthal and elevational planes, when the stimulus bandwidth is narrow or when particular localization cues are removed. Hence, it does not surprise that the owls had difficulties in determining stimulus elevation in low-frequency narrowband stimuli where ILD information is sparse, or with stimuli at 5 kHz frequency from which the ILD was removed (section 6). These results, however, do also show that the 1/3 octave bandwidth yielded sufficient cues to determine in which hemisphere (left or right) the sound originated, which is most likely due to a matching of the characteristic ITD at the stimulus position (±40° azimuth) with the available ILD cues as implied in Euston and Takahashi (2002). This stands in contrast for example to guinea pigs, where neurons in the core of the inferior colliculus (ICc) responded omnidirectionally to 1/3 octaveband stimulation (Sterbing et al., 2003), a fact that implies an inability of the guinea pig to localize such stimuli, though not tested behaviorally in the cited study.

In sum, my results demonstrate that owls use ILDs not only to discriminate stimulus elevations, but also can use the level differences to resolve azimuthal spatial coding ambiguities. In other words, when the ILD of virtual stimuli with 5 kHz center frequency was artificially set to 0 dB, the owls could no longer determine stimulus elevation and also seemed to experience phantom sound sources. They did not localize stimuli in the correct hemisphere as they did with unmanipulated stimuli of the same frequency, but rather exhibited a preference for either the left one or the right hemisphere.

Those results emphasize the importance of combined spatial cues for spatially precise localization, among which binaural cues (ITD and ILD) are of specific relevance. The differential use of ILDs and monaural cues for localization in barn owls and mammals is also one of the major differences between these two groups of species. In the following section, the additional possible role of monaural frequency spectra to sound localization will therefore be discussed, the contribution of which is sparsely investigated in the barn owl.

7.2 The role of monaural frequency spectra

My findings are consistent with the hypothesis that barn owls seemingly do not use monaural frequency characteristics for sound localization, as suggested by Poganiatz and Wagner (2001). This holds at least for narrowband filtered stimuli with 1/3 octaveband width as used in section 6. However, one should be careful in drawing definite conclusions, because the fact that specific sound features have no impact on the performance in a concrete task does not necessarily imply that the respective sound cue *cannot be used* at all. The possibility of a dominance hierarchy for localization cues was discussed above (section 6.4.5).

For instance, the owl might still benefit from information provided by monaural spectra, such as peaks or notches at characteristic frequencies, if sound sources are for example displaced along iso-ILD lines. Corresponding confusions, namely front-back or back-front reversals, for sound sources along either median or horizontal planes are a common problem in humans (Gardner and Gardner, 1973; Hill et al., 2000; Wenzel et al., 1993; Zahorik et al., 2006). Humans use spectral cues to resolve such ambiguities (Carlile et al., 1999), and also other mammalian species such as cats are known to use spectral notches in the high-frequency range (>10 kHz) for elevational localization (cat: Musicant et al., 1990; Tollin and Yin, 2003; rat: Koka and Tollin, 2008 ferret: Carlile, 1990). This may explain why cats experience illusory elevational sound sources under stereophonic stimulation (Tollin and Yin, 2003).

Valuable spectral cues occur only in wideband sounds. In very narrowband sounds or in tones, frequency-characteristic filtering leads to simple amplitude changes of that frequency without resulting in specific ratios between the amplitudes of different frequencies. If, for example, a 5 kHz tone is replayed to the owl, the filtering of the ruff will attenuate the tone's amplitude depending on the sound source position. Likewise, a 7 kHz tone may be attenuated more strongly than the 5 kHz tone. If each tone is regarded separately, the owl may detect their different sound amplitudes, but this does not provide information on the sound source position, because the owl cannot infer the initial amplitude of the tone. However, integration of both frequencies yields a specific and direction-dependent ratio of their amplitudes. From changes in that ratio, the owl may infer the sound location. Since each frequency is attenuated in a characteristic way (Fig. 27, von Campenhausen and Wagner, 2006; Keller et al., 1998), inferring the sound location from the ratio between single frequency bands gets easier, the broader the available frequency information is and vice versa. As a consequence, narrowband noise limits across-frequency integration and evaluation of direction-dependent spectral patterns as a cue for sound source position. It might thus be that in effect, barn owls are able to extract and use spectral cues in sound signals, but that the signal's 1/3 octave bandwidth (see chapter 6) was insufficient for accurate elevational sound localization.

Poganiatz and Wagner (2001) held the mean ILD of wideband noise (4 to 10 kHz) constant and concluded that such wideband ILDs contributed to elevational head-turn angles. My

experiments took that approach a step further by investigating the contribution of frequency-specific ILDs to elevational sound localization. Although it became obvious from my results that owls can use narrowband ILDs but not narrowband monaural spectra to determine stimulus elevation, it might still be that broadband monaural spectra yield sufficient elevational cues. Poganiatz et al. (2001) held the ITD of broadband stimuli constant while varying broadband ILD and spectral cues together, and Poganiatz and Wagner (2001) held broadband ILD constant while varying the ITD and spectrum together. The first approach does not allow statements on the respective contribution of ILD and monaural spectra. The latter approach led to the conclusion that ILDs were not the only relevant cue to determine stimulus elevation, however without answering how exactly ITD and/or spectral cues could contribute to head-turn elevation.

For that reason, it would be a worthwile future project to use broadband sound sources systematically displaced along the vertical midline (resulting in zero ITD), where elevational localization is most accurate (Hausmann et al., 2009), with native monaural spectra but fixated ILD to see if barn owls were able to determine stimulus elevation based on variations in the monaural spectra alone. Virtual acoustic stimuli offer a feasible way to realize the required manipulations. If no changes of elevational head-turn angles in response to variations in monaural spectra occurred, then the relevant cue for elevational localization in the barn owl must be the direction-dependent combination of ILD and ITD.

An alternative possibility is a restricted use of monaural spectra in certain spatial regions, in the case of which at least some changes in head-turn elevation should be apparent in the above proposed experimental design. For example, Poganiatz and Wagner (2001) observed an increase in head-turn elevation in the lower but not the upper hemisphere or vice versa depending on stimulus azimuth when only the broadband ILD of virtual stimuli was fixed at $\pm 6\,\mathrm{dB}$. This would be explained if the owl used spectral cues for defined regions of space while spectral information was irrelevant in other regions, meaning a direction-dependent combination of localization cues. Such a mechanism would also be plausible considering studies in mammalian species showing that frequency-specific spectral notches help to determine stimulus elevation (cat: Musicant et al., 1990; Tollin and Yin, 2003; rat: Koka and Tollin, 2008 ferret: Carlile, 1990).

Another approach to investigate the role of monaural spectra more closely in the owl would be to manipulate the magnitude of spectral notches. While the role of spectral notches that vary systematically with stimulus elevation is confirmed for many mammalien species (see above), comparable systematic investigations for the owl are missing so far. One could introduce additional spectral notches into high-frquency sounds, or vary the amplitude of naturally occurring notches. Again, the Virtual Space Technique provides a powerful tool to implement the according manipulations of dichotic stimuli.

7.3 The role of pinna movements

In contrast to many mammalian species, the barn owl is unable to move its pinnae and direct them to the sound direction. For that reason the bird has to move its head in order to bring auditory targets into the sensory focus (Knudsen et al., 1979). One the one hand, this may be disadvantageous because head-turn latencies are usually longer than those for pinna movements, as was for example measured for the cat. Pinna movements to auditory targets had a latency of about 35 ms (Populin and Yin, 1998b), whereas latencies ranged from less than 100 ms for unexpected sound bursts (Thompson and Masterton, 1978) to about 300 ms for voluntary head movements (May and Huang, 1996).

On the other hand, being unable to move head and pinnae independently also provides the advantage that the auditory focus coincides with the visual focus, and the neuronal spatial receptive fields do not need to be adapted to varying target locations depending on the initial eye and pinna position. The latter is the case for example in primates, where the extent of eye saccades to auditory targets compensates for the initial eye position in rhesus monkeys (Metzger et al., 2004). For example, an azimuthal difference of 12° in the initial eye position resulted in only a small azimuthal difference in the final saccade to the auditory target (i.e., the final gaze position) of 0.6 to 1.6° (Metzger et al., 2004).

Also in cats, the initial position of the eyes was found to have little effect on the accuracy of saccadic eye movements to auditory targets in cats besides the consequential mismatch between auditory and visual spatial representations (Hartline et al., 1995).

The behavioral observations are mirrored in the neuronal representation. Changes in eye position lead to an according shift of spatial auditory receptive fields in the superior colliculus of monkeys (Jay and Sparks, 1984), and the auditory spatial tuning in the cat's superior colliculus is likewise adapted to the position of the pinna (Middlebrooks and Knudsen, 1987). Consequently, neuronal representations of the auditory and visual modalities usually form superimposed spatial maps in primates or cats regardless of the potentially different alignment of sensory reference frames (Jay and Sparks, 1984; Middlebrooks and Knudsen, 1984; Hartline et al., 1995)

Saccades to auditory targets are usually subject to undershooting of the target position in a broad range of species (barn owl: Knudsen and Konishi, 1979, monkey: Metzger et al., 2004; Populin, 2006, cat: Populin and Yin, 1998a, ferret: Nodal et al., 2008). One possible reason that is discussed for the increasing localization errors with increasing target periphery is that the extent of auditory saccades may not suffice to fully compensate for differences in the initial eye position, as reviewed in Metzger et al. (2004). If so, undershooting errors should not, or to a smaller extent, occur in species with immobile eyes or pinnae. However, the study of Metzger et al. (2004) rather refutes this hypothesis, and the explanation might also not hold for the barn owl which typically commits strong undershooting errors in the periphery though due to the eyes' relative immobility (Steinbach, 1972) a potential mismatch

between auditory and visual axes should not occur. Underestimation of peripheral targets does also occur in humans, whose pinnae are likewise immotile (reviewed in Zahorik et al., 2005). On the other hand, localization accuracy strongly decreases when an animal's head is restrained, allowing eye movements only, compared to when it is freely moveable (Jay and Sparks, 1990; Populin, 2006), suggesting that there is no inherent "failsafe" compensational mechanism for mismatches between eye, pinna or head.

Taken together, localization errors do not seem to be unambiguously related to the motility of eyes or pinnae relative to the auditory and visual axes, or to be restricted to species with moveable sensory organs.

7.4 Outlook

Besides extensive research on the field of auditory processing, many aspects of this astonishing sense remain obscure. The barn owl as an auditory specialist has been established as a model animal during the last decades, resulting in a vast range of comparative data. Together with the computational power that emerged in the past years and powerful methodological approaches such as the Virtual Space technique used here, this species offers an immense potential for behavioral, electrophysiological or modeling studies. Single aspects of auditory processing may be investigated systematically, for instance by sequentially breaking down physical cues that usually coercively coincide in natural free-field sounds. Such a reduction to the most basic sound features allows focused analyses of how binaural and monaural cues are extracted, processed and combined in order to accomplish the complex task of sound localization.

Apart from the promotion of established techniques used for studies in the barn owl so far, a better understanding of the fundamentals of sound localization could also be achieved by introducing techniques such as magnetic resonance imaging to the research in owls, and by making use of newly developed approaches such as detachable headphone devises for auditory stimulation in freely moving animals (Nodal et al., 2010) or electrophysiological recordings in awake, behaving owls.

Another important but often neglected aspect of sound localization in the barn owl is the evaluation of sound source distance cues. Kim and coworkers (2010) recently presented distance-dependend HRTFs for rabbits, but comparable data for the owl are missing so far. It would thus be a promising step to vary sound source distance during HRTF recordings also for the barn owl, the more as distance evaluation turned out to be a critical parameter in free-flight localization tasks (Hausmann et al., 2008; Singheiser et al., 2010).

8 References

Akeroyd M (2006) Akeroyd ma (2006) the psychoacoustics of binaural hearing. *Intern J Audiol* 45:S25–S33.

Algazi V, Avendano C, Duda R (2000) Elevation localization and head-related transfer function analysis at low frequencies. *J Acoust Soc Am* 109(3):1110–1122.

Aytekin M, Grassi E, Sahota M, Moss C (2004) The bat head-related transfer function reveals binaural cues for sound localization in azimuth and elevation. *J Acoust Soc Am* 116:3594–3605.

Bala A, Spitzer M, Takahashi T (2003) Prediction of auditory spatial acuity from neural images on the owl's auditory space map. *Nature* 424:771–774.

Bala A, Spitzer M, Takahashi T (2007) Auditory spatial acuity approximates the resolving power of space-specific neurons. *PloS One* 2:e675.

Bühler P, Epple W (1980) The vocalizations of the barn owl. *J Ornithol* 121:36–70.

Bizley J, Nodal F, Nelken I, King A (2005) Functional organization of ferret auditory cortex. *Cerebral Cortex* 15:1637–1653.

Blauert J (1997) *Spatial Hearing* MIT Press, Cambridge, Massachusetts.

Brainard M, Knudsen E, Esterly S (1992) Neural derivation of sound source location: resolution of spatial ambiguities in binaural cues. *J Acoust Soc Am* 91:1015–1027.

Bronkhorst A (1995) Localization of real and virtual sound sources. *J Acoust Soc Am* 98:2542–2553.

Brown C, Beecher M, Moody D, Stebbins W (1978) Localization of primate calls by old world monkeys. *Science* 201:753–754.

Cai H, Carney L, Colburn H (1998a) A model for binaural response properties of inferior colliculus neurons. i. a model with interaural time difference-sensitive excitatory and inhibitory inputs. *J Acoust Soc Am* 103(1):475–493.

Cai H, Carney L, Colburn H (1998b) A model for binaural response properties of inferior colliculus neurons. ii. a model with interaural time difference-sensitive excitatory and inhibitory inputs and an adaptation mechanism. *J Acoust Soc Am* 103(1):494–506.

Calford M (1988) Constraints on the coding of sound frequency imposed by the avian interaural canal. *J Comp Physiol A* 162:491–502.

Calford M, Piddington R (1988) Avian interaural canal enhances interaural delay. *J Comp Physiol A* 162:503–510.

Calmes L, Lakemeyer G, Wagner H (2007) Azimuthal sound localization using coincidence of timing across frequency on a robotic platform. *J Acoust Soc Am* 121:2034–2048.

Carlile S (1990) The auditory periphery of the ferret. ii: The spectral transformations of the external ear and their implications for sound localization. *J Acoust Soc Am* 88:2195–2204.

Carlile S, Delaney S, Corderoy A (1999) The localisation of spectrally restricted sounds by human listeners. *Hear Res* 128:175–189.

Carlile S, Leong P, Hyams S (1997) The nature and distribution of errors in sound localization by human listeners. *Hear Res* 114:179–196.

Carr C, Konishi M (1988) Axonal delay lines for time measurement in the owl's brainstem. *Proc Natl Acad Sci USA* 85:8311–8315.

Carr C, MacLeod K (2010) Microseconds matter. *PLoS Biology* 8(6):e1000405.

Casseday J, Neff W (1973) Localization of pure tones. *J Acoust Soc Am* 54(2):365–372.

Christensen-Daalsgard J, Manley G (2005) Directionality of the lizard ear. *J Exp Biol* 208:1209–1217.

Colburn H (1973) Theory of binaural interaction based on auditory-nerve data. i. general strategy and preliminary results on interaural discrimination. *J Acoust Soc Am* 54(6):1458–1470.

Coles R, Guppy A (1988) Directional hearing in the barn owl (tyto alba). *J Comp Physiol A* 163:117–133.

Dietz M, Ewert S, Hohmann V (2009) Lateralization of stimuli with independent fine-structure and envelope-based temporal disparities. *J Acoust Soc Am* 125:1622–1635.

Drager U, Hubel D (1975) Physiology of visual cells in mouse superior colliculus and correlation with somatosensory and auditory input. *Nature* 253:203–204.

DuLac S, Knudsen E (1990) Neural maps of head movement vector and speed in the optic tectum of the barn owl. *J Neurophysiol* 63:131–146.

Dyson M, Klump G, Gauger B (1998) Absolute hearing thresholds and critical masking ratios in the european barn owl: a comparison with other owls. *J Comp Physiol A* 182:695–702.

Egnor S (2001) Effects of binaural decorrelation on neural and behavioral processing of interaural level differences in the barn owl (tyto alba). *J Comp Physiol A* 187:589–595.

Ehret G, Dreyer A (1984) Localization of tones and noise in the horizontal plane by unrestrained house mice (mus musculus). *J Exp Biol* 109:163–174.

Ehret G, Schreiner C (1997) Frequency resolution and spectral integration (critical band analysis) in single units of the cat primary auditory cortex. *J Comp Physiol A* 181:1351–1432.

Euston D, Takahashi T (2002) From spectrum to space: the contribution of level difference cues to spatial receptive fields in the barn owl inferior colliculus. *J Neurosci* 22:284–293.

Fay R, Feng A (1987) *Mechanisms for directional hearing among nonmammalian vertebrates. In: Directional Hearing* Springer, New York.

Fischer B (2007) Optimal models of sound localization by barn owls. *NIPS* abstract 38.

Fischer B, Christianson B, Pena J (2008) Cross-correlation in the auditory coincidence detectors of owls. *J Neuroscience* 28(32):8107–8115.

Fletcher H (1940) Auditory patterns. *Reviews of Modern Physics* 12:47–65.

Fujiki N, Riederer K, Jousmäki V, Mäkelä J, Hari R (2002) Human cortical representation of virtual auditory space: differences between sound azimuth and elevation. *Europ J Neuroscience* 16(11):2207–2213.

Gardner M, Gardner R (1973) Problem of localization in the median plane: effect of pinnae cavity occlusion. *J Acoust Soc Am* 53:560–575.

Gatehouse R, Shelton B (1978) Sound localization in bobwhite quail (colinus virginianus). *Behav Biol* 22:533–540.

Goldberg J, Brown P (1968) Functional organization of the dog superior olivary complex: an anatomical and electrophysiological study. *J Neurophysiol* 31:639–656.

Goldberg J, Brown P (1969) Response of binaural neurons of dog superior olivary complex to dichotic tonal stimuli: some physiological mechanisms of sound localization. *J Neurophysiol* 22:613–636.

Gordon B (1973) Receptive fields in deep layers of cat superior colliculus. *J Neurophysiol* 36:157–178.

Harper N, McAlpine D (2004) Optimal neural population coding of an auditory spatial cue. *Nature* 430:682–686.

Harris L, Blakemore C, Donaghy M (1980) Integration of visual and auditory space in the mammalian superior colliculus. *Nature* 5786:56–59.

Hartline P, Vimal R, King A, Kurylo D, Northmore D (1995) Effects of eye position on auditory localization and neural representation of space in superior colliculus of cats. *Exp Brain Res* 104:402–408.

Hartmann W, Wittenberg A (1996) On the externalization of sound images. *J Acoust Soc Am* 99:3678–3688.

Hausmann L, Singheiser M, Plachta D, Brill S, Wagner H (2008) In-flight corrections in free-flying barn owls (tyto alba) during sound localization tasks. *Journal of Experimental Biology* 211:2976–2988.

Hausmann L, von Campenhausen M, Endler F, Singheiser M, Wagner H (2009) Improvements of sound localization abilities by the facial ruff of the barn owl (tyto alba) as demonstrated by virtual ruff removal. *PLoS One* 4:e7721.

Hausmann L, von Campenhausen M, Wagner H (2010) Properties of low-frequency head-related transfer functions in the barn owl (tyto alba). *J Comp Physiol A* 196:601–612.

Heffner R, Heffner H (1988) Sound localization and use of binaural cues by the gerbil (meriones unguiculatus). *Behav Neurosci* 102(3):422–428.

Heffner R, Koay G, Heffner H (1996) Sound localization in chinchillas iii: Effect of pinna removal. *Hear Res* 99:13–21.

Hill K, Lewis D, Hutchings M, Coles R (1980) Directional heraing in the japanese quail (coturnix coturnix japonica). i. acoustical properties of the auditory system. *J Exp Biol* 68:135–151.

Hill P, Nelson P, Kirkeby O, Hamada H (2000) Resolution of front-back confusion in virtual acoustic imaging systems. *J Acoust Soc Am* 108:2901–2910.

Huang A, May B (1996) Spectral cues for sound localization in cats: effects of frequency domain on minimum audible angles in the median and horizontal planes. *J Acoust Soc Am* 100:2347–2160.

Hwang S, Park Y, Park Y (2008) Modeling and customization of head-related impulse responses based on general basis functions in time domain. *Acta Acustica united with Acustica* 94:965–980.

Hyson R, Overholt E, Lippe W (1994) Cochlear microphonic measurements of interaural time differences in the chick. *Hear Res* 81:109–118.

Jay F, Sparks D (1990) *Localization of auditory and visual targets for the initiation of saccadic eye movements. In: Comparative perception. Basic mechanisms* New York: Wiley.

Jay M, Sparks D (1984) Auditory receptive fields in primate superior colliculus shift with changes in eye position. *Nature* 309:345–347.

Jeffress L (1948) A place theory of sound localisation. *J Comp Physiol Psychol* 41:35–39.

Johnen A, Wagner H, Gaese B (2001) Spatial attention modulates sound localization in barn owls. *J Neurophysiol* 85:1009–1012.

Johnston R (1990) Variation in size and shape in pigeons, columbia livia. *Wilson Bull* 102:213–225.

Kacelnik O, Nodal F, Parsons C, King A (2006) Training-induced plasticity of auditory localization in adult mammals. *PLoS Biology* 4(4):e71.

Keller C, Hartung K, Takahashi T (1998) Head-related transfer functions of the barn owl: measurement and neural responses. *Hear Res* 118:13–34.

Keller C, Takahashi T (2005) Localization and identification of concurrent sounds in the owl's auditory space map. *J Neurosci* 25:10446–10461.

Kettler L (2010) Master's thesis, RWTH Aachen.

Kim D, Bishop B, Kuwada S (2010) Acoustic cues for sound source distance and azimuth in rabbits, a racquetball and a rigid spherical model. *JARO* .

Kim S, Choi W (2005) On the externalization of virtual sound images in headphone reproduction: a wiener filter approach. *J Acoust Soc Am* 117:3657–3665.

King A, Calvert G (2001) Multisensory integration: perceptual grouping by eye and ear. *Current Biology* 11(8):R322–R325.

King A, Carlile S (1994) Responses of neurons in the ferret superior colliculus to the spatial location of tonal stimuli. *Hear Res* 81:137–149.

King A, Kacelnik O, Mrsic-Flogel T, Schnupp J, Parsons C, Moore D (2001) How plastic is spatial hearing? *Audiol Neurootol* 6:182–186.

Klump G (2000) *Comparative Hearing: Birds and Reptiles* Springer Handbook of Auditory Research, New York.

Knudsen E (1981) The hearing of the barn owl. *Scientific American* 245:113–125.

Knudsen E, Blasdel G, Konishi M (1979) Sound localization by the barn owl (tyto alba) measured with the search coil technique. *J Comp Physiol A* 133:1–11.

Knudsen E, Esterly S, Knudsen P (1984) Monaural occlusion alters sound localization during a sensitive period in the barn owl. *J Neurosci* 4:1001–1011.

Knudsen E, Knudsen P (1986) The sensitive period for auditory localization in the barn owl is limited by age, not by experience. *J Neurosci* 6:1918–1924.

Knudsen E, Konishi M (1978) A neural map of auditory space in the owl. *Science* 200:795–797.

Knudsen E, Konishi M (1979) Mechanisms of sound localisation in the barn owl (tyto alba). *J Comp Physiol A* 133:13–21.

Koay G, Kearns D, Heffner H, Heffner R (1998) Passive sound-localization ability of the big brown bat (eptesicus fuscus). *Hear Res* 119:37–48.

Koka K, Tollin D (2008) The acoustical cues to sound location in the rat: measurements of directional transfer functions. *Acoust Soc Am* 123:4297–4309.

Konishi M (1973a) How the owl tracks its prey. *American Scientist* 61:414–424.

Konishi M (1973b) Locatable and nonlocatable acoustic signals for barn owls. *The American Naturalist* 107:775–785.

Konishi M (2003) Coding of auditory space. *Annual Review Neuroscience* 26:31–55.

Köppl C (1997) Phase locking to high frequencies in the auditory nerve and cochlear nucleus magnocellularis of the barn owl, tyto alba. *J Neuroscience* 17:3312–3321.

Köppl C, Gleich O (1997) Evoked cochlear potentials in the barn owl. *J Comp Physiol A* 103:601–612.

Köppl C, Gleich O, Manley G (1993) An auditory fovea in the barn owl cochlea. *J Comp Physiol A* 171:695–704.

Kulkarni A, Colburn H (1998) Role of spectral detail in sound-source localization. *Nature* 396:747–749.

Langendijk E, Bronkhorst A (2002) Contribution of spectral cues to human sound localization. *J Acoust Soc Am* 112:1583–1596.

Larsen O, Dooling R, Michelsen A (2006) Role of pressure difference reception in the directional hearing of budgerigars (melopsittacus undulatus). *J Comp Physiol A* 192:1063–1072.

Larsen O, Dooling R, Ryals B (1997) *Roles of intracranial air pressure in bird audition) Diversity in auditory mechanics* World Scientific, Singapore.

Leibold C (2010) Influence of inhibitory synaptic kinetics on the interaural time difference sensitivity in a linear model of binaural coincidence detection. *J Acoust Soc Am* 127:931–942.

Lewald J (1987) The acuity of sound localization in the pigeon (columbia livia). *Naturwissenschaften* 74:296–297.

Lewald J (1990) The directionality of the ear of the pigeon (columbia livia). *J Comp Physiol A* 167:533–543.

MacPherson E, Middlebrooks J (2002) Listener weighting of cues for lateral angle: The duplex theory of sound localization revisited. *J Acoust Soc Am* 111:2219–2236.

Makous J, Middlebrooks J (1990) Two-dimensional sound localization by human listeners. *J Acoust Soc Am* 87:2188–2200.

Manley G, Koeppl C, Konishi M (1988) A neural map of interaural intensity differences in the brain stem of the barn owl. *J Neuroscience* 8:2665–2676.

Martin R, Webster W (1987) The auditory spatial acuity of the domestic cat in the interaural horizontal and median vertical planes. *Hear Res* 30:239–252.

May B, Huang A (1996) Sound orientation behavior in cats. i. localization of broadband noise. *J Acoust Soc Am* 100:1059–1069.

Mazer J (1998) How the owl resolves auditory coding ambiguity. *Proc Natl Acad Science USA* 95:10932–10937.

McAlpine D, Jiang D, Palmer A (2001) A neural code for low-frequency sound localization in mammals. *Nat Neurosci* 4:396–401.

Meredith M, Stein B (1986) Visual, auditory, and somatosensory convergence on cells in superior colliculus results in multisensory integration. *J Neurophysiol* 56:640–662.

Metzger R, Mullette-Gillman A, Underhill A, Cohen Y, Groh J (2004) Auditory saccades from different eye positions in the monkey: Implications for coordinate transformations. *Journal of Neurophysiology* 92:2622–2627.

Michelsen A, Larsen O (2008) Pressure difference receiving ears. *Bioinsp Biomim* 3:1–18.

Middlebrooks J (1999) Virtual localization improved by scaling nonindividualized external-ear transfer functions in frequency. *J Acoust Soc Am* 106:1493–1510.

Middlebrooks J, Green D (1991) Sound localization by human listeners pp. 135–159.

Middlebrooks J, Knudsen E (1984) A neural code for auditory space in the cat's superior colliculus. *J Neurosci* 4:2621–2634.

Middlebrooks J, Knudsen E (1987) Changes in external ear position modify the spatial tuning of auditory units in the cat's superior colliculus. *J Neurophysiol* 57:672–687.

Mills W (1972) *Modern Auditory Theory*, chapter Auditory localization Academic Press, New York.

Moiseff A (1989a) Bicoordinate sound localization by the barn owl. *J Comp Physiol A* 164:637–644.

Moiseff A (1989b) Binaural disparity cues available to the barn owl for sound localization. *J Comp Physiol A* 164:629–636.

Moiseff A, Konishi M (1981a) Neuronal and behavioral sensitivity to binaural time differences in the owl. *J Neuroscience* 1:40–48.

Moiseff A, Konishi M (1981b) The owl's interaural pathway is not involved in sound localization. *J Comp Physiol* 144:299–304.

Mrsic-Flogel T, King A, Jenison R, Schnupp J (2001) Listening through different ears alters spatial response fields in ferret primary auditory cortex. *J Neurophysiol* 86:1043–1046.

Musicant A, Chan J, Hind J (1990) Direction-dependent spectral properties of cat external ear: New data and cross-species comparisons. *J Acoust Soc Am* 87:757–781.

Nienhuys T, Clark G (1979) Critical bands following the selective destruction of cochlear inner and outer hair cells. *Acta Oto-laryngologica* 88:350–358.

Nodal F, Bajo V, Parsons C, Schnupp J, King A (2008) Sound localization behavior in ferrets: Comparison of acoustic orientation and approach-to-target responses. *Neuroscience* 154:397–408.

Nodal F, Keating P, King A (2010) Chronic detachable headphones for acoustic stimulation in freely moving animals. *J Neuroscience Methods* 189:44–50.

Ohayon S, Harmening W, Rivlin E (2008) Through a barn owl's eyes: interactions between scene content and visual attention. biological cybernetics. *Biological Cybernetics* 98:115–132.

Okanoya K, Dooling R (1987) Hearing in passerine and psittacine birds: A comparative study of absolute and masked auditory thresholds. *J Comp Psych* 101:7–15.

Olsen J, Knudsen E, Esterly S (1989) Neural maps of interaural time and intensity differences in the optic tectum of the barn owl. *J Neurosci* 9:2591–2605.

Parsons C, Lanyon R, Schnupp J, King A (1999) Effects of altering spectral cues in infancy on horizontal and vertical sound localization by adult ferrets. *J Neurophysiology* 82:2294–2309.

Payne R (1962) How the barn owl locates prey by hearing. *The Living Bird First Annual Of The Cornell Lab Of Ornithology* pp. 151–159.

Payne R (1971) Acoustic location of prey by barn owls (tyto alba). *J Exp Biol* 54:535–573.

Pena J, Konishi M (2001) Auditory spatial receptive fields created by multiplication. *Science* 13(292):249–252.

Phillips D (2007) A perceptual architecture for sound lateralization in man. *Hear Res* 238:124–132.

Plenge G (1974) On the differences between localization and lateralization. *J Acoust Soc Am* 56:944–951.

Poganiatz I, Nelken I, Wagner H (2001) Sound-localization experiments with barn owls in virtual space: influence of interaural time difference on headturning behavior. *JARO* 2:1–21.

Poganiatz I, Wagner H (2001) Sound-localization experiments with barn owls in virtual space: influence of broadband interaural level difference on head-turning behavior. *J Comp Physiol A* 187:225–233.

Populin L (2006) Monkey sound localization: Head-restrained versus head-unrestrained orienting. *J Neuroscience* 26:9820–9832.

Populin L (2008) Human sound localization: measurements in untrained, head-unrestrained subjects using gaze as a pointer. *Exp Brain Res* 190:11–30.

Populin L, Yin T (1998a) Behavioral studies of sound localization in the cat. *J Neuroscience* 18:2147–2160.

Populin L, Yin T (1998b) Pinna movements of the cat during sound localization. *Journal of Neuroscience* 18:4233–4243.

Quine D, Konishi M (1974) Absolute frequency discrimination in the barn owl. *J Comp Physiol* 93:347–360.

Rayleigh L (1907) On our perception of sound direction. *Philos Mag* 13:214–232.

Rose J, Gross N, Geisler C, Hind J (1966) Some neural mechanisms in the inferior colliculus of the cat which may be relevant to localization of a sound source. *J Neurophysiol* 29:288–314.

Rosowski J, Saunders J (1980) Sound transmission through the avian interaural pathway. *J Comp Physiol A* 130:183–190.

Roulin A (2001) Food supply differentially affects sibling negotiation and competition in the barn owl (tyto alba). *Behav Ecol Sociobiol* 49:514–519.

Roulin A, Kölliker M, Richner H (2000) Barn owl (tyto alba) siblings vocally negotiate resources. *Proc R Soc Lond B* 267:459–463.

Ruhland J, Yin T (2008) Localization of high pass, low pass, and narrow band sounds by cats In *Abstract 586, Session O31, on ARO Midwinter Meeting in Phoenix, Arizona, USA*.

Saberi K, Farahbod H, Konishi M (1998) How do owls localize interaurally phase-ambiguous signals? pp. 6465–6468.

Saberi K, Takahashi Y, Egnor R, Farahbod H, Mazer J, Konishi M (2002) Detection of large interaural delays and its implication for models of binaural interaction. *J Assoc Res Otolaryngol* 3:80–88.

Saberi K, Takahashi Y, Farahbod H, Konishi M (1999) Neural bases of an auditory illusion and its elimination in owls. *Nat Neurosci* 2:656–659.

Saberi K, Takahashi Y, Konishi M, Albeck Y, Arthur B, Farahbod H (1998) Effects of interaural decorrelation on neural and behavioral detection of spatial cues. *Neuron* 21:789–798.

Schwartzkopff J (1952) Untersuchungen über die arbeitsweise des mittelohres und das richtungshören der singvögel unter verwendung von cochlea-potentialen. *Z Vergl Physiol* 34:46–68.

Searle C, Braida L, Cuddy D, Davis M (1975) Binaural pinna disparity: another auditory localization cue. *J Acoust Soc Am* 57:448–455.

Seidl A, Grothe B (2005) Development of sound localization mechanisms in the mongolian gerbil is shaped by early acoustic experience. *J Neurophysiol* 94:1028–1036.

Shackleton T, Meddis R, Hewitt M (1991) Across frequency integration in a model of lateralization. *J Acoust Soc Am* 91(4):2276–2279.

Shackleton T, Skottun B, Arnott R, Palmer A (2003) Interaural time difference discrimination thresholds for single neurons in the inferior colliculus of guinea pigs. *J Neuroscience* 23(2):716–724.

Shifferman E, Eilam D (2004) Movement and direction of movement of a simulated prey affect the succes rate in barn owl tyto alba attack. *Journal of Avian Biology* 35:111–116.

Singheiser M, Plachta D, Bremen P, Brill S, Wagner H (2010) Target-approaching behavior of barn owls (tyto alba): influence of sound frequency. *J Comp Physiol A* 196:277–240.

Slattery WI, Middlebrooks J (1994) Monaural sound localization: acute versus chronic unilateral impairment. *Hear Res* 75:38–46.

Spezio M, Keller C, Marrocco R, Takahashi T (2000) Head-related transfer functions of the rhesus monkey. *Hear Res* 144:73–88.

Spitzer M, Semple M (1991) Interaural phase coding in auditory midbrain: influence of dynamic stimulus features. *Science* 254:721–724.

Spitzer M, Takahashi T (2006) Sound localization by barn owls in a simulated echoic environment. *J Neurophysiol* 95:3571–3584.

Steinbach M (1972) Eye movements of the owl. *Vision Research* 13:889–891.

Sterbing S, Hartung K, Hoffmann K (2003) Spatial tuning to virtual sounds in the inferior colliculus of the guinea pig. *J Neurophysiol* 90:2648–2659.

Stern R, Zeiberg A, Trahiotis C (1988) Lateralization of complex binaural stimuli: A weighted-image model. *J Acoust Soc Am* 84:156–165.

Takahashi T, Konishi M (1986) Selectivity for interaural time difference in the owl's midbrain. *Journal of Neuroscience* 6:3413–3422.

Takahashi T, Bala A, Spitzer M, Euston D, Spezio M, Keller C (2003) The synthesis and use of the owl's auditory space map. *Biol Cybern* 89:378–387.

Takahashi T, Konishi M (1988) The projections of the cochlear nuclei and nucleus laminaris to the inferior colliculus of the barn owl. *J Comp Neurol* 274:190–211.

Takahashi T, Moiseff A, Konishi M (1984) Time and intensity cues are processed independently in the auditory system of the owl. *J Neurosci* 4:1781–1786.

Takahashi T, Wagner H, Konishi M (1988) The role of the commissural projections in the representation of bilateral space in the barn owl's inferior colliculus. *J Comp Neurol* 281:545–554.

Thompson G, Masterton R (1978) Brain stem auditory pathways involved in reflexive head orientation to sound. *J Neurophysiol* 41:1183–1202.

Tollin D, Koka K (2009) Postnatal development of sound pressure transformations by the head and pinnae of the cat: Monaural characteristics. *J Acoust Soc Am* 125:980–994.

Tollin D, Yin T (2002) The coding of spatial location by single units in the lateral superior olive of the cat. ii. the determinants of spatial receptive fields in azimuth. *J Neuroscience* 22:1468–1479.

Tollin D, Yin T (2003) Spectral cues explain illusory elevation effects with stereo sounds in cats. *J Neurophysiol* 90:525–530.

von Campenhausen M, Wagner H (2006) Influence of the facial ruff on the sound-receiving characteristics of the barn owl's ears. *J Comp Physiol A* 192:1073–1082.

Vonderschen K, Wagner H (2009) Tuning to interaural time difference and frequency differs between the auditory arcopallium and the external nucleus of the inferior colliculus. *J Neurophysiol* 101:2348–2361.

Wada Y (1924) Beiträge zur vergleichenden physiologie der gehörorgane. *Pflugers Arch Ges Physiol* 202:46–69.

Wagner H (1993) Sound-localization deficits induced by lesions in the barn owl's auditory space map. *J Neuroscience* 13:371–386.

Wagner H (2002) *Directional hearing in the barn owl: psychophysics and neurophysiology* Dänemark.

Wagner H (2004) A comparison of neural computations underlying stereo vision and sound localization. *J Physiol* 98:135–145.

Wagner H, Asadollahi A, Bremen P, Endler F, Vonderschen K, von Campenhausen M (2007) Distribution of interaural time difference in the barn owl's inferior colliculus in the low- and high-frequency ranges. *J Neurosci* 27:4191–4200.

Wagner H, Takahashi T, Konishi M (1987) Representation of interaural time difference in the central nucleus of the barn owl's inferior colliculus. *J Neuroscience* 7:3105–3116.

Walker B, Lindsay J (2006) Navigation performance with a virtual auditory display: effects of beacon sound, capture radius, and practice. *Human Factors* 48:265–278.

Wanrooij MV, Opstal AV (2004) Contribution of head shadow and pinna cues to chronic monaural sound localization. *J Neuroscience* 24:4163–4171.

Weber T, Thorson J, Huber F (1981) Auditory behaviour of the cricket. i. dynamics of compensated walking and discrimination paradigms on the kramer treadmill. *J Comp Physiol A* 141:215–232.

Wenzel E, Arruda M, Kistler D, Wightman F (1993) Localization using nonindividualized head-related transfer functions. *J Acoust Soc Am* 94:111–123.

Wenzel E, Wightman F, Kistler D, Foster S (1988) Acoustic origins of individual differences in sound localization behavior. *J Acoust Soc Am* 84:S79.

Whittington D, Hepp-Reymond M, Flood W (1981) Eye and head movements to auditory targets. *Exp Brain Res* 41:358–363.

Wightman F, Kistler D (1989a) Headphone simulation of free-field listening. i: Stimulus synthesis. *J Acoust Soc Am* 85:858–867.

Wightman F, Kistler D (1989b) Headphone simulation of free-field listening. ii: Psychophysical validation. *J Acoust Soc Am* 85:868–878.

Wightman F, Kistler D (1992) The dominant role of low-frequency interaural time differences in sound localization. *J Acoust Soc Am* 91(3):1648–1661.

Winkowski D, Knudsen E (2006) Top-down gain control of the auditory space map by gaze control circuitry in the barn owl. *Nature* 439:336–339.

Witten I, Knudsen P, Knudsen E (2010) A dominance hierarchy of auditory spatial cues in barn owls. *PLoS One* 5(4):e10396.

Wotton J, Haresign T, Simmons J (1995) Spatially dependent acoustic cues generated by the external ear of the big brown bat, eptesicus fuscus. *J Acoust Soc Am* 98:1423–1445.

Yin T, Kuwada S (1983) Binaural interaction in low-frequency neurons in inferior colliculus of the cat. iii. effects of changing frequency. *J Neurophysiol* 50:1020–1042.

Zahorik P, Bangayan P, Sundareswaran V, Wang K, Tam C (2006) Perceptual recalibration in human sound localization: learning to remediate front-back reversals. *J Acoust Soc Am* 120:343–359.

Zahorik P, Brungart D, Bronkhorst A (2005) Auditory distance perception in humans: A summary of past and present research. *Acta Acustica united with Acustica* 91:409–420.

9 Appendix

Virtual ruff removal (chapter 5)

The detailed distribution of ITDs and ILDs in the owls' HRTFs are presented for the behaving owls H, S and P as well as for the reference animal owl 39 with normal and removed ruff.

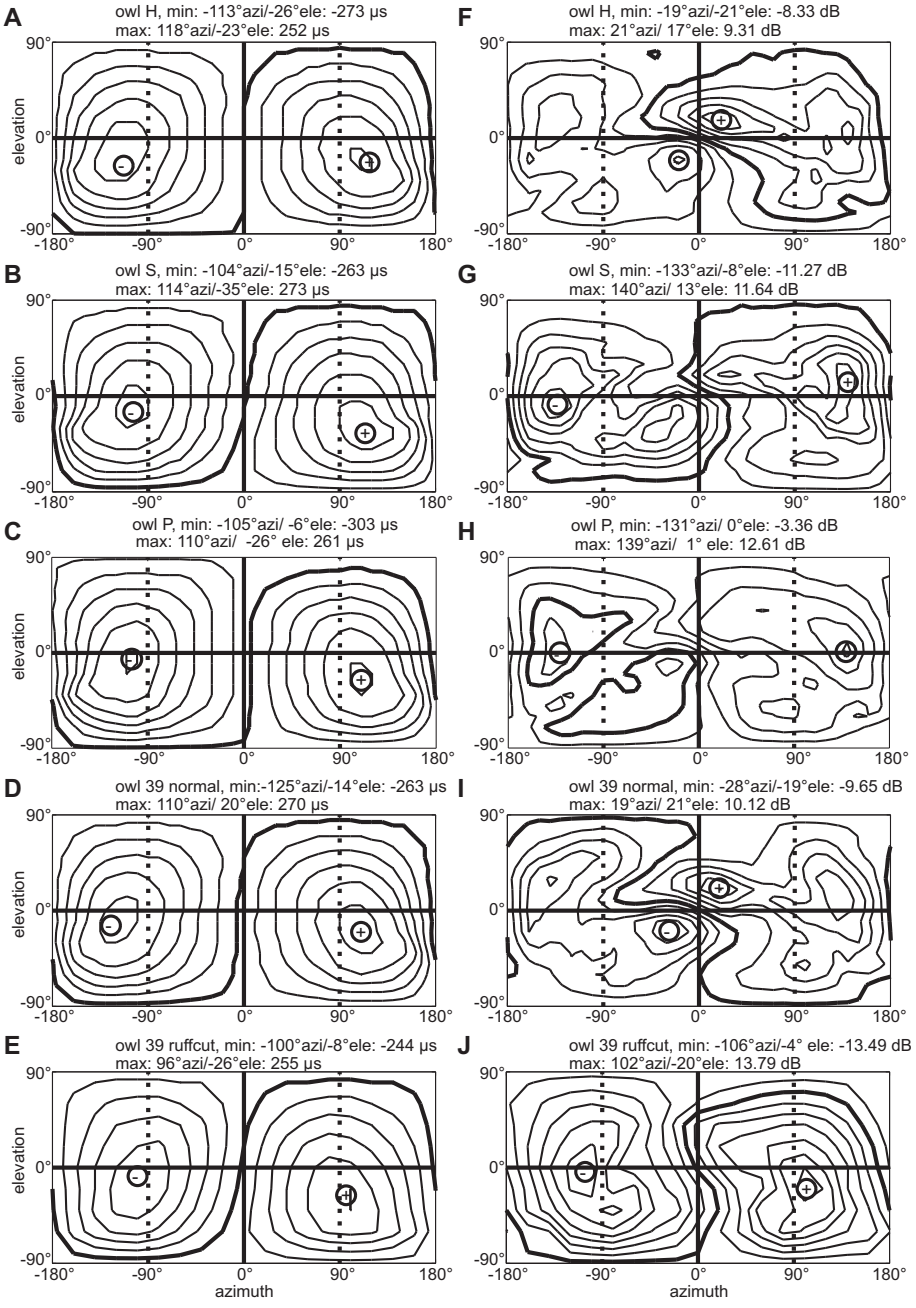

Figure 35: Broadband ITD and ILD distributions

The distribution of ITDs (**A-E**) and ILDs (**F-J**) in dependence of the azimuthal (ordinate) and elevational (abscissa) sound-stimulus positions is shown for owl H (A+F), owl S with intact ruff (B+G) and owl P (C+H), for owl 39 with intact ruff (D+I) and for owl 39 with removed ruff feathers (E+J). Angular values refer to the position in a spherical coordinate system relative to the midsagittal plane (azimuth) and the horizontal plane through the owl's eyes (elevation). Negative azimuthal angles correspond to positions to the left of the owl. Negative elevational angles correspond to positions below the equator. Bold lines indicate the positions where the ITD respectively ILD is zero, i.e., the sound reaches the left and the right ear at the same time. Thin black lines connect points with equal ITD (iso-ITD line) in steps of 50 µs or equal ILDs (iso-ILD line) in steps of 2 dB. The maximum negative ITD respectively ILD is marked with a "–" sign, whereas the maximum positive ITD and ILD are marked with a "+" sign. The angular position of the extrema is given above each panel, together with the corresponding ITD (in µs) and ILD (in dB), respectively.

The differences in ITDs and ILDs between individualized HRTFs and those of owl 39 normal respectively owl 39 ruffcut are shown for owl S (Fig. 36) and for owl P (Fig. 37).

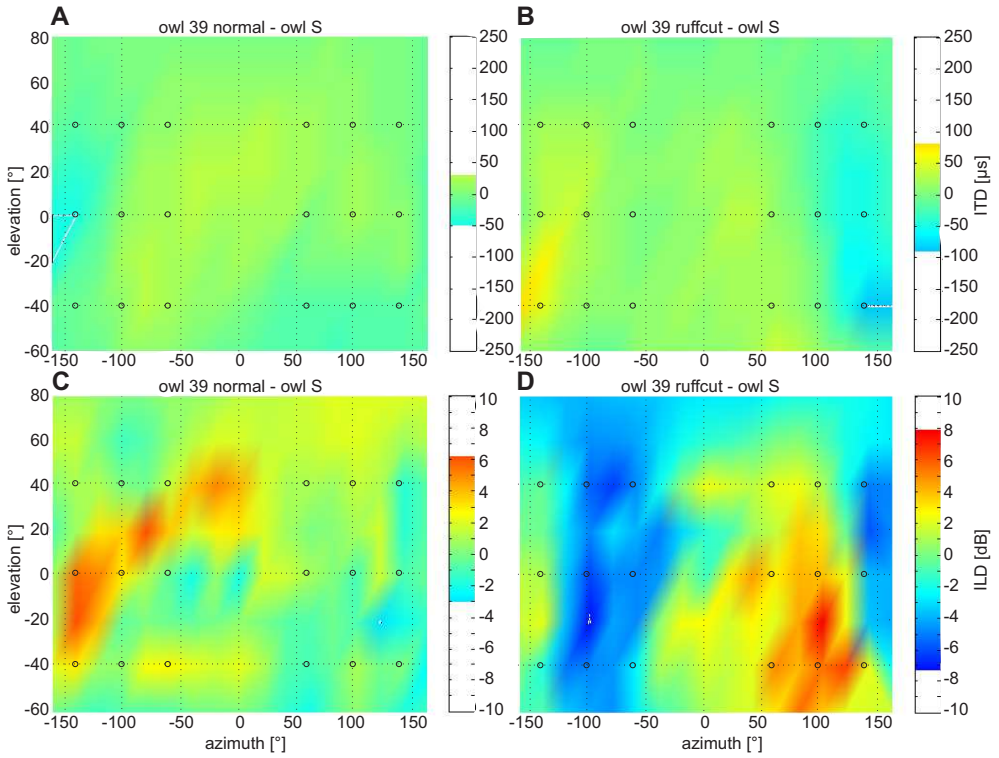

Figure 36: ITD and ILD differences between normal and ruffcut HRTFs
As in 15, but for owl S.

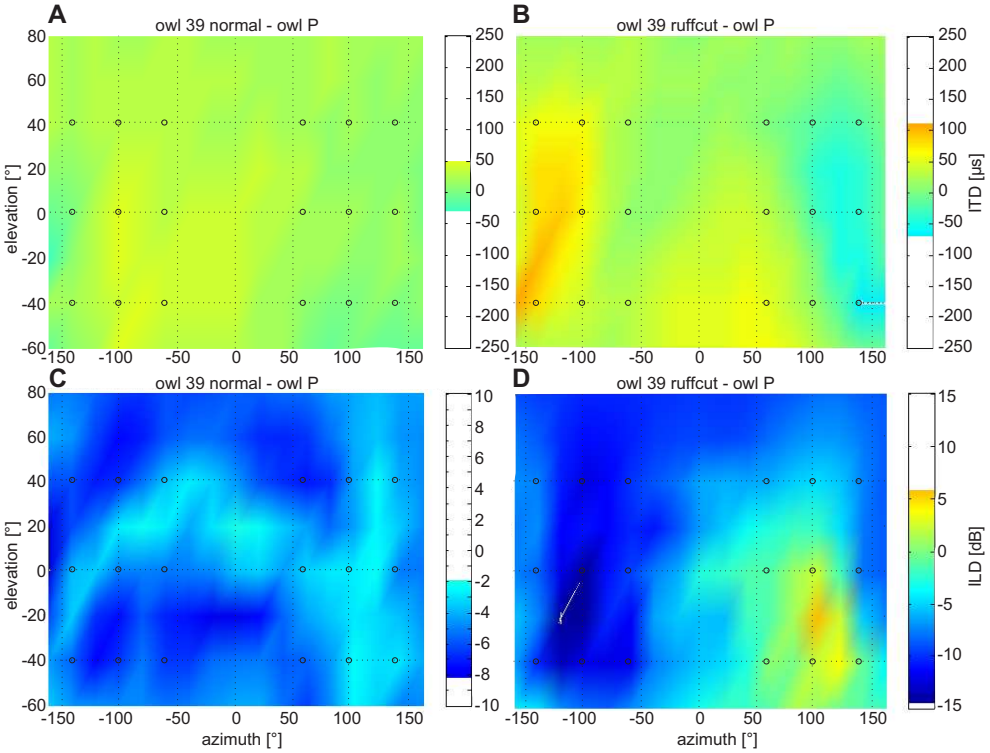

Figure 37: ITD and ILD differences between normal and ruffcut HRTFs
As in 15, but for owl P.

As additional information to the analysis of azimuthal head-turn angles (tables 3 and 4 in section 5.3.3), the following tables 9 and 10 give the results of ANOVA analyses of variance.

Table 9: ANOVA with Scheffé post-hoc test for azimuthal head-turn angles

For pooled data from the three owls, the HRTF set alone (individualized, owl 39 normal or ruffcut) as well as the interaction terms between owl and HRTF (owl*HRTF) had no influence on the azimuthal head-turn angle. In contrast, the influence of all other factors and interaction terms was highly significant ($p<0.001$, bold printed). That is, for example, azimuthal (azi) and elevational (ele) stimulus angles or the interaction of HRTF and azimuth (azi*HRTF) influenced the amplitude of the azimuthal head-turn angle. Degree of freedom (df), test statistic (F) and significance level (p) as indicated, significant terms are bold printed.

	df	F	significance (p)
azimuth	5	8297.339	**0.000**
elevation	2	42.853	**0.000**
HRTF	2	0.306	0.736
owl	2	78.053	**0.000**
azi*ele	10	14.194	**0.000**
azi*HRTF	10	73.763	**0.000**
azi*owl	10	5.111	**0.000**
ele*HRTF	4	4.683	**0.031**
ele*owl	4	4.309	**0.002**
owl*HRTF	4	0.974	0.420
azi*ele*HRTF	20	2.493	**0.000**
azi*owl*HRTF	20	1.305	0.164
azi*ele*owl	20	2.001	**0.005**
azi*ele*HRTF	20	2.493	**0.000**
ele*owl*HRTF	20	1.542	0.138
azi*ele*owl*HRTF	20	1.542	**0.008**

Table 10: Scheffé post-hoc test for azimuthal head-turn angles

The interaction term of azimuthal stimulus angle and A) HRTF set (ind. = individualized, 39n = owl 39 normal, 39c = owl 39 ruffcut) respectively B) stimulus elevation (-40°, 0° or 40°) as shown in Table 9 was more closely analyzed with a Scheffé post-hoc test whose results (p values, bold printed if significant) are given for each owl and azimuth (left column). The test revealed that the difference was due to differences at peripheral stimulus angles (±140°), whereas responses to more central stimulus angles mostly did not differ.

	owl H			owl S			owl P		
A)	**ind/39n**	**39n/39c**	**ind/39c**	**ind/39n**	**39n/39c**	**ind/39c**	**owl H/39n**	**39n/39c**	**owl H/39c**
-140°	0.459	**0.000**	**0.000**	0.413	**0.000**	**0.000**	0.775	**0.000**	**0.000**
-100°	0.742	0.946	0.559	0.635	0.103	**0.012**	0.974	**0.036**	**0.072**
-60°	**0.077**	0.283	0.785	0.777	0.322	0.118	0.031	0.629	0.226
60°	**0.016**	0.997	**0.009**	**0.049**	**0.023**	0.931	0.863	0.566	0.276
100°	0.556	0.173	0.702	0.848	**0.003**	**0.015**	0.762	0.175	**0.028**
140°	0.873	**0.000**	**0.000**	0.971	**0.000**	**0.000**	0.607	**0.000**	**0.000**

B)	**-40°/0°**	**-40°/40°**	**0°/40°**	**-40°/0°**	**-40°/40°**	**0°/40°**	**-40°/0°**	**-40°/40°**	**0°/40°**
-140°	0.156	0.983	0.110	**0.000**	0.986	**0.0004**	**0.048**	0.552	**0.000**
-100°	0.954	0.860	0.681	0.6996	0.991	0.999	**0.001**	**0.025**	0.367
-60°	**0.000**	**0.000**	0.791	**0.016**	**0.000**	0.140	**0.000**	**0.000**	0.678
60°	0.139	0.980	0.198	0.839	**0.0295**	0.290	0.985	0.153	0.212
100°	**0.039**	0.789	**0.005**	0.568	**0.005**	**0.000**	0.375	**0.000**	**0.000**
140°	0.992	**0.003**	**0.001**	0.435	**0.000**	**0.000**	0.593	**0.000**	**0.000**

Responses to 1/3 octaveband-filtered noise (chapter 6)

The width of 1/3 octaveband filters for the various center frequencies calculated as shown in Fig. 2 are provided in the following table:

Table 11: Bandwidth of 1/3 octaveband filters of various frequency

For each center frequency in kHz, the bandwidth (lower and upper border) of a third-order butterworth filter with 1/3 octave bandwidth is indicated. Below and above these cutoff frequencies, the amplitude of a signal filtered with the corresponding octaveband filter fell below the indicated attenuation in dB.

	3 dB attenuation at...		20 dB attenuation at...		30 dB attenuation at...	
frequency [kHz]	**lower border [kHz]**	**upper border [kHz]**	**lower border [kHz]**	**upper border [kHz]**	**lower border [kHz]**	**upper border [kHz]**
1	0.89608	1.1157	0.7902	1.2647	0.7098	1.4078
2	1.7922	2.2314	1.5804	2.5294	1.4196	2.8157
3	2.6882	3.349	2.3706	3.7941	2.1294	4.2216
5	4.4784	5.5824	3.949	6.3216	3.5451	7.0275
7	6.2706	7.8157	5.5255	8.8431	4.9569	9.8157
9	8.0608	10.049	7.098	11.3569	6.3627	12.5804

Below, supplementary information is provided on the owls' head-turn latencies in response to 1/3 octaveband-filtered noise, giving the mean and median latencies in ms for each center frequency and owl.

Table 12: Latencies to 1/3 octaveband-filtered and broadband noise

For each of the three owls, mean as well as median response latencies and the corresponding standard deviation (SD) for various stimulus frequencies are indicated in ms.

	center frequency [kHz]	mean [ms]	median [ms]	SD [ms]
owl H	**1**	181.7	171	84.8
	2	201.8	169	92.7
	3	194.1	162	104.8
	5	170.1	149	88.4
	7	170.3	140	83.6
	9	175.8	143	100.1
	broadband	132.4	109.5	66.2
	fixILD	186.1	152	91.7
owl S	**1**	218.1	186	110.3
	2	225.2	186	105.5
	3	197.2	161	112.8
	5	195.4	169	85.7
	7	215.8	179	114.8
	9	192.2	159.5	110.8
	broadband	138.4	126	56.6
	fixILD	170.5	154	55.4
owl P	**1**	183.8	157	84.3
	2	159.6	154	42.8
	3	153.0	140	69.6
	5	156.9	142	61.0
	7	163.0	147	77.6
	9	151.8	128.5	85.0
	broadband	174.9	157	70.8
	fixILD	142.0	131	52.5

10 Acknowledgements

I would like to thank Prof. Dr. Hermann Wagner for being my first reviewer - and even more importantly, for steady support whenever needed, but also for giving me plenty of rope to realize my own ideas.

Special thanks to Prof. Dr. Harald Luksch, who found the time for being my second reviewer despite his workload as a professor in Munich. It is a pity not having you in Aachen any more.

Dr. Mark von Campenhausen earns my gratitude for teaching me how to program in MatLab and C^{++}, and for many valuable discussions. The very same holds for Frank Endler, who was always a good friend and who I owe a lot because he generously shared his vast experience in programming.

To my parents, Prof. Dr. Axel Hausmann and Brigitte Hausmann, my deepest gratitude for always being there for me and supporting me all years long. I owe you a lot. Also, I want to thank Matthias Berger who takes me as I am, for better or for worse. My little sister, Lea, knew how to keep me motivated whenever lazy owls frustrated me - thank you for your mental support. Of course, also my sister Kathrin, my brother-in-law Tom and my nephews Paul and Linus, as well as my brother Philipp, did everything they could (at least I hope so) to be the best family I could imagine.

Many thanks to Martin Singheiser, my understanding fellow sufferer, who helped me not to forget why we are researchers. Thank you for endless talks and delightful dinners, and for all your support. I would also like to thank Dr. Benedikt Mönig who reminded me that there exists a world outside working - thank you for being who you are.

To the entire Institute of Biology II - especially my colleagues Sandra, Wolf, Petra, Thomas, Stefan and Tom, Jörg and Susanne - I would like to express my gratitude. I liked working with people who have a good sense of humor, and I will certainly miss you a lot.

Finally, the owls: Hurin, Scottie and Pavarotti and many others - thank you for providing me with lots of data.

11 Curriculum Vitae

Persönliche Daten:

Name:	Elena Laura Hausmann
Staatsangehörigkeit:	deutsch

Qualifikationen:

2002	Abitur am Städtischen Gymnasium St. Leonhard, Aachen
2002 - 2007	Studium der Biologie an der RWTH Aachen, Abschluss zur Diplom-Biologin
2005 - 2007	Wirtschaftswissenschaftliches Zusatzstudium an der RWTH Aachen, Abschluss mit Master in Business Administration
2005 - 2006	Studentische Hilfskraft am Institut für Biologie II, Lehrstuhl für Zoologie und Tierphysiologie, RWTH Aachen
2007 - 2010	Promotionsstipendium der RWTH Aachen
2007 - 2010	Wissenschaftliche Angestellte am Institut für Biologie II
2007 - 2010	Promotion am Institut für Biologie II